APPLICATION OF MASS SPECTROMETRY TO THE ANALYSIS OF MIXTURES

A thesis submitted by

David Mitchell, B.Sc.

for the degree of

Doctor of Philosopy

in the University of Warwick

Contents

List of Figures

List of Tables

Acknowledgements

Firstly I would like to thank my two supervisors Prof Keith Jennings at Warwick and Dr Jim Scrivens at ICI for their invaluable help and encouragement.

I would also like to thank all members of the mass spectrometry research group at Warwick from 1984-1987 for their intellectual and social support. Special mention goes to Dr Rod Mason, Dr David Newton and Dr Richard Bowen. I am indebted to the support services and technicians of the Department of Chemistry at Warwick, especially the mechanical and electrical workshops. I would also like to thank the people at ICI especially Mr Gary Manton and Dr Trevor Blease for their time and patience whilst I was there.

Specific acknowledgments go to Dr David Catlow for obtaining the Field Desorption spectra and Dr Trevor Blease for the low energy collisionally activated daughter ion spectra, Dr Aiden Harrison for the NMR spectra and Dr Gilberto de Nucci for his typing expertise.

I would also like to acknowledge the financial support of ICI for this CASE award.

Declaration

The work presented in this theses is my own and original except were due reference or acknowledgment is given. Some of this work has been previously presented at conferences or accepted for publication.

Mass Spectra of 2-Aryl-3-Nitrochromans and 2-Aryl-3-Nitrochromenes, D. Mitchell, R.D. Bowen, K.R. Jennings, R.S. Varma, G.W. Kabalka, J. Chem. Soc. Perkin II, 1495,1987

Mass Spectra of 2-Aryl-chroman-3-one Oximes, R.D. Bowen, D. Mitchell, R.S. Varma, G.W. Kabalka, Org. Mass Spectrom., 22, 231, 1987.

Fast Atom Bombardment Mass Spectra of Surfactants and Tin Stabilisers, D. Mitchell, K.R. Jennings, J.H. Scrivens, 10th International Mass Spectrometry Congress, Swansea, 1985.

Mass Spectra of 2-Aryl-3-Nitrochroman and 2-Aryla-3-Nitrochromenes, D.Mitchell R.D. Bowen, K.R. Jennings, R.S. Varma, G.W. Kabalka, British Mass Spectrometry Society Meeting, Brighton, 1986,

Mass Spectra of Tin Stabilisers, D. Mitchell, K.R. Jennings, J.H. Scrivens, Royal Society of Chemistry Annual Congress, Swansea, 1987,

Thermospray Mass Spectra of Quaternary Ammonium Salts, D. Mitchell, K.R. Jennings, J.H. Scrivens, American Society for Mass Spectrometry, 35th Annual meeting, Denver, 1987,

Fast Atom Bombardment Mass Spectrometry of Anionic Surfactants, D. Mitchell, K.R. Jennings, J.H. Scrivens, British Mass Spectrometry Society Meeting, 1987, York,

Summary

The work presented in this thesis involves the application of mass spectrometry to the analysis of a number of both commercial products and model organic compounds. Use of soft ionisation techniques for thermally labile and ionic compounds (mainly fast atom bombardment, field desorption and thermospray) has been extensively explored for the provision of both qualitative and quantitative information. More established ionisation techniques (electron impact and chemical ionisation) have also been utilized in order to obtain qualitative data. In many cases comparisons have been made between different ionisation modes, and some discussion of the processes occuring is given. Ion structures and decomposition pathways have been elucidated by both tandem mass spectrometry and high mass resolution measurements.

Analysis of both complex mixtures and pure compounds has been performed. The systems studied were: surfactants (anionic - sodium alcohol ether sulphates, nonionic - alcohol ethoxylates, cationics - mainly quaternary ammonium salts), organotin PVC heat stabilisers and organic heterocyclic compounds (some chromans, chromenes and corresponding oximes).

Abbreviations

mmHg	millimeters of mercury
KV	kilovolts
$KJmol^{-1}$	kilojoules per mole
s	seconds
Vm^{-1}	volts per meter
FTICR	Fourier transform ion cyclotron resonance
$secdec^{-1}$	seconds per decade
mA	milliamps
µl	microliters
K	degrees Kelvin
NMR	nuclear magnetic resonance
MHz	mega Hertz
$C\mu g^{-1}$	Coulombs per microgram
RI	Relative Intensity

Chapter I

INSTRUMENTAL TECHNIQUES

1.1 Mass Spectrometry[1-3]

A mass spectrometer may be defined as an instrument which separates gaseous ions according to their mass to charge ratio (m/z) by some physical means.

Development of mass spectrometry began in the early part of this century[4-6]. Mass spectrometers were first applied to the determination of the different elemental isotopes, and their relative abundances. Application of mass spectrometers widened to usage in the chemical industry for mixture analysis of oils. This practice ceased with the advent of gas chromatography[7] in the 1960s, which is considerably simpler and less expensive instrument for mixture analysis. Mass spectrometry retained analytical usage mainly due to its ability to provide accurate mass and structural information.

Since the 1960s extensive development in the field of mass spectrometry has occured. Notable inovations include: the coupling of chromatography with mass spectrometry, new ionisation techniques, fast scanning, use of computers, high mass range options, and tandem mass spectrometry. These, together with the inherent sensitivity, specificity, and adaptability of mass spectrometers, has led to their high profile in analytical laboratories.

The operation of a mass spectrometer can be considered as four sequential parts: (a) Sample introduction. (b) Ion production. (c) Ion separation. (d) Ion detection, amplification and presentation.

1.1.1. Sample introduction

There are a number of methods of admitting a sample into a mass spectrometer. Choice of method used for a particular sample depends upon its: (a) Volatility. (b) Thermal stability. (c) Whether the sample is known to be pure or a mixture.

The only instrumental constraints are: the necessity of operating the mass spectrometer at low pressure (10^{-1}-10^{-8} Torr, where 1 Torr = 1 mmHg), and often at high source voltages (magnetic sector instruments).

1.1.2. Ion Production

Over the last two decades or so a comprehensive array of ionisation methods have been developed. Often an analyst has a number of ionisation techniques that can be applied to a sample. Which technique used depends upon: (a) The physical state of the sample. (b) Thermal stability of the sample. (c) What information is required.

The different methods of ion production will be discussed in some detail later.

1.1.3. Ion Separation

After an ion has been produced in the ion source it is transmitted into an analyser region. There are five major types of analyzer: (a) Magnetic sector[8,9]. (b)

Quadrupole[10]. (c) Ion cycloton resonance (ICR)[11]. (d) Time of flight (TOF.)[12]. (e) Ion trap[13].

It is possible to combine magnetic and quadrupole sectors into what are known as hybrid mass spectrometers[14,15].

The results presented and discussed within this thesis have been obtained almost exclusively using magnetic sector instruments, although some use has been made of a hybrid machine.

There are two possible geometries for double focusing magnetic sector instruments: (a) Forward, or Nier-Johnson, where the ESA (electrostatic analyzer) preceeds the magnet[8]. (b) Reverse, where the magnet preceeds the ESA[9].

Forward geometry instruments have been used predominantly for this work. Fig. 1.1 shows a schematic diagram of this type. Ions formed in the ion source are accelerated at a high potential (1 - 10 KV) through a series of focusing lenses, resolution slits, and first field free region into the ESA. Field free (or drift) regions are sections of the mass spectrometer where the ions are not under the influence of electric or magnetic fields.

An ion of mass (M), travelling with a velocity (v) and which has a number (z) of electronic charges (e), accelerated by a voltage (V), will have, on leaving the

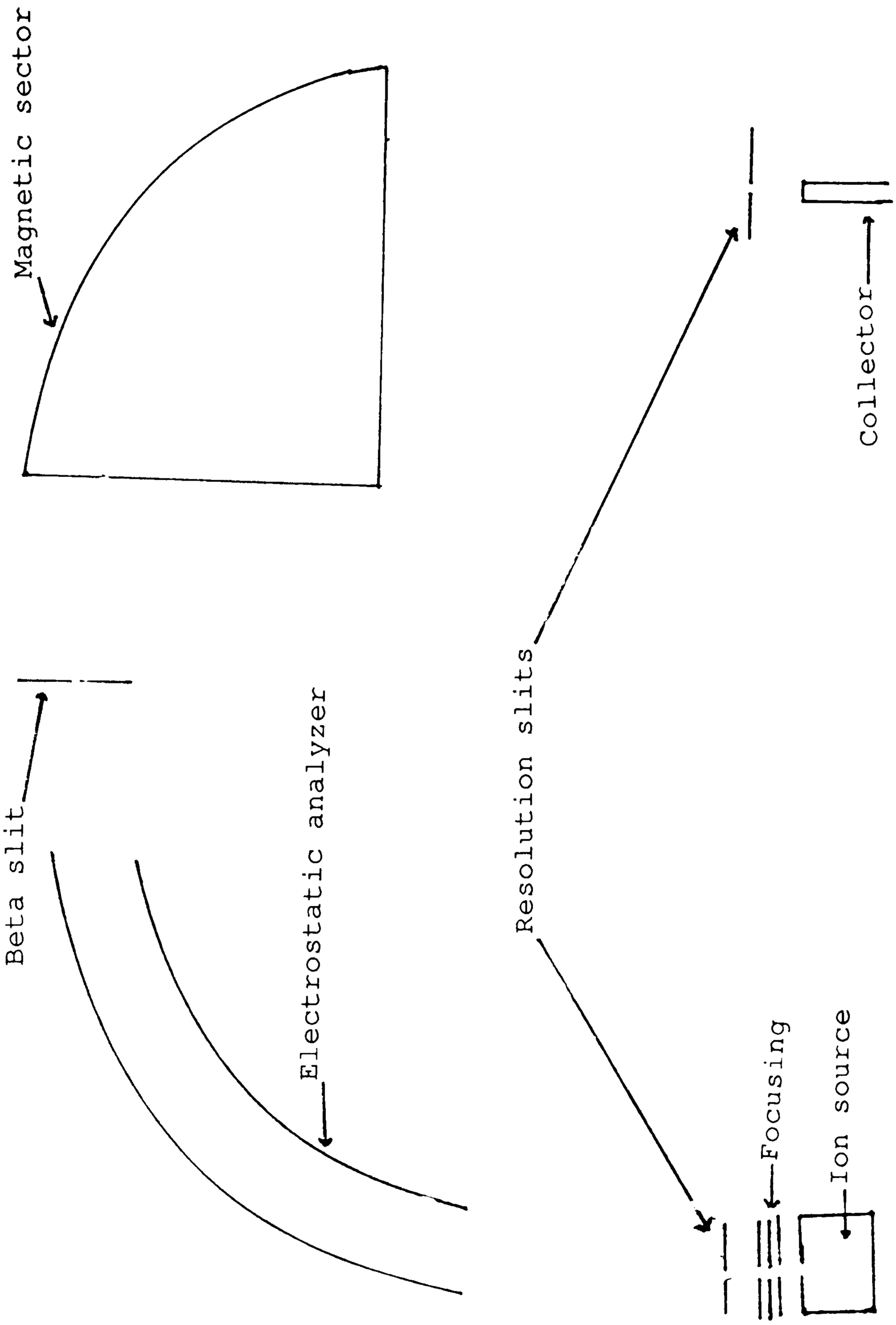

Fig 1.1. Forward geometry magnetic sector mass spectrometer.

ion source, a kinetic energy given by

$$\frac{1}{2} mv^2 = ezV \qquad (1)$$

The initial spread of translational energies of gaseous molecules within the source results in a slight spread of kinetic energies of ions leaving the source. This places severe restrictions upon the mass resolution of the instrument. Alleviation of this problem by the use of an ESA is common. The ESA comprises of two quarter circular parallel plates (of radius R), across which is applied a potential difference. Ions passing between the plates are forced to travel in a circular path of radius R_e dictated by

$$R_e = \frac{2V}{E} \qquad (2)$$

Where V is the accelerating voltage, and E the electric field strength between the plates. Hence, the ESA is a kinetic energy analyzer. Therefore, placing a slit between the ESA and the magnet results in ions of only a closely defined kinetic energy passing through the second field free region and into the magnetic analyzer.

In a magnetic field of strength (B), an ion will

experience a force of magnitude F

$$F = Bevz \tag{3}$$

towards the center of a circle of radius r. This force is equal to the centrifugal force on the ion. Hence, the following expression can be obtained

$$Bzev = \frac{mv^2}{r} \tag{4}$$

which can be combined with equation (1) to give

$$\frac{m}{z} = \frac{B^2r^2e}{2V} \tag{5}$$

Although it is possible to bring all the ions to strike the detector simultaneously[16], it is normal to scan the instrument. Scanning enables ions of differing m/z ratios to pass sequentially through a slit and onto the detector. From equation (5) it is obvious that one of two parameters may be varied (magnetic field or accelerating voltage), whilst the other is maintained at a constant value. Since sensitivity is proportional to the accelerating voltage, magnetic field scanning is the preferred option.

It is necessary to briefly mention quadrupole mass analyzers because of their presence on the hybrid

instrument used in this work. Quadrupole mass analysers consist of four parallel hyperbolic rods. A dc (direct current) potential, and a Rf (radio frequency) potential are applied across opposite rods. The electric field created cause the ions to oscillate. The equations of motion of the ions in a quadrupole are complex. It is sufficient to say that the m/z value of the transmitted ions depends upon the rod separation, the radio frequency, and the potentials applied. Ions of differing m/z rations can be given stable trajectories sequentially by either sweeping the radio frequency at constant potentials, or scanning the potentials such that the ratio of the dc to Rf potentials are constant. The latter method is preferred as it provides a linear mass range.

The practical differences between magnetic and quadrupole analysers are: (a) The latter requires substantially lower source voltages (several volts, as opposed to kilovolts). It is important, therefore, to decelerate ions leaving the magnetic sector region of an hybrid machine, before entering the quadrupole section. (b) Quadrupoles are capable of faster scan speeds. (c) But lower mass range, maximum of 4000 amu (atomic mass units) compared with over 20,000 amu on magnetic sector instruments. (d) Also quadrupoles can only give nominal mass resolution, whereas with magnetic sectors, mass resolving powers of 100,000 are possible. (e) Quadrupoles simultaneously eject positive and negative ions. (f) They are also much more compact, and less expensive than sector instruments.

1.1.4. Ion Detection, and Data Presentation

There are basically two types of ion detection systems used with magnetic sector instruments. As mentioned earlier an instrument may, or may not be scanned. The former is rarely used, but offers the advantage of high sensitivity since all the ions that pass through the analyzer are detected. A photosensitive plate is normally used as a detector.

The scanning instruments are less sensitive as only a fraction of scan time is spent on each specific mass, but they offer the powerful advantages of fast data acquisition, and simple interfacing to computers. In this type of instrument either a photomultiplier, or more commonly an electron multiplier detector is used. The detector produces an electric current which is proportional to the number of ions striking it (often a gain of 10^4 - 10^6 is obtainable). This signal is normally then transmitted to either a uv (ultra violet) recorder or computer.

Sensitivity of a scanning instrument can be improved (up to a thousand fold) by fixing the instrument parameters to allow ions of one, or a small number of masses to pass through the analyzer. Using this technique femtogram detection is possible.

Recently use has been made of array detectors[17]. Here a small portion (4%) of the mass range can be detected simultaneously.

All other instrument types normally use either photomultiplier or electron multiplier detection.

1.2. Ion Production

Methods of ion production in organic mass spectrometry can be categorised into two groups: (a) Vapour phase, ionisation of vapours and (b) Desorption, ionisation of condensed phases.

1.2.1. Vapour Phase Techniques

These are generally the older, more established ionisation methods. They involve the presentation of sample molecules, in the vapour phase, into the ion volume. Although the main two are electron impact (EI) and chemical ionisation (CI), other methods of some importance include: photoionisation[18], atmospheric pressure ionisation[19] and field ionisation[20].

1.2.1.1. Electron Impact

Electron impact is the oldest and still the most commonly used form of ionisation. Electrons are produced from an heated filament and then are accelerated into the ion volume by a potential difference between the filament and the source. The magnitude of this potential difference determines the average energy of the electrons. An electron beam with an average energy of 70 eV (electron volts, 1 eV = 96 $KJmol^{-1}$) is typically used. 70 eV represents a section of the ionisation efficiency curve where small changes in electron energy do not

affect the ion beam intensity to any appreciable extent, so enabling good reproducibility. These high energy electrons interact with the vapourised sample molecules (M) to form excited radical cations ($M^{+\cdot}$).

$$M + e \longrightarrow M^{+\cdot} + 2e \qquad (6)$$

Most organic molecules have ionisation energies which lie in the range 7 - 15 eV. Therefore it is possible for a radical cation to contain an excess of internal energy, the magnitude of which depends upon: (a) The strength of interaction between the ionising electron and the molecule. (b) Ionisation potential of the molecule. (c) Thermal energy of the molecule.

Variation of parameters (a) and (c) for a specific sample result in a distribution of internal energies for the molecular cations. Since excess internal energy cannot be lost through collisions (because of the low source pressure, approximately 10^{-6} Torr), it is randomised throughout the ion in the form of vibrational energy. Accumulation of sufficient energy within a specific bond can result in a unimolecular decomposition. This is the basis of the Quasi Equilibrium Theory (QET)[21], which in its simplist form leads to the

following expression

$$k = v(E-E_0/E)^{s-1} \quad (7)$$

where k is the rate constant for a specific unimolecular decomposition, E_0 is the energy required for the reaction, E is the internal energy contained within the ion, v is a frequency factor, and s is the effective number of oscillators.

$$s = \frac{3n-6}{3} \quad (8)$$

Where n is the number of atoms in the molecule.

There are basically two types of unimolecular reactions that can occur in an EI source: (a) Simple cleavage. For this type of reaction v tends to be high, and constant. The only necessary constraint is the flow of sufficient energy to a specific bond. (b) Intramolecular rearrangement. In these cases v is generally low. For a rearrangement to occur accumulation of sufficient energy in a specific bond is no longer the only reaction requirement. In addition, the ion must have the correct spatial orientation. This geometrical constraint lowers the frequency factor, and hence the reaction rate.

Since an ion resides in the source for about 10^{-6} s, reactions having a rate constant of less than 10^6 s^{-1} do

not lead to any observed fragment ions. Therefore, even if an ion contains enough energy to decompose, the rate constant may be too slow for it to do so. This explains the predominance of simple cleavage over rearrangement reactions in the EI source, for although the former require more energy, they occur at a faster rate than the latter.

If a reaction has a rate constant between 10^4 - 10^6 s^{-1} then the ion may fragment after leaving the source, but before reaching the detector. These are termed metastable decompositions. These reactions can normally only be observed if they occur in the second field free region. Metastable peaks appear in the "normal" mass spectrum using a uv recorder, as being broad (due to the energy release during fragmentation), and are of low intensity in relation the normal mass peaks. These metastable peaks arise at apparent, rather than real masses. It is possible to calculate their actual masses by the equation

$$M^* = \frac{M_2^2}{M_1} \qquad (9)$$

Where M_1 is the mass of the parent ion, M_2 the daughter ion, and M^* the apparent mass observed in the spectrum. Metastable decompositions occuring in the first field free region, and ESA are filtered out by the ESA. Those decompositions in the magnetic region are deflected out by the magnetic fields. Metastable reactions in the

third field free region are not normally seen, and a special detector is required to study them[22].

Thermochemistry determines which of several simple cleavage reactions an ion may undergo (since v values are very similar)

Generally a radical cation ($M^{+\cdot}$) can fragment by a simple cleavage

$$M^{+\cdot} \longrightarrow A^{+} + B^{\cdot} \qquad (10)$$

to form an even electron ion (A^{+}) and a radical ($B^{\cdot}$) Conversely it may decompose via rearrangement to lose a neutral molecule (D).

$$M^{+\cdot} \longrightarrow C^{+\cdot} + D \qquad (11)$$

The even electron ion (A^{+}) can now fragment only by the loss of a neutral species (even electron rule). Inherent stability of even electron ions as compared to radical ions constitutes the reason for this rule. Exceptions to this rule are rarely observed, and only occur when the products are exceptionally stable (e.g. di-iodides, which may lose successive iodide radicals[23]).

1.2.1.2. Chemical Ionisation

One of the major problems associated with EI is the often large, and unknown degree of energy deposited in

the molecular cation. If the activation energy for the first unimolecular decomposition is low, molecular ions of low abundance are the result. The obvious consequence of this is difficulty in the determination or confirmation of a sample's chemical identity. Molecular ion abundance can often be improved by using low energy electrons (up to 20 eV)[24]. Wide application of this technique has been hampered by several problems, mainly lower total ion currents, and difficulties in maintaining reproducibility of results.

A series of soft ionisation techniques have become available, which have been developed to overcome the problem of excessive fragmentation commonly seen with EI. Soft ionisation methods can be defined as those that provide enhanced molecular, or pseudo-molecular ion peaks as compared to results obtained from EI. The most commonly used is chemical ionisation (CI)[25].

Chemical ionisation involves the collision of a sample molecule with a reagent ion to form a sample product ion.

The reagent gas, or a mixture of gases is admitted into the source at a pressure of approximately 1 Torr. Sample is introduced at a low concentration (around 0.1%) relative to the reagent gas(es). This is to ensure that as little EI of the sample occurs as possible. A high energy electron beam is accelerated into the source (typically 100 - 400 eV) to produce a plasma of ions.

The major advantage of CI is that it enables the transfer of a specific amount of energy to the sample

molecules, hence controlling the extent of fragmentation. There are several CI techniques that may be employed.

(a) Charge Transfer

This simply involves the transfer of an electron from an ionised reagent gas species (normally a monoatomic gas) to a sample molecule. A well defined amount of energy is transferred to the sample molecule, which is equal to the recombination energy of the reagent gas. The magnitude of internal energy contained within the resultant sample ion is equal to the difference between the recombination energy of the reagent gas, and the ionisation energy of the sample. Thus, it is possible to select the level of sample ion internal energy by choice of reagent gas.

In general charge transfer offers no practical advantage over EI for molecular weight determination because the residual internal energies tend to be sufficient to cause comparable fragmentation.

(b) Proton Transfer

This is the most popular form of CI used at present. Basically it involves the transfer of a proton from a protonated reagent ion (AH^+) to a sample molecule (M) to form the protonated molecular ion (MH^+).

$$AH^+ + M \longrightarrow MH^+ + A \qquad (12)$$

AH^+ is formed in high concentrations at high reagent gas pressures. For example, in methane at a source pressure of 1 Torr 90% of the total ion current consists of CH_5^+ and $C_2H_5^+$ ions.

The exothermicity of reaction (12) determines the internal energy deposited within the protonated sample molecular ion. Therefore, the degree of fragmentation can be influenced by judicious choice of the reagent gas. A second factor that improves the molecular ion region with proton transfer CI as compared to EI, is the inherent stability of the protonated molecular ions. Such ions are even electron, and so do not readily undergo simple cleavage decompositions to form radicals as is commonly seen with EI.

From table 1.1 it can be seen that methane is a relatively harsh CI reagent gas, whereas use of isobutane will cause less fragmentation, with ammonia being the "softest" popular CI reagent gas.

Reagent Gas	Reagent Ion	Proton Affinity (KJ mol^{-1})
Ammonia	NH_4^+	861.0
Isobutane	$C_4H_9^+$	826.9
Methane	CH_5^+	548.1

Table 1.1 - Proton affinities for some common reagent gases.

(c) Hydride Ion Transfer

This involves the abstraction of an hydride ion from a sample molecule (M) to a reagent ion (X^+).

$$X^+ + M \longrightarrow XH + M\text{-}H^+ \qquad (13)$$

This reaction is possible whenever the hydride ion affinity of X^+ is greater than that of M-H. Hydride ion transfer has found little practical use.

(d) Reagent Ion Capture

If the proton affinity of the reagent ion is greater than that of the sample proton transfer becomes slow. In which case other reactions, such as condensation, may become important. The products of ion-molecule condensation reactions are often seen when ammonia is used as reagent gas. Both proton transfer and association reactions may occur. This can be useful for determination of the relative molecular weight of a sample.

(e) Negative Ion Chemical Ionisation

This can take the form of; (i) Reagent ion reaction, (ii) Proton abstraction, (iii) Resonant electron capture.

(i) Reagent ion reactions with sample molecules are often observed if oxygen is present. The reactive species is $O^{-\cdot}$. A typical reaction of $O^{-\cdot}$ is the alkyl

displacement from carbonyl groups[26].

$$R_2CO + O^{-\cdot} \longrightarrow RCO_2^- + R^{\cdot} \qquad (14)$$

(ii) Proton abstraction CI is possible when a strong Bronstead base (B) is present in the source.

$$B^- + M \longrightarrow BH + M\text{-}H^- \qquad (15)$$

The exothermicity of this reaction is decided by the difference in proton affinities of the acid, and the sample. Since most of the excess energy resides in the newly formed bond (BH), the sample deprotonated molecular anion tends to have a low internal energy. Consequently spectra typically show intense deprotonated molecular anion peaks and little fragmentation. $CH_3CO^{-\cdot}$ is sometimes used as a reagent ion by use of methyl nitrite reagent gas (proton affinity 1593 $KJmol^{-1}$)[27].

(iii) Resonant electron capture is not strictly CI. It involves the adhearence of an electron to a sample molecule

$$M + e \longrightarrow M^* \qquad (16)$$

Under normal CI conditions (70 eV electrons) the kinetic energy of the electrons is too high to allow for

sufficient molecule electron interaction to result in a stable anion. This problem is overcome by using a CI gas as an electron moderator so producing the near thermal energy electrons (approximately 0 ev) required. Resonance capture may now take place, providing the sample molecule has a sufficiently high electron affinity to allow the anion to have a sufficiently long lifetime to be stabilized by collision.

Electron capture reactions (15) tend to have very fast reaction rates(400 times the diffusion limit for an ion molecule reaction). Hence in favourable cases, improvements in sensitivity of several orders of magnitude can be obtained over EI or positive ion CI. Typical electron capture spectra show intense radical molecular anion peaks, with little fragmentation.

An unfortunate problem with this method of ionisation is the dependence of the results on experimental conditions (source pressure, temperature etc). Marked differences in results are often observed from day to day, and from lab to lab.

1.2.2. Desorption Techniques

All vapour phase ionisation techniques suffer from one serious drawback; the need to volatilise the sample prior to ionisation. Therefore it is necessary for the analyte to be thermally stable, or to be derivatised before mass spectral analysis can be performed. The exception to this; pyrolysis mass spectrometry[28], involves the study of thermal degradation products.

Pyrolysis mass spectrometry has mainly been applied to the fingerprinting of polymers,and biological systems. This technique aside, the thermal stability of an analyte can constitute a serious problem, which excludes a significant number of potential systems from mass spectrometric study.

Extensive research has been expended on the development of new methods of ionisation with a view to overcoming the thermal stability problem.

This has led to the introduction of a wide range of desorption methods which have found to be useful for analysing thermally labile and ionic samples. The following sections discusses some of those techniques which have been used for or are referenced to, the work presented in this thesis. The only major desorption technique not mentioned is Plasma Desorption Mass Spectrometry (PDMS)[29].

1.2.2.1 Desorption Chemical Ionisation (DCI)[30,31]

A probe extension is used to place the sample directly into the ion volume. The sample is rapidly heated, normally in a CI environment.

Ionisation of the sample is thought to involve thermal desorption of ions which have been produced on the probe (surface ionisation), and/or evaporation of neutrals from the probe that are subsequently ionised via CI processes in the source.

Evaporation of intact ions and or neutrals occurs because rapid heating of sample allows the possibility of

thermal desorption. Say a certain sample undergoes thermal decomposition at a temperature T, and thermal desorption at a higher temperature T′. If then the sample can be heated sufficiently quickly through T to T′ before the sample thermally degrades, then thermal desorption of the intact species may occur. This phenomenon is central to a number of desorption methods.

Even though DCI enables molecular weight information to be accessible for thermally labile systems, via the presence of a protonated molecular ion peak. It is of limited use because the heating of the sample up to T′ can not be performed rapidly enough to prevent some thermal decomposition occuring, and products from this process typically dominate the spectra. A second problem is the transience of the ion beam formed, the sample being lost off of the probe tip very quickly. This problem disables the performance of experiments requiring an ion beam of reasonable longevity.

1.2.2.2 Laser Desorption

A pulsed infra-red laser is used to induce rapid heating of a solid sample. Heating to T′ is much more efficient than with DCI, so no thermal degradation products are observed. Intense protonated molecular ions with little fragmentation are the norm.

Major problems associated with this instrumentation are the high cost of the laser, and the transience of the ion beam. The consequence of the later

is that laser desorption can only be applied with either a TOF, or Fourier Transform (FT) ICR analyzer.

1.2.2.3 Field Desorption[33]

Field desorption (FD) was developed from field ionisation. Fig 1.2 shows a schematic diagram of a FD source.

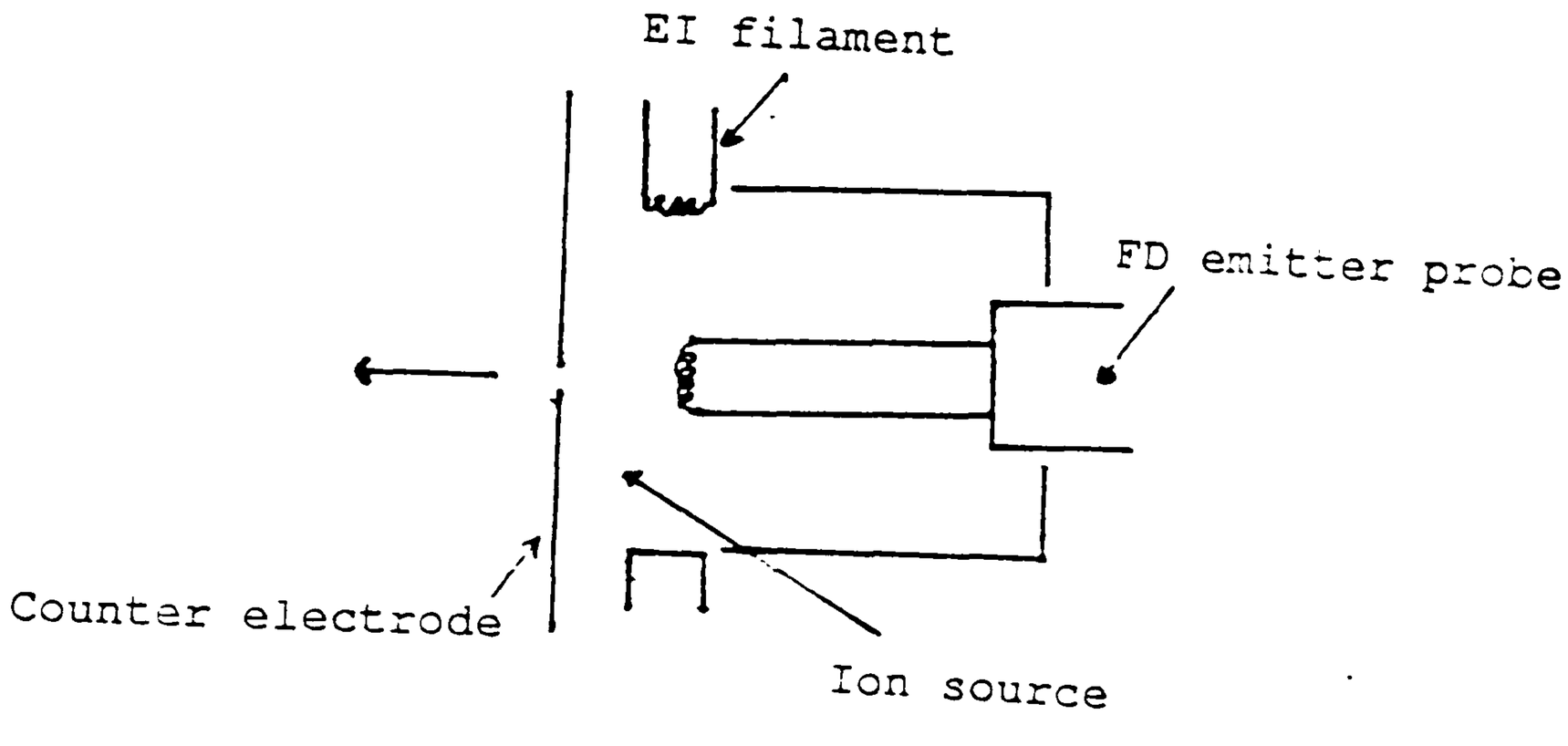

Fig. 1.2. FD ion source

The sample is deposited on an emitter, which is normally a fine "comb-like" anode. A high potential difference is applied between the anode and cathode, so generating very high electric fields at the emitter tips (typically 10^8 - 10^{10} Vm^{-1}). These high fields aided by heating of the emitter results in ionisation of the sample. A detailed understanding of the ionisation mechanism(s) involved with FD is still not available.

It is thought that heating of the emitter has two effects: (a) causes thermal ionisation. (b) allows rapid movement of sample to the emitter tips. High electric

fields at the emitter tips induce electron tunnelling from sample molecules to the anode to form radical cations. Protonated or cation adduct molecular ions are formed by the field extraction of surface sample molecules whilst solvating a proton or metal ion. With ionic materials the purpose of the field is to extract the preformed ions from the condensed phase. These processes leave the resultant ions with very little internal energy, and with the ion's short source residence time (10^{-9}-10^{-11}s) result in spectra displaying little fragmentation. Therefore, this technique relies heavily on field induced ionisation.

Major problems with FD are: (a) Poor reproducibility. Results are strongly dependent upon experimental conditions. (b) Transient ion beams of low abundance. (c) Difficulties in operation. It is a highly skilled job to produce good emitters.

1.2.4. Fast Atom Bombardment

Although neutral beam SIMS (secondary ion mass spectrometry) was developed some time ago[34], the use of neutral beam bombardment did not become widespread until Barber et al[35] introduced the role of a liquid matrix in 1981. The major disadvantage with solid SIMS is the short lived nature of the resulting ion beam due to the quick sputtering off of sample from the target surface. Use of a liquid matrix allows the surface under bombardment to be continuously refreshed by diffusion of molecules from the bulk. This has resulted in long lived (sometimes for

hours), strong (comparable to EI 10^{-11} - 10^{-10} $C\mu g^{-1}$)[36] ion currents, so enabling tandem mass spectrometry and high mass resolution experiments to be performed.

Fig. 1.3 shows the arrangement of a typical Fast Atom Bombardment (FAB) experiment

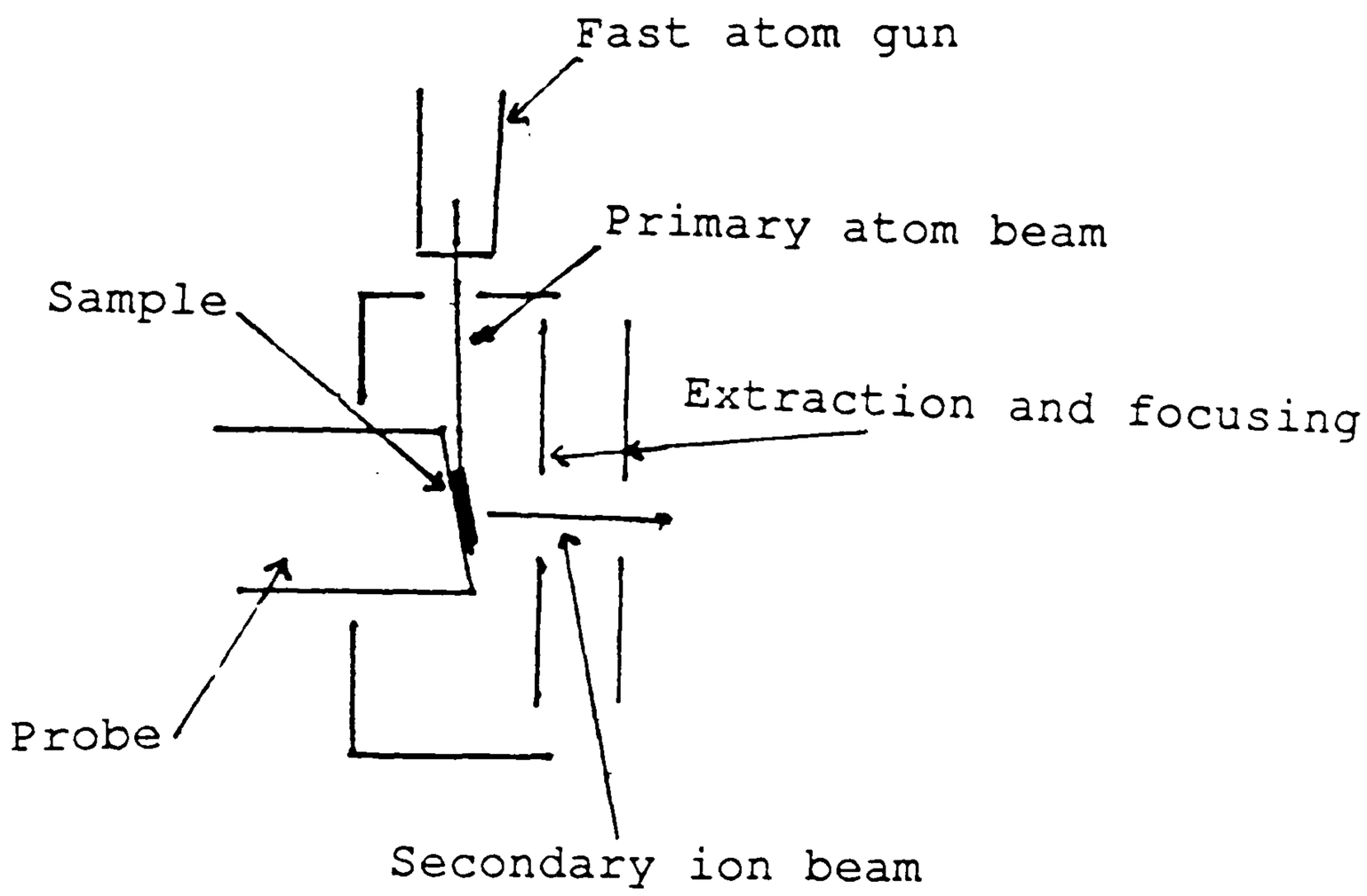

Fig. 1.3. - FAB experimental arrangement

The general procedure involves the desolving of the sample in a polar, viscous matrix of suitable type[37]. A few microliters of this solution are placed in the path of a high energy neutral atom beam (charge exchanged ions which have been accelerated across a 4-8 KV potential) and floated at source potential. Normally Xenon is used

as the bombarding medium, its popularity is due to its inertness, high mass and reasonable cost.

Generally FAB is thought of as a soft ionisation technique. Ionic materials dissociate in solution, and strong ion signals are observed which are characteristic of the ions formed in solution. Polar, non-ionic materials normally form protonated (or deprotonated for negative ion FAB) pseudo-molecular ions. Adduct or cluster ions are also a common feature. Occasionally radical cations[38,39] are observed for non-polar, or low redox potential compounds.

The processes of ion formation occuring under FAB conditions are still open to debate, but a number of reasonable mechanisms have been proposed. It is thought that, in general, the bombarding atom beam does not play a role in the actual formation of ions. The major purpose of the atom beam is to sputter off particles from the liquid surface, be they ions, neutrals, or conglomerates of both. This is thought to occur via momentum transfer from the bombarding atoms to the liquid molecules, which results in the formation of a collision cascade[40]. It now becomes possible for surface particles to obtain sufficient kinetic energy to be ejected from the liquid into the gas phase.

Ion formation for a particular sample when subjected to FAB is thought to involve one or more of the following processes.

(a) Preformation of ions in solution. There is no doubt that this explains the origin of ions from ionic

materials. Ionic compounds readily dissociate in the polar matrix, and hence display spectra characteristic of the separated ions.

The application of the "preformed ion" theory is more controversial with non-ionic analytes. In these cases it is thought that protonated molecular ions are formed through proton transfer from an acidic matrix molecule. Experimental evidence arises from the occurrence of multiple protonated ions with some peptides. The relative abundance of these ions are pH dependent[41]. Further evidence comes from pKa[42], and enzyme kinetic[43] measurements obtained by FAB experiments which correspond favourably with values generated by solution techniques, and from occurrence of MH^+ of prophyrin in acidic solution correlated with visible spectroscopy[43].

FAB spectra often show cluster and adduct ions (especially when salt solutions are added). This is thought to occur via the desorption of particle containing a sample molecule (M), cation (C^+), and matrix (A) molecules. Desolvation of this particle occurs to leave the ion (MC^+)

$$MCA^+_n \longrightarrow MC^+ + nA \qquad (17)$$

The relative abundances of MC^+ to AC^+ has some dependence on the relative abilities of M and A to compete for C^+.[44]

(b) Ion-molecule reactions in CI type reactions just above the liquid surface (selvedge).

$$AH^+ + M \longrightarrow MH^+ + A \qquad (18)$$

Evidence for this comes from studies involving compounds of differing trends in gas phase and solution bascities. It was noted that the relative abundances of protonated molecular ions is dependent upon gas phase rather than solution basicities[45]. Also the relative abundances of matrix clusters can be predicted on the basis of gas phase basicities[46]. It can also be argued that adduct ion formation can occur in the selvedge[47].

(c) Collisional activation between the impinging beam and gas phase neutrals. This has been shown to occur with volatile samples[48], to give radical molecular ions.

(d) Electron transfer processes. Oxidation-reduction reactions have been observed[49]. These compounds normally have low redox potentials. The mechanism(s) are unknown, although it appears to involve the bombarding beam[48].

1.2.2.5. Thermospray

Development of interfaces between HPLC (high performance liquid chromatography) systems and mass spectrometry has been a major area of research over the last fifteen years or so. This task has two severe problems to overcome: (a) The high pressure difference between the HPLC and the mass spectrometer source.

HPLC

HPLC uses flow rates of around 2 ml min^{-1}, and the mass spectrometer source operates at 10^{-5} Torr. (b) Ionisation of the sample in the source.

These problems have been solved, and there are a number of successful systems in use. Each system has a number of advantages and disadvantages over one-another. One of the most common interfaces in use is thermospray[50], which offers the advantage of being an ionisation technique as well as a competent interface.

A typical thermospray system is shown in Fig 1.4.

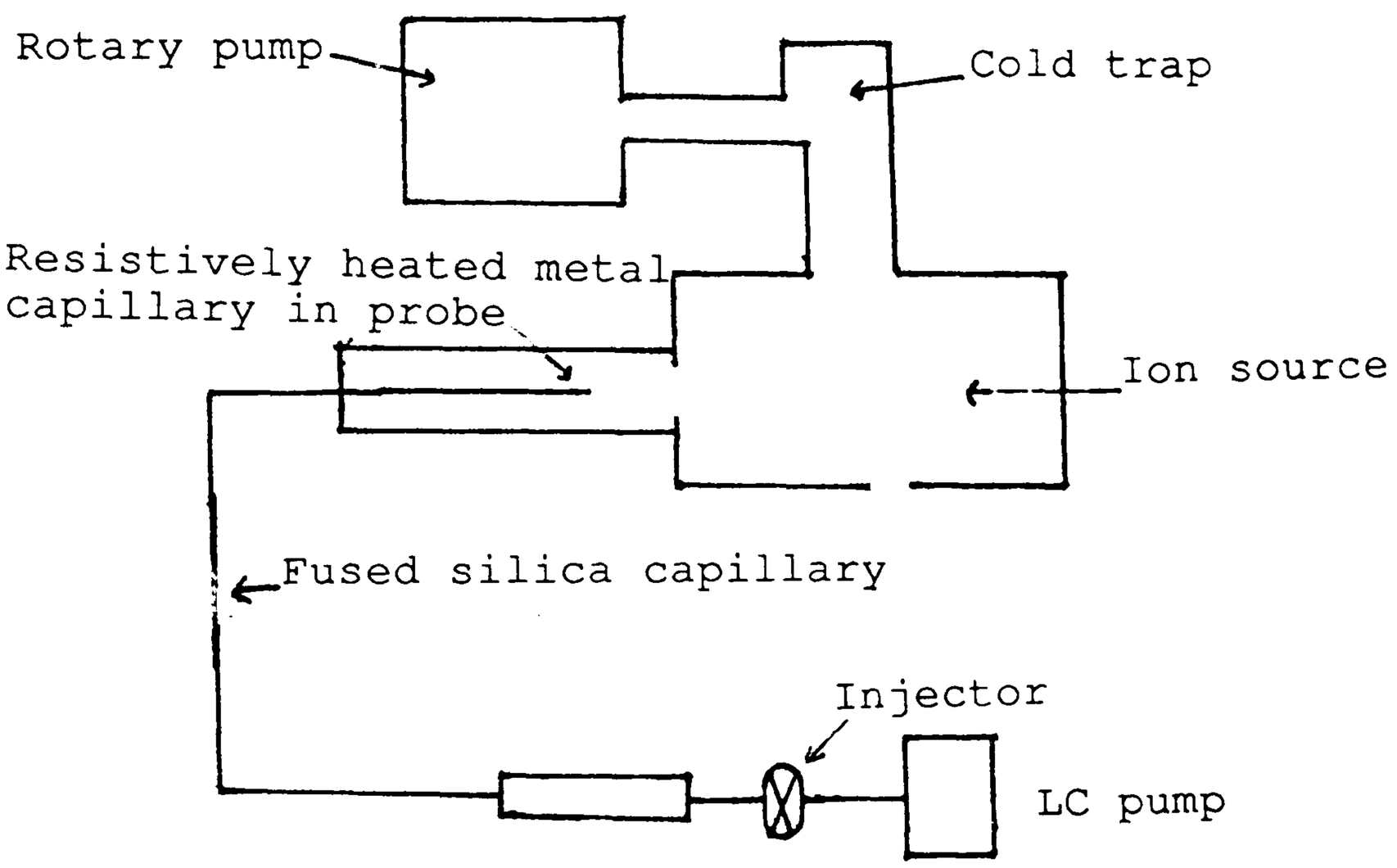

Fig. 1.4. - Thermospray experimental arrangement

The sample is introduced via an injection port into a normal HPLC system. Eluent from the HPLC column passes into a 25m capillary column, the end of which is

resistively heated. This heating converts the liquid into a superheated mist, which is then sprayed into the mass spectrometer. Most of the solvent has been vaporised and is pumped away by a mechanical pump attached to the source housing. The less volatile sample particles are retained in droplets, formed in the vaporised mist, which reach the source. Since most of the solvent is easily removed high flow rates (approximately 2 ml min^{-1}) can be utilized.

Ionic samples dissociate in solution, and spectra showing peaks responding to dissociated ions are obtained. Polar, non-ionic samples show intense protonated (or deprotonated in negative ions mode) molecular ion peaks. Cluster ions are also common.

Ionisation of non-ionic analytes is thought to occur via gas-phase ion-molecule reactions[51]. A strong electrolyte solution, normally 0.1 mol dm^{-3} ammonium acetate, is added to the flow before or after the HPLC column. The presence of a strong electrolyte ensures that mist droplets have overall positive or negative charges, so creating high electric fields. This facilitates the field evaporation of ions from the droplet. CI type ion-molecules reactions may occur between ammonium ions and sample molecules (M)

$$NH_4^+ + M \longrightarrow MH^+ + NH_3 \qquad (19)$$

It is possible to use a filament in the source for an alternative method of ionisation, this results in CI type spectra being observed. "Filament on" ionisation is normally used if the necessary concentration of electrolyte cannot be maintained (if non-polar HPLC solvents are required). Electrons from the filament interact with the solvent to produce reagent ions, which may then undergo ion-molecule reactions with sample molecules. The problem with using the filament is a lowering of sensitivity compared to thermospray.

1.3. Mixture Analysis

The most common method of mixture analysis involves the chromatographic separation of the components, until the utilization of some detection system. Chromatographic analysis has a number of problems associated with it: (a) The often involved work up of the sample. (b) Inability to provide structural information.

Mass spectrometry is a viable alternative, because although expensive, it offers sensitivity, versatility, speed of analysis, and a wealth of structural information. The major instrumental problem with mass spectrometric mixture analysis is the occurrence of spectral interferences. A molecular ion peak of one component may be obscured by the presence of a fragment ion peak of another component. There are number of ways around this problem, which are discussed below.

1.3.1. On-line Chromatographic Techniques

Use is made of a chromatographic system to separate each component in the mixture. Each separated component then travels into the ion source, either directly or via some interface, where it is ionised and analysed as normal. The major problem with interfacing gas (GC), liquid (LC) or super-critical fluid (SFC) chromatographic systems to a mass spectrometer, is the pressure difference between operational chromatography and mass spectrometry. This problem has now been solved, and GC/MS, LC/MS, and to some extent SFC/MS are well established.

The original chromatographic problem of having to work the sample up still applies.

1.3.2. Soft Ionisation

Methods of soft ionisation produce spectra consisting mainly of pseudo-molecular ion peaks, with little fragmentation. Therefore, the level of spectral interference is greatly reduced. The soft ionisation techniques used, or referred to, in this work have already been discussed.

1.3.3. High Resolution Mass Spectrometry

By international convention an atom of the main carbon isotope has a mass of exactly 12 amu. On this scale all other elemental masses are non exact (e.g. ^{1}H = 1.007825 amu, ^{16}O = 15.994914 amu, ^{14}N = 14.003074 amu). Therefore, although some ions with differing elemental

compositions may have the same nominal mass, they do not have equivalent exact masses. For example C_5H_{12} and C_4H_8O both have a nomimal mass of 72 amu but exact masses of 72.0930 and 72.0575 amu respectively, a difference of 0.0364 amu. A resolving power of 10,000 would be more than adequate to resolve between these two masses. Two masses are said to be resolved when the height of the valley between the two peaks is 10% or less than the height of the peaks. Changing the resolving power of a magnetic sector instrument is performed by varying the width of two sets of slits, one just after the source, the other just before the detector. Reduction of slit width increases the resolving power. The consequences of improving the resolving power are; a reduction in the incidence of spectral interferences due to the improvement in the mass specificity of the instrument, and a loss of ion current as the slits are closed down.

1.3.4. Tandem Mass Spectrometry[52]

Tandem mass spectrometry makes use of a mass spectrometer both as a component separator, and a mass analyser. The basis of these experiments is the observation of unimolecular decompositions in the field free regions. As already stated naturally occuring metastable transitions give rise to peaks of low intensity. To improve the sensitivity of these experiments it is necessary to increase the number of metastable decompositions by excitation of an optimum number of ions passing through the region. The most

common procedure is to use a collision gas[53], usually helium. Although lasers[54], surfaces[55], and electron filaments[56] have been used.

Two types of tandem instrumentation have been utilized in this work.

(a) Forward geometry double focusing magnetic sector instrument[57]. Fig. 1.1 shows the location of the three field free regions in this type of instrument. The third field free region is generally not used for studying metastable decompositions. It is possible to use the second field free region, but the mass resolution of the parent ion is poor. The preferred region for observing metastable decompositions is in between the source and ESA. To study these reactions it is necessary to scan both the electric and magnetic sectors simultaneously. The scan routine required depends upon the analysis to be performed. There are three possible analysis that all tandem configurations can perform.

(i) Daughter ion. All fragment ions resulting from a specific parent ion. To perform this analysis on a magnetic sector instrument the magnetic (B) and electric (E) sectors need to be scanned in such a manner that the ratio of the two remains constant

$$\frac{B}{E} = \text{constant} \qquad (20)$$

(ii) Parent ion. In this study all parent ions which give rise to a specified daughter ion are reported. In order

to perform this experiment on sector instruments of forward geometry it is necessary to scan the magnet and ESA such that equation (21) is obeyed.

$$\frac{B^2}{E} = \text{constant} \qquad (21)$$

(iii) Constant neutral loss. In this case the peaks observed are the result of the loss of a specified neutral molecule. For forward geometry magnetic sector instruments it is necessary to scan the magnetic and electric fields such that

$$\frac{(B/E)^2}{1-E'} = \text{constant} \qquad (22)$$

$$E' = \frac{E_2}{E_1} \qquad (23)$$

Where E_1 and E_2 are the electrostatic fields required to enable the parent and daughter ion to be transmitted.

Similar results may be obtained by repeatedly scanning the magnet and reducing the ESA voltage by a series of steps, this is termed metastable mapping[57]. Although this technique has the advantage of performing all three types of analysis in one experiment, it has the serious drawback of being time consuming requiring the acquisition of several hundred scans.

A major advantage of using forward geometry magnetic sector instruments, over the other tandem systems, is the relative ease of performance with existing double focusing machines. The main limitation is the severely reduced mass resolution obtained.

(b) The second tandem instrument type used in this work involves the coupling of quadrupoles to a magnetic sector instrument (hybrid). Two quadrupoles are generally used, the first an Rf only quadrupole is not used for mass analysis, but may be filled with a collision gas to enable collision induced decomposition experiments to be performed. The second quadrupole is used for mass analysis. It now becomes possible to study unimolecular decompositions at low kinetic energies, as opposed to high energy collisions in magnetic sector instruments. In a magnetic sector instrument the ions have high kinetic energies (due to the high accelerating source voltage) and variation of these energies is strictly limited according to sensitivity and mass range. No such limitations arise with the use of quadrupoles (except that the kinetic energies need to be lower), collision energies in the range of 10-500 eV can be employed. This allows variation of two parameters; (i) gas pressure (ii) collision energy, upon which the unimolecular decompositions observed in the quadrupole collision region show a heavy dependence. Generally the higher the collision energy and gas pressure, the greater the degree of decomposition[58]. The major disadvantage with hybrid

systems is that the mass range and mass resolution of the daughter ions is limited by the quadrupole analyzer.

Although not used in this work there are a number of other tandem systems in used which include; triple quadrupoles[59], multi sectors[60], FTICR[61], and ion traps[62]. All these types of instrumentation have their relative merits and demerits.

1.3.5. Quantitative Mixture Analysis[63]

Reliable quantitative results require the presence of an internal standard, which needs to be as similar to the analyte as possible. In order of preference: (a) Isotopically labelled analogue. (b) A close homologue. (c) An isomer. (d) Same chemical type. The level of analyte in a sample can be calculated by comparison of the signal intensity for the analyte to that obtained for the known concentrations of internal standard.

If a suitable internal standard is not available an external calibration may be used. Responses for differing, known concentrations of analyte are obtained, from which a calibration graph can be drawn. The unknown concentration of analyte can be determined by comparing the signal for the analyte with the calibration graph.

1.4. Ion Decomposition Pathways and Structure Elucidation

Of prime importance in qualitative mass spectrometry is the determination of how an ion fragments in order to deduce its structure. This can be normally be determined

by application of known rules, and/or intuition, to the mass spectra obtained.

It is often necessary to either confirm, or determine an unknown ion structure by instrumental means. A reasonable estimate of an ion's empirical formula can be made by comparison of the isotope peak ratios for postulated ion structures and those determined experimentally. A much more accurate method of empirical formula determination is high mass resolution. As previously described it is possible to determine the mass of an ion to a high degree of accuracy, and so establish the empirical formula of that ion. There are problems with this method; (a) Reduction in mass specificity as the mass of the ion increases, and consequently an increase in the number of empirical formulations. (b) Loss of ion signal as mass resolution increases.

A very powerful instrumental technique for elucidating ion decomposition pathways and ion structures is by the use of tandem mass spectrometry. It is possible to "select" an ion of interest with the "first" mass spectrometer, induce decomposition and examine the daughter ion spectra. Even without tandem instrumentation, useful information can often be gleaned by investigation of the metastable peaks within the normal mass spectrum obtained on a UV recorder.

Chapter II

ANALYSIS OF ANIONIC AND NON-IONIC SURFACTANT MIXTURES BY FAST ATOM BOMBARDMENT MASS SPECTROMETRY (FABMS)

2.1. Introduction

This work involves the analysis of commercial anionic and non-ionic surfactant (surface-active agent) mixtures by Fast Atom Bombardment Mass Spectrometry (FABMS).

2.1.1. Detergents[64]

Water is by far the most common cleaning solvent in use despite two serious drawbacks: (a) Water is highly polar making it inefficient for solubilising non-polar substances. (b) Water has a high surface tension (0.07275 Nm^{-1} at 291 K)[65], therefore it has poor wetting and fibre penetration properties. These problems can be overcome by the addition of a detergent. A Detergent may be defined as a combination of surfactants with other substances, formulated to enhance the cleaning performance of the surfactants alone. A wide variety of detergents are available whose composition depend upon their particular applications.

2.1.2. Surfactants[66,67]

Surfactants are the major cleaning agents present in detergents. They have the following general characteristics.

(a) Amphipatic structure. Surfactant molecules contain two moieties with differing solubility tendencies, ie, separate hydrophilic (water loving) and hydrophobic (water hating) parts.

(b) Surfactant molecules form orientated monolayers at the liquid surface.

(c) At equilibrium the surface concentration of a surfactant is greater than within the bulk solution.

(d) Micelle formation. The critical micelle concentration (CMC) is the concentration of surfactant which provides a monolayer covering the whole surface. Addition of more surfactant will cause the formation of micelles. A micelle is a cluster of surfactant molecules in which the solvent soluble moiety is on the outside and the solvent phobic moiety points inside. Such a particle is soluble in the solvent because of the solvent-phillic micelle face.

Surfactant addition to water markedly improves its cleaning ability due to the following two effects:

(a) Reduction of surface tension. Surface tension arises from strong attractive forces between water molecules. The attractive forces between surfactant molecules at the surface is much lower than those between the water molecules, thus surfactant addition lowers surface tension.

(b) Solubilisation of non-polar substances. The hydrophobic moieties of the surfactant molecules are soluble in non-polar substances. This results in a covering of the surface of the substance surface with hydrophilic "heads", thus enabling the substance to be removed into the water. Once in solution the surfactant molecules remain in place, preventing redeposition of the substance upon the cleaned surface.

Commercial surfactants are manufactured as complex mixtures. The physical and chemical properties of which are dependent upon the surfactant composition. Also there tends to be significant amounts of impurities present; raw materials, fatty acids, alcohols, and hydrocarbon precursors.

Surfactants are normally classified according to the charge they carry in solution

(a) Anionic surfactants. These constitute the largest group of surfactants, generally comprising about 80% of world-wide production. Their ability to ionise in solution gives them good dispersing properties, and enables dirt particles to be held in solution.

A wide range of anionic surfactants are currently in use, but the work presented in this thesis was obtained using one type of surfactant - alcohol ether sulphates.

These chemicals have the general formula

$$RO(CH_2CH_2O)_nSO_3^-M^+ \qquad (1)$$

where the counter ion (M^+) is usually sodium or, less commonly potassium or ammonium. R is an alkyl group, which imparts the hydrophobic properties upon the molecule. The size of R can vary from C_9H_{19} to $C_{20}H_{41}$, although the range $C_{10}H_{21}$ to $C_{15}H_{31}$ are generally preferred.

The hydrophilic properties of the molecule arise from the presence of the $(-OCH_2CH_2O-)_nSO_3$ moiety. Hydrophilicity of the molecule increases with the ethoxy chain length. Values for n can range from 0 - 20.

A typical mixture suitable for detergent use would comprise of a number of homologous series, each series differs by the alkyl chain length, and within the series by the number of ethoxylate units.

(b) Non-ionic surfactants

As is the case with anionic surfactants, a wide range of non-ionic surfactants are in use, and they are manufactured as complex mixtures. The class of non-ionic surfactant studied in this work was the alcohol ethoxylates.

$$RO(CH_2CH_2O)_nOH \qquad (2)$$

These surfactants are particularly good at removing greasy oils, and are generally used in detergent formulations together with an excess of anionic surfactants.

(c) Cationic surfactants. The cationic surfactants used in this work have the general formula

$$(R_4R_3R_2R_1)N^+ \quad X^- \qquad (3)$$

where R_1 - R_4 are typically, but not always alkyl groups and X^- is usually chloride. They are manufactured as mixtures which tend to contain less components than in anionic or non-ionic surfactant mixtures. This category of surfactant is discussed in greater detail in chapter three.

(d) Amphoteric surfactants. These are not involved in this work. Amphoteric surfactants are zwitterionic.

2.1.3. Surfactant Analysis[73]

The analysis of surfactant mixtures is important for quality control because:

(a) Surfactant properties are dependent upon their composition

(b) Presence of some impurities cause toxicology problems

A number of analytical techniques, mainly volumetric[68], chromatographic[69,70], spectrophotometric[71], and potentiometric[72], have been applied to surfactant analysis. The use of mass spectrometry has been severely limited by the involatility of these chemicals, so making them difficult to analyze by classical ionisation techniques, although GC/MS has been used to analyse some non-ionic[74]. Some success has been achieved by the application of desorption ionisation methods. Good qualitative data was obtained with FD[75,76], laser desorption[77,78], DCI[79,80] and FAB in conjunction with tandem mass spectrometry[81,82]. No attempt has been made to make any quantitative statements, or to analyze directly untreated commercial mixtures by FABMS. The basic aim of this work was to try and establish an analytical protocol using FABMS for anionic and non-ionic surfactants which involved as little pre-treatment as possible.

2.1.4. Mixture Analysis by FABMS

FAB offers three major advantages for analysing surfactants:

(a) Speed and ease of operation, so enabling a high turnover of samples.

(b) FAB is a soft ionisation technique. As described earlier soft ionisation produce simple spectra, so keeping the level of spectral interferences to a minimum.

(c) FAB tends to show a certain degree of selectivity. Peaks which have arisen from ionic species dominate the spectra.

There is one significant problem associated with FAB ionisation for mixture analysis. It is well established that FAB is a surface sampling technique[83,84]. Spectra obtained by FAB are mainly representative of the liquid surface composition, with only a minor contribution from the bulk solution. Any differences in surface activity of the various components leads to an enhancement or suppression of individual components at the surface and therefore in the FAB spectra, so that the relative bulk concentrations of components are difficult to determine. This problem was first highlighted when attempting to analyse mixture of peptides[85]. Relative molar responses of peptides in mixtures have been correlated with their hydrophobicities at water/air surfaces[86].

A number of methods have been tried, with some success, to overcome the problem of differential desorption efficiencies:

(a) Derivatisation. Making all the components more hydrophobic has been found to reduce surface activity differentials[86].

(b) Addition of a counter surfactant of opposite[87], or the same sign[88]. This is discussed in some detail later in this chapter.

(c) Calibration curves, or response factors can be calculated if standards are available over the concentration range of interest[89].

2.2. Experimental

The positive ion FAB results were obtained using an MS50 mass spectrometer, whereas negative ion FAB were run on an MS80 (Kratos Analytical). Both of these are forward geometry instruments as described earlier. A scan speed of 10 secdec^{-1}, and mass resolution of 1000 were used. The MS50 was operated with a source potential of +6 KV (mass range up to 1300 amu), and MS80 at -2 KV (up to 1200 amu). A S120 Eclipse computer (Data General) with a DS55 data system (Kratos Analytical) was used for data acquisition and processing. Both instruments were fitted with a fast atom gun (Ion Tech) which was operated at a potential between 6 and 8 KV and a gun current of 1 mA. Both Argon and Xenon (British Oxygen Company) were used as bombarding gases.

Unless otherwise stated, the general experimental procedure was as follows; the surfactant mixture (Imperial Chemical Industries) was dissolved in 50 microl of triethanolamine (Aldrich). A few microliters of sample was placed on the probe tip and into the ion source to come under bombardment at the beginning of the second scan. Twelve scans in total were acquired. The data presented here are an average of scans four to eight.

2.3. Anionic Surfactant Results

Although these mixtures contain other substances in addition to the surfactants, the major peaks in the FAB spectra can be assigned to either surfactant components, or to ions formed from the matrix.

Table 2.1. shows the alcohol ether sulphate mixtures studied in this work.

Reference	R	Average n
C_{12}/C_{14} 2EO	$C_{12}H_{25}/C_{14}H_{29}$	2
C_{12}/C_{14} 3EO	$C_{12}H_{25}/C_{14}H_{29}$	3
C_{13}/C_{15} 2EO	$C_{13}H_{27}/C_{15}H_{31}$	2
C_{13}/C_{15} 3EO	$C_{13}H_{27}/C_{15}H_{31}$	3
C_{10} 4EO	$C_{10}H_{21}$	4

Table 2.1 - Standard alcohol ether sulphates.

Where reference is the terminology used throughout this work for that particular sample. R and M refer to general formula (1) described earlier. The alkyl group series are in a 3:1 ratio.

The average n value, or degree of ethoxylation (E) is an important commercial parameter. It is possible to calculate an experimental value for E using the relative

peak intensities (i) of each component, and the following expression:

$$E = \bar{m} - 1 \qquad (24)$$

$$\bar{m} = \sum_{k=1}^{n} i_k(k+1) \Big/ \sum_{k=1}^{n} i_k \qquad (25)$$

for a mixture with n components.

2.3.1. Negative Ion FAB

Fig 2.1. shows a typical negative ion FAB spectrum for C_{12}/ C_{14} 2EO.

As may be expected, the anionic surfactant component peaks completely dominate the spectrum, with the matrix ions completely suppressed.

Two series of ions of general formula (4), differing by 44 amu were observed

$$RO(CH_2CH_2O)_nSO_3^- \qquad (4)$$

The major series (R = $C_{12}H_{25}$) show ions at m/z 265, 309, 353, 397, 441, 485, 529, 553, 597 and 641 (ie up to n = 9). The minor series differ from the major by 28 amu (R = $C_{14}H_{29}$) and show ions at m/z 293, 337, 381, 425, 459, 513, 557, 601 and 645 (ie up to n = 8).

No evidence of any fragment ions was observed.

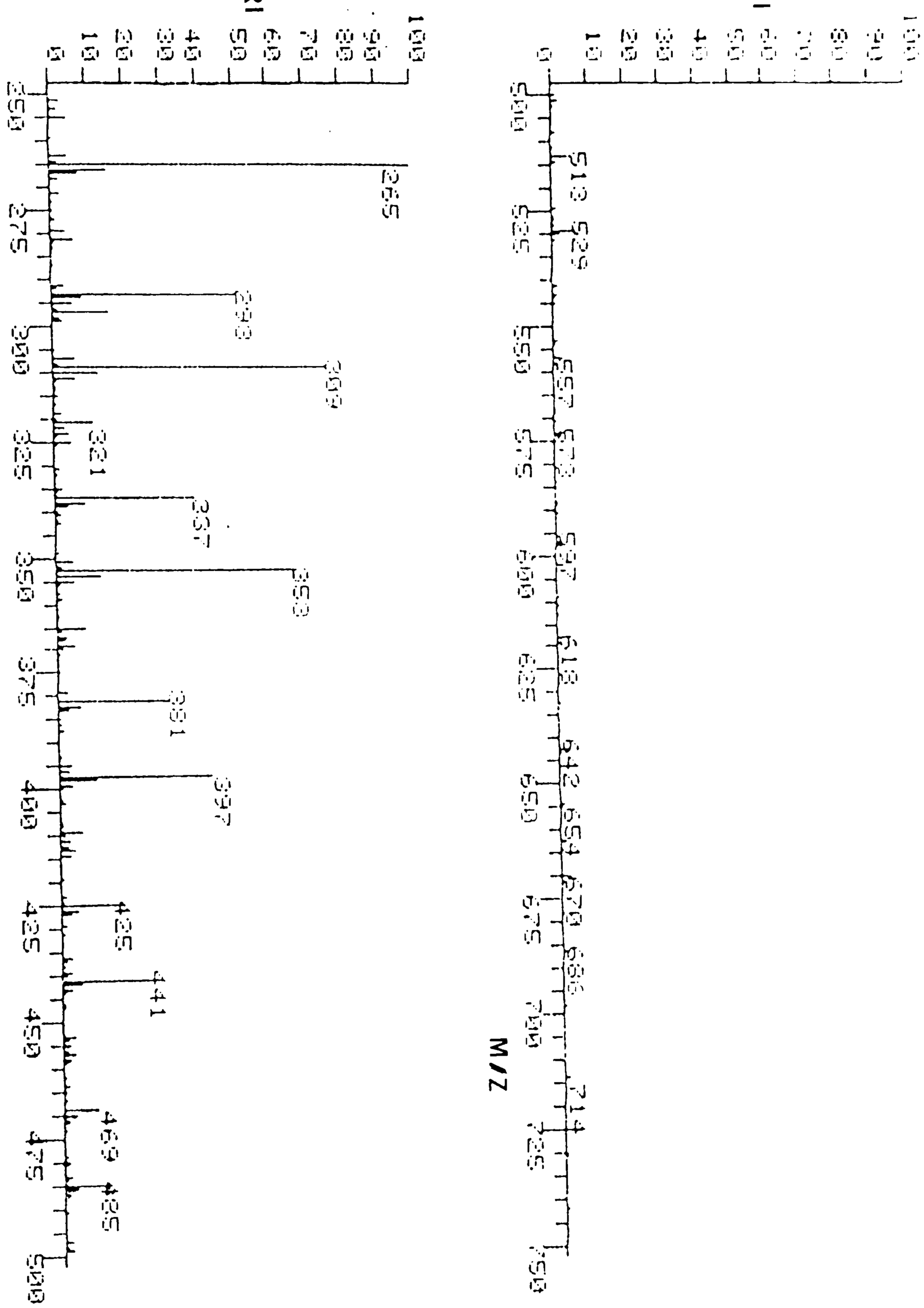

Fig. 2.1. Negative ion FAB spectrum for C13/C15 2EO.

Table 2.2. reports the relative peak intensities (as a percentage of base peak) for each separate ethoxy component within the major alkyl series. Also shown is the experimentally calculated E, which in each case, except for the C_{10}4E0 mixture, was too low. Another point of interest from these results was that the relative intensities of the n = 0 - 5 species were dependent upon the size of the major alkyl series.

n	C_{12}2EO	C_{12}3EO	C_{13}3EO	C_{13}2EO	C_{10}4EO
0	100	99	100	100	49
1	85	91	70	57	67
2	69	83	68	40	95
3	41	64	52	24	100
4	23	42	35	17	89
5	12	28	24	12	72
6	7	18	17	7	55
7	4	12	12	3	40
8	2	6	8	2	30
9	1	4	5	1	20
10	-	2	3	-	14
11	-	2	2	-	9
$\bar{n}$	1.7	2.4	2.4	1.4	4

Table 2.2 - Relative peak intensities for ethoxy components in major homologous series.

Since FAB is mainly a surface sampling technique, the spectra produced from these mixtures gave an "n" distribution which was representative of the surface concentration of the components in the matrix. The surface concentration of each component is dependent upon that component's relative surface activity, and its actual sample concentration. As the ethoxy chain confers polar solubility upon the molecule, the shorter the ethoxy chain the greater that components' relative surface activity.

Relative differences in the component surface activities appear to be dependent upon the size of the hydrophobic moiety as spectral dominance of the lower molecular weight components appears to be greater the longer the alkyl chain. At shorter alkyl chain lengths (eg $C_{10}H_{21}$) the differences are negligible, and so a true picture of the relative concentrations of the components was observed. The problem with this statement is that both major and minor homologous series showed the same "n" distribution.

Comparison of the relative peak intensities of components of both the major and minor series leads to experimental values for the ratios of the two series. Both the 2E0 mixtures gave a ratio of 1.7, and the 3E0 mixtures a ratio of 1.5. These numbers indicate that the minor series is enhanced with respect to the major, and again this discrimination appears to be heightened by chain length. Surface chemistry again provides an explanation. The larger hydrophobe confers a greater degree of surface activity upon the molecule, and so its surface concentration is enhanced with respect to the smaller hydrophobe component.

Different matrices were tried to determine whether a change in matrix conditions would have any effect on the distributions. Theoretically a less polar matrix should enhance the higher molecular weight "n" components with respect to the lower. Obviously the range of matrices to choose from was limited, it must be sufficiently viscous, and have a large enough dielectric constant to enable

dissociation of the surfactant salts. No significant change was observed with matrix. Matrices used were glycerol, triethanolamine, thioglycerol and polyethylene glycols.

2.3.2. Positive Ion FAB

The general formula of the pseudo-molecular ions observed in the positive ion made is shown below.

$$[RO(CH_2CH_2O)_nSO_3Na_2]^+ \qquad (5)$$

Fig 2.2. displays a typical positive ion FAB spectrum for the C_{12}/C_{14} 2EO mixture.

Sample ion currents were not as strong as those observed in the negative ion mode. Matrix peaks dominated the spectrum. Normally an addition of approximately 10 µl of a saturated sodium chloride solution was required to increase the sample ion peaks to a sufficient intensity to enable reliable results to be obtained.

Again the spectra show ions corresponding to the two homologous series. The major series ions range from m/z 311 to 795, and the minor series at 28 amu higher at m/z 339 to 823.

Table 2.3. shows the relative peaks intensities (normalized to the main surfactant component peak) of the major alkyl homologous series for the mixture studied, along with average degrees of ethoxylation, and ratios of major to minor homologous series.

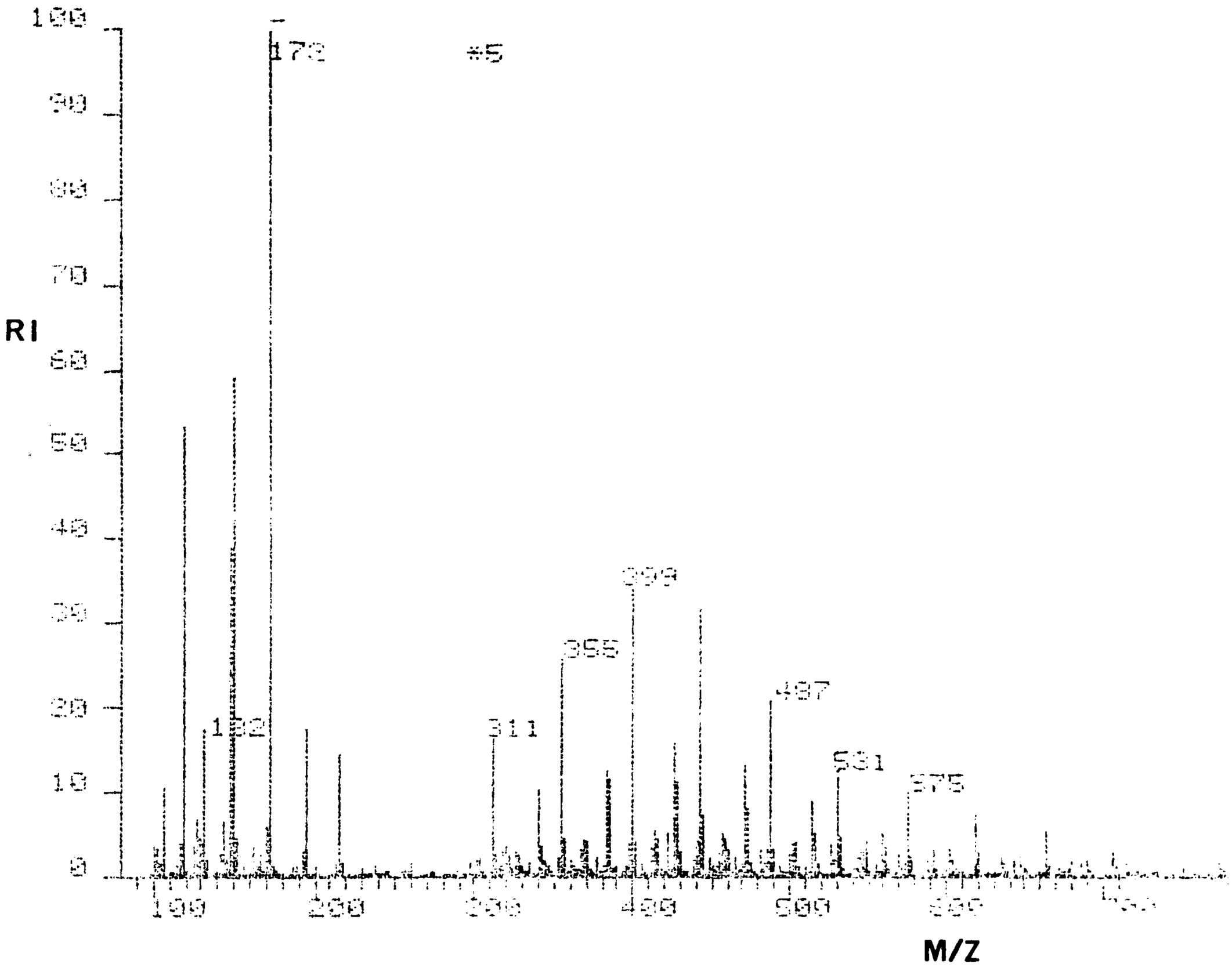

Fig. 2.2. Positive ion FAB spectrum for C13/C15 2EO.

n	C_{12}2EO	C_{12}3EO	C_{13}3EO	C_{13}2EO	C_{10}4EO
0	55	30	45	63	32
1	75	64	49	69	44
2	100	89	96	100	83
3	81	100	99	90	100
4	48	82	75	52	84
5	28	68	59	31	65
6	21	62	52	23	67
7	15	50	45	20	51
8	9	39	32	11	34
9	8	27	23	8	22
10	4	21	15	4	15
11	3	14	8	3	11
12	-	6	5	-	6
$\bar{n}$	2.9	4.4	4.3	3	4.5

Table 2.3 - Relative positive ion peak intensities for ethoxy componentes of major homologous series.

This table indicates that positive ion FAB yields completely different "n" distributions to those obtained when negative ion detection was employed. The enhancement of major to minor alkyl series was still observed, indicating that surface chemistry played an important role in the ion distributions. The strong similarity between the major and minor series ratios for both positive and negative ion results, and the large differences in the "n" distributions, indicate that

differences in ion formation efficiencies (ethoxy chain length dependent) is an important factor in providing the positive ion distribution.

The lower molecular weight components (ie n = 0,1,2, and 3) appear to have relatively low ion formation efficiencies, although it does increase with length of the ethoxy chain.

Above n = 4 however, the relative peak intensities were dependent upon the relative concentration of the components. Differences in ion formation efficiencies are difficult to rationalise, although it may be postulated that the ethoxy chain is instrumental in binding of the second counter ion. For example if n = 3

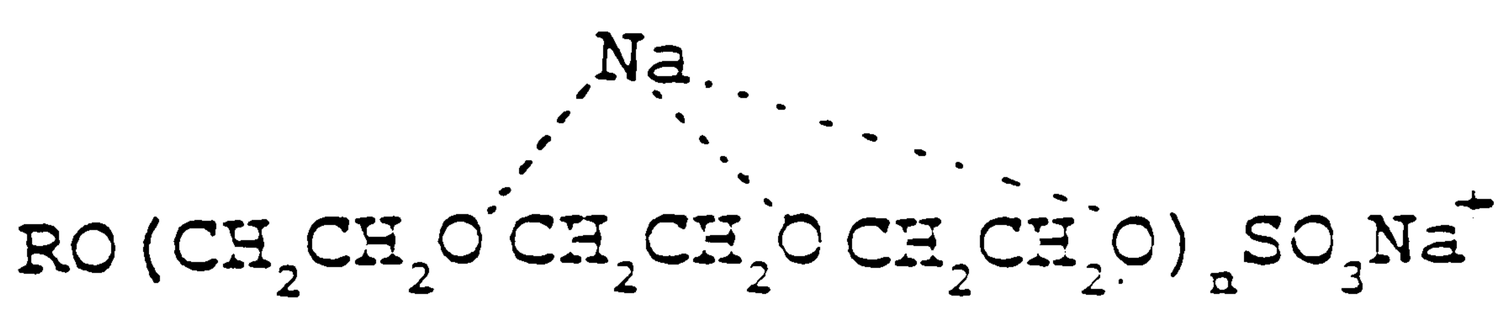

(6)

The problem with this theory is that no dependence of "n" distribution upon counter ion size was observed. Similar distributions arose when sodium was replaced by different singly charged ions (NH_4^+, K^+, Li^+, H^+). Doubly charged counter ions (magnesium or calcium) gave spectra which did not contain surfactant related peaks.

2.3.3. Counter Surfactant Addition

Obviously neither positive or negative ion FAB is suitable for quantitative analysis of these systems.

As mentioned earlier there are a number of methods used for overcoming the problem of differences in components' relative surface activity. Derivatisation is not really applicable. Calibration curves or molar response factors could not be derived because of the non-availability of pure components of the surfactant mixtures. That leaves the addition of a counter surfactant. Dorn and Ligon first suggested this technique in 1983. They added a negative counter surfactant (sodium stearate) to a mixture of cationic surfactants (acylcarnitines) and found that the molar responses of the mixture components reflected bulk concentration after addition of sodium stearate. They postulated that excess amounts of oppositely charged (to the ions detected) counter surfactant leads to domination of the surface by the counter surfactant. Hence, a FAB "transparent" layer is formed under the matrix surface. Therefore, the surface contribution for the total FAB spectra is reduced and a they become more representative of the bulk concentration.

The anionic nature of these mixtures implied the use of positive counter surfactant, and operation of the mass spectrometer under negative ion conditions. A negative counter surfactant (sodium stearate) was tried, using positive ion detection, but no change in ion distribution occurred.

A series of cationic surfactants was added to the samples ranging from pure compounds to complex commercial surfactant mixtures, in an attempt to improve the molar responses of the anionic surfactant mixtures under study.

(a) Tetramethyl - Octyl Ammonium Salts

These compounds had a purity greater than 98%. Addition of these counter surfactants had no effect upon the negative ion distribution of any of the anionic surfactant mixtures studied.

(b) Synprolam 35TMQC

Synprolam 35TMQC is a commercial cationic surfactant mixture of general formula

$$RN^{+}(CH_3)_3Cl^{-} \qquad (7)$$

Where R is a $C_{13}H_{27}$ or $C_{15}H_{31}$ alkyl group, in a 3:1 ratio. Addition of this counter surfactant did not effect either of the C_{13}/C_{15} 2EO or C_{13}/C_{15} 3EO mixtures, It did, however, have a dramatic effect upon the other mixtures. On addition of a counter surfactant a gradual change in the "n" distribution was observed until a limiting set of values was achieved. Table 2.4. shows the final "n" distributions for the major alkyl homologous series of each mixture.

The relative intensities for the n = 5 - 9 components remained largely unchanged for the two C_{12}/C_{14} mixtures. A dramatic change occurred for the n = 0 - 3 components, with only a small increase in the relative intensity of

the n = 4 species. Overall the ion current fell, reflecting the surface dominance of the "invisible" cationic surfactant.

Addition to the C_{104EO} mixture resulted in an increase in the relative intensities of the n = 0 - 3 species, with a reduction for the n = 4 - 12 components.

	SYNPROLAM 35TMQC			KENAMINE
n	$C_{12}{}^{2EO}$	$C_{12}{}^{3EO}$	$C_{10}{}^{4EO}$	$C_{10}{}^{4EO}$
0	64	68	91	75
1	94	87	93	62
2	100	100	100	79
3	59	74	88	100
4	29	47	64	97
5	15	26	44	81
6	7	16	28	61
7	3	8	17	44
8	1	5	10	30
9	1	3	6	21
10	-	2	5	20
11	-	-	2	12
12	-	-	1	7
$\bar{n}$	2	2.5	2.8	4.2

Table 2.4 - Relative peak intensities after addition of synprolam 35TMQC or kenamine.

(c) Kenamine

Kenamine is a three component industrial cationic surfactant mixture, of the same general as synprolam

35TMQC (7). In this case R is a mixture of $C_{18}H_{37}$, $C_{20}H_{41}$, and $C_{22}H_{45}$ alkyl groups.

Kenamine addition only affected the C_{10}4EO mixture. Table 2.4 also shows the final distribution obtained for kenamine addition to C_{10}4EO. An increase in the relative peak intensities for the n = 0 and n = 4, 5, and 6 species with a decrease for n = 1 and 2 was observed

(d) Synprolam F3

The general formula of this commercial cationic surfactant mixture is shown below

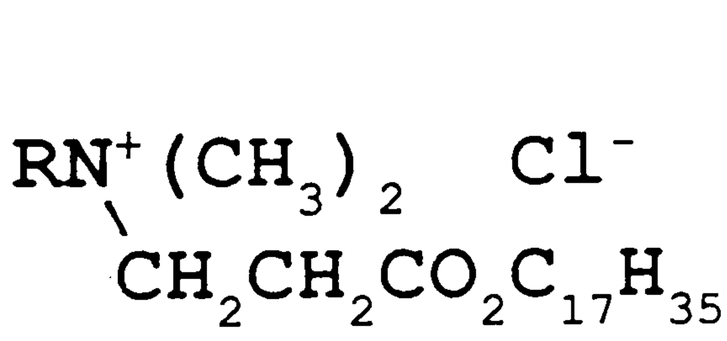

(8)

Where R is a mixture of $C_{13}H_{27}$ and $C_{15}H_{31}$ alkyl groups. Table 2.5. shows the resulting final "n" distribution for the major homologous series.

n	SYNPROLAM F3		
	C_{12}2EO	C_{13}3EO	C_{10}4EO
0	33	85	30
1	42	75	40
2	96	100	85
3	100	90	100
4	54	65	83
5	32	46	63
6	14	30	43
7	11	17	31
8	4	12	20
9	2	7	12
10	-	4	8
11	-	3	5
12	-	-	2
$\bar{n}$	2.9	2.9	3.9

Table 2.5 - Relative peak intensities after synprolam F3 addition.

Addition to the C_{12}/C_{14} 2EO mixture resulted in a reduction of the relative peaks due to the n = 0, and 1 components, with a marked increase for the n = 2 - 9 species. Therefore, the effect of synprolam F3 on the "n" distribution was similar, but more pronounced than the synprolam 35TMQC counter surfactant.

A similar result was observed with the C_{13}/C_{15} 3EO mixture.

Addition of synprolam F3 to the $C_{10}4EO$ mixture reduced the relative intensities of all the peaks with respect to that for the n = 3 components, but did not otherwise affect their relative intensities.

d) Synprolam DHQC

This commercial cationic surfactant mixture has the general formula

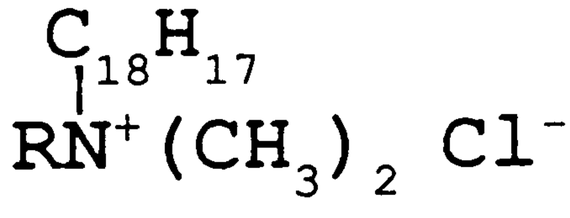

(9)

Where R is a mixture of C_9H_{19} and $C_{11}H_{33}$ alkyl groups. Table 2.6 shows the results obtained for synprolam DHQC addition.

n	SYNPROLAM DHQC		
	$C_{12}2EO$	$C_{13}3EO$	$C_{10}4EO$
0	100	100	92
1	65	59	69
2	45	48	100
3	25	35	91
4	12	25	67
5	6	14	46
6	3	12	31
7	3	5	20
8	1	3	30
9	-	2	9
10	-	1	4
11	-	-	2
12	-	-	1
$\bar{n}$	1.4	2	3

Table 2.6 - Relative peak intensities of ethoxy components after addition of synprolam DHQC.

For both the C_{12}/C_{14} 2EO and C_{13}/C_{15} 3EO mixtures the relative abundances of the n = 0 component was enhanced with respect to the others. Addition to the $C_{10}4EO$ mixtures resulted in an apparent increase of the n = 0, 1 and 2 components relative abundances.

The major to minor alkyl ratios obtained an addition of various counter-surfactants are displayed in Table 2.7.

COUNTER SURFACTANT	C_{13}/C_{15}		C_{12}/C_{14}	
	2EO	3EO	3EO	2EO
SYNPROLAM 35TMQC	-	-	2.3	3.0
SYNPROLAM DHQC	-	2.1	-	2.7
SYNPROLAM F3	-	2.1	-	4.3

Table 2.7 - Major to minor homologous series ratios upon addition of counter surfactant.

In all cases the ratios calculated were significantly higher than those obtained without the counter surfactant present.

It is difficult to provide a rationale for those results due to the complexity of the systems. Clearly Dorn and Ligon's theory discussed earlier does not provide a satisfactory explanation.

The most plausible explanation involves the differential interactions between anionic and cationic species.

(a) Bulk interactions. Formation of mixed micelles may occur within the bulk solution creating a soluble medium for the more hydrophobic species. This would result in the reduction of the relative intensities of the lower molecular weight components in some instances.

(b) Surface interactions. Addition of a counter surfactant may change the surface properties of the matrix by formation of a hydrophobic layer on the surface, so creating a soluble medium at the surface for more hydrophobic components. This would explain the

enhancement of lower molecular weight components in some cases.

The effect of counter surfactant addition was dependent upon both surfactant mixtures concerned and therefore cannot be considered as a general analytical method for surfactant analysis.

2.4. Non-Ionic surfactant Analysis

The non-ionic surfactant mixture studied was similar to the C_{13}/C_{15} 3EO anionic surfactant except that the ethoxy chain was terminated by an hydroxyl rather than a sulphate group.

2.4.1. Negative Ion FAB

No surfactant related peaks were observed in the negative ion FAB spectra. Base was added in an attempt to deprotonate sample molecules, without success. Also salt (sodium chloride) solution were added to produce cluster ions between surfactant molecules and chloride ions. Salt addition gave spectra which showed unusual and uninterpretable peaks (Fig 2.3.)

2.4.2. Positive Ion FAB

Fig 2.3 shows a positive ion FAB spectrum of the non-ionic surfactant, after addition of a sodium chloride solution. The general formula of the ions detected is shown below

$$RO(CH_2CH_2O)_nHNa^+ \qquad (10)$$

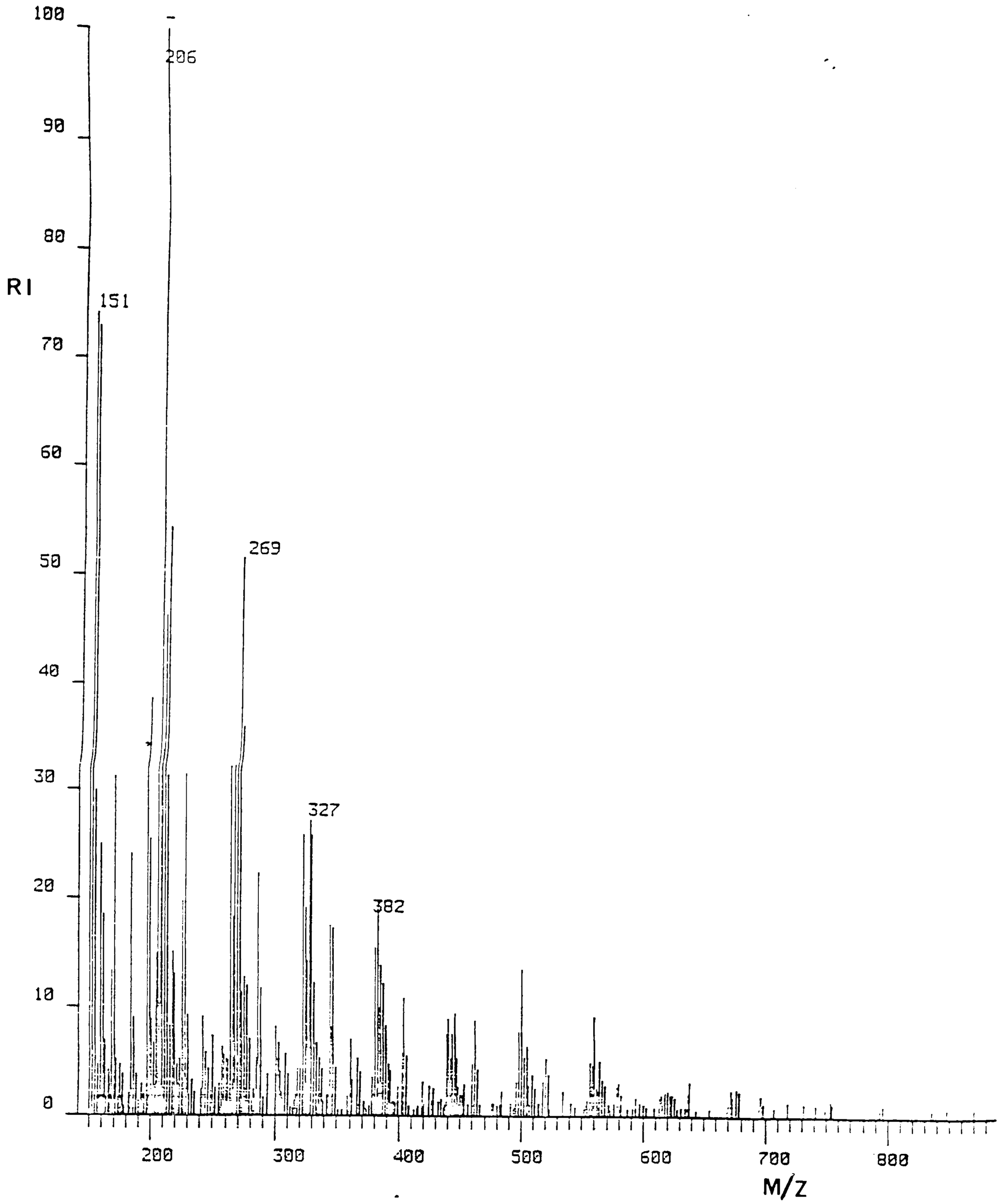

Fig. 2.3. Negative ion FAB spectrum for C_{13}/C_{15} 3EO alcohol ethoxylate.

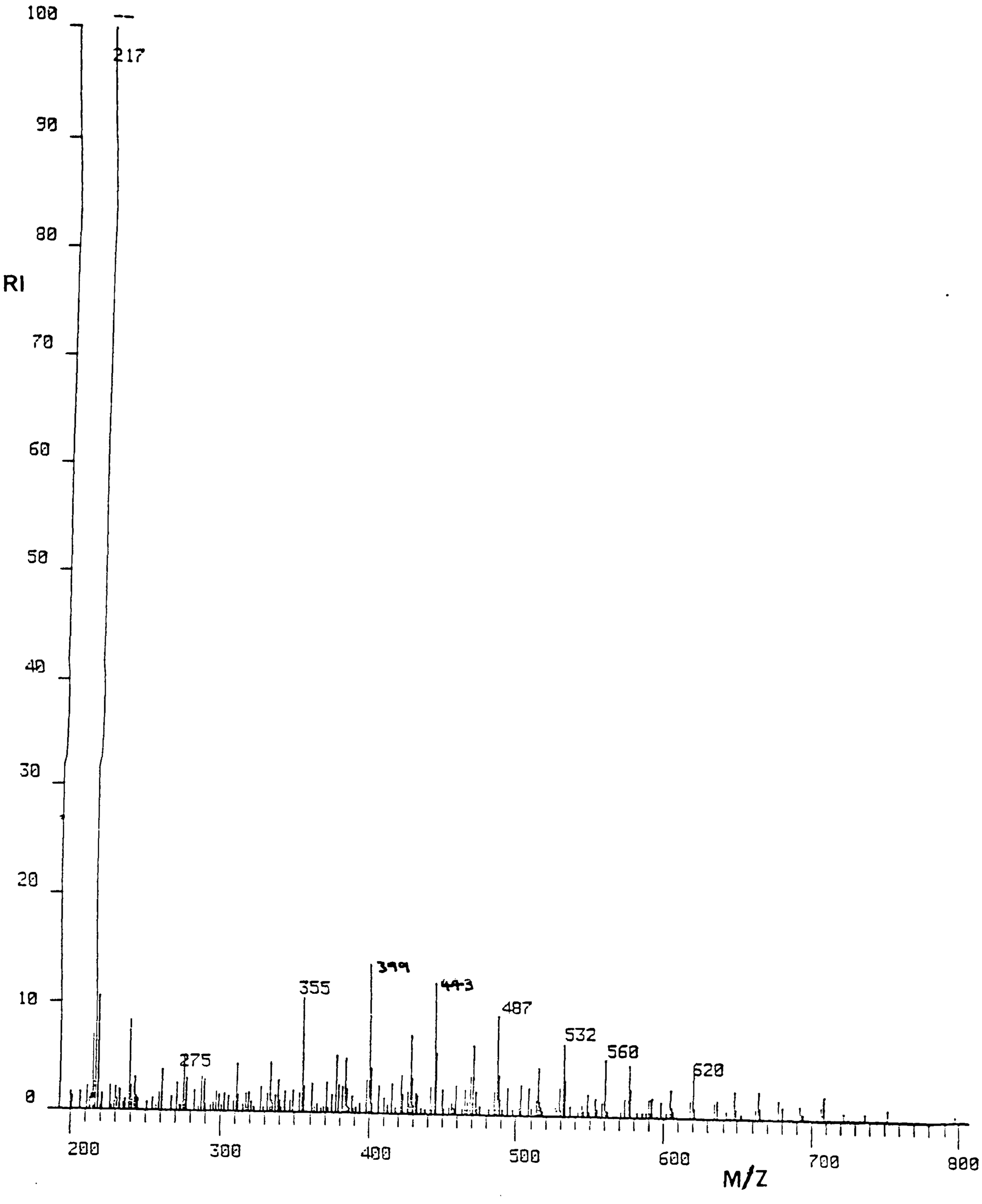

Fig. 2.3. Positive ion FAB spectrum for C_{13}/C_{15} 3EO alcohol ethoxylate.

Peaks corresponding to the major alkyl series occur at m/z 223, 267, 311, 355, 399, 443, 487, 531, 575, 619, 663, 707, 751. Table 2.8 shows the relative peak intensities of the ethoxy components for the major homologous series.

n	m/z	%
0	283	0
1	267	9
2	311	32
3	355	72
4	399	100
5	443	88
6	487	67
7	531	48
8	575	35
9	619	30
10	663	18
11	707	15
12	754	7

Table 2.8 - Relative peak intensities of ethoxy components of major alkyl series.

The average "n" value was 5.5. This is significantly higher than that expected, and that obtained for the corresponding anionic surfactant. This implies that the optimum chain length for ion formation is longer in non-ionic than anionic surfactants. It could also be argued that the lower molecular weight components are not soluble in the polar matrix since non-ionic surfactants do not have the benefit of the sulphate group to aid hydrophilicity. Evidence against this was the independence of the ethoxy distribution upon matrix. Also the ratio of major to minor alkyl series was 2.0, which is closer to the actual value than that obtained for anionic mixtures. If differential solubilities was an important factor then the larger R group would be less soluble and so show a lower ratio.

2.5. Conclusions

Sodium alcohol ether sulphate mixtures showed differing component distributions depending on whether positive or negative ion detection was employed. The negative ion distribution was dictated by surface activities as well as actual concentrations. Positive ion distribution was mainly dependent upon ionisation efficiencies. Addition of a cationic counter surfactant changed the distribution, the actual change was dependent upon both the analyte and counter surfactant. Therefore FAB ionisation was not found useful for quantitative analysis.

Non-ionic alcohol ethoxylates did not give negative ion FAB peaks. Positive ion FAB gave distributions which were dictated by ionisation efficiencies. Therefore, again FAB was found not to provide quantitative results.

Although quantitative information could not be obtained, this data does provide good qualitative information. This is of some importance for quality control of such complex mixture.

Chapter III

THERMOSPRAY ANALYSIS OF CATIONIC SURFACTANTS AND LONG CHAIN AMINES

3.1 Introduction

The chemical industry manufactures a range of quaternary ammonium salts for use as cationic surfactants. This category of surfactant are not utilised in domestic detergents because of their lack of surface activity under the required alkaline conditions. They have, however, found extensive applications in fabric conditioner formulations. This is due to the ability of cationic surfactants to absorb onto fibres with hydrophilic surfaces protecting these fibres and reducing the amount of matting.

As with anionic surfactants, the properties of cationic surfactants are dependent upon their composition[90], it is therefore important to be able to perform accurate analysis for quality control.

The various methods of analysis have been reviewed[91], the common technique employed being colorimetry[92,93].

Mass spectrometric analysis of these compounds has been difficult in the past because of their involatility. Electron impact ionisation provides no ions which may be assigned to intact quaternary ammonium ions[94]. Thermal decomposition occurs to form the tertiary amine,and alkyl halide. The tertiary amine is then ionised and beta cleavage occurs to form the $R_1R_2N{=}CH_2$ ion (where R_1 and R_2 alkyl groups).

DCI spectra do show peaks arising from intact quaternary ammonium ions[95], although the major peaks in

the spectra arise from dealkylation with subsequent protonation of the product amine.

FAB and FD ionisation techniques have also been applied to these compounds[95]. In both cases spectra were obtained whose major peaks arose from quaternary ammonium ions, with little fragmentation. As outlined earlier, there are problems associated with these techniques. FD is difficult to operate and obtain reproducible results, FAB analysis of mixtures is unreliable due to discrimination effects.

Thermospray is a soft ionisation technique applicable to involatile materials, and does not have the problems associated with FD and FAB.

Thermospray spectra have previously been obtained for single component samples of dicationic quaternary ammonium salts[96,97]. The spectra of these compounds had a dominant peak which may be assigned to the doubly charged quaternary ammonium ion, with only a small degree of fragmentation.

The work presented in this chapter is based on the study of thermospray as an ionisation technique for the qualitative and possibly quantitative analysis of commercial quaternary ammonium salt mixtures.

3.2 Experimental

The thermospray results were obtained on a MS80Rf (Kratos Analytical) forward geometry mass spectrometer fitted with a thermospray source and inlet system.

Unless stated otherwise the experimental conditions used were as follows:vaporiser temperature : 543 K; source temperature : 513 K; sample flow rate : 1ml min^{-1}; solvent : distilled water; ammonium acetate concentration: 0.1 $moldm^{-3}$.

The mass spectrometer was operated with an accelerating voltage of 4 KV (mass range up to 600 amu), with a mass resolving power of 1000, and a scan speed of 3 $secdec^{-1}$.

No HPLC column was used in the inlet line, so no separation of the components occurred prior to ionisation. The source was operated with the filament off, therefore all the ions formed arose from the thermospray process.

The FAB spectra were obtained on the same instrument, using 8 KV Xenon atoms (produced from an Ion-Tech FAB gun).

Triethanolamine (Aldrich) was used as a matrix. Operating conditions for the mass spectrometer were similar to those used for FAB.

The FD results were obtained on a Jeol with a source potential of 10 KV, and emitter current of 20 mA.

All surfactant mixtures were supplied by Imperial Chemical Industries. The single component quaternary ammonium salts were purchased from Aldrich.

3.3 Analysis of Commercial Mixtures

FAB and Thermospray spectra were obtained for a series of commercial quaternary ammonium salt mixtures (listed in table 3.1)

FD was also used for one of these mixtures - Arquad N.F.

The general observations made for this series are typified by those results obtained for Softlan JGE 9JE. A FAB spectrum of this mixture is shown in Fig 3.1.

This spectrum shows strong quaternary ammonium ion peaks at m/z 494 ($R_1 = R_2 = C_{16}H_{33}$), m/z 522 ($R_1 = C_{16}H_{33}$, $R_2 = C_{18}H_{37}$), and m/z 536 ($R_1 = R_2 = C_{18}H_{37}$). A thermospray spectrum (Fig 3.2) of the same mixture contains no peaks which could be assigned to intact quaternary ammonium ions, but only those from fragment ions.

Possible ion structures are shown below

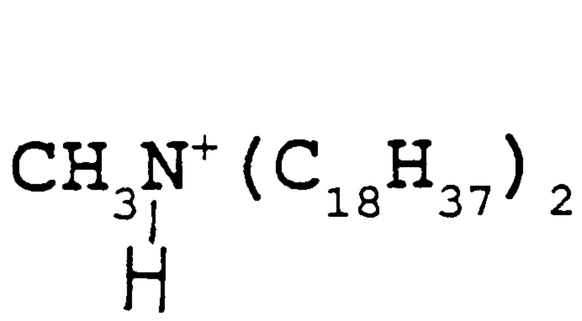

m/z 526

(11)

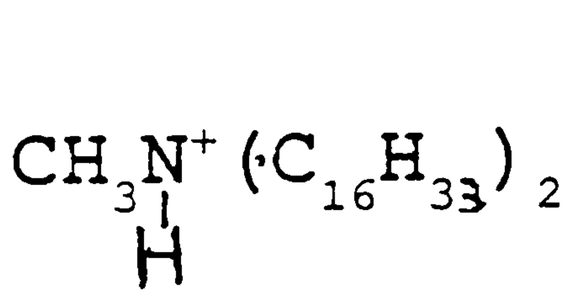

m/z 480

(12)

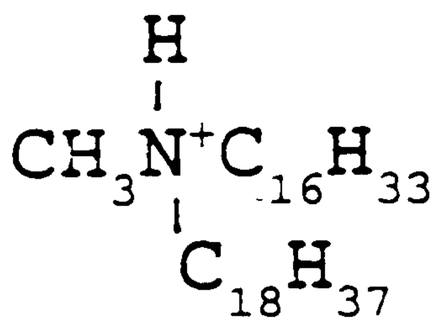

m/z 508

(13)

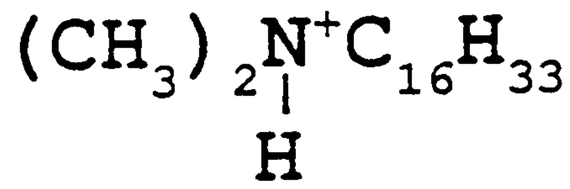

m/z 270

(14)

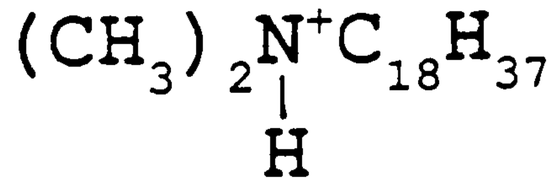

m/z 298

(15)

Name	Formula	R	R'
Arquad 550	$(CH_3)_3NR$	C_{18}	-
Softlan JGE 930 Softlan JGE 931	$(CH_3)_3NR$	$C_{18}/C_{16}/C_{14}$	-
Arquad 12/50	$(CH_3)_3NR$	C_{14}	-
Lenor active 927 Arquad HC Tesco fabric conditioner Lenor active 697	$(CH_3)_2NRR'$	C_{16}/C_{18}	C_{16}/C_{18}
Arquad NF	$(CH_3)_2NRR'$	C_8	C_{10}
Arquad T-20	$(CH_3)_2NRR'$	range of alkyl groups	
Synprolam FS JGE 960	$RN(CH_3)_2CH_2CH_2CO_2R'$	C_{13}/C_{15}	C_{15}/C_{17}

Table 3.1. Commercial quaternary ammonium salts studied.

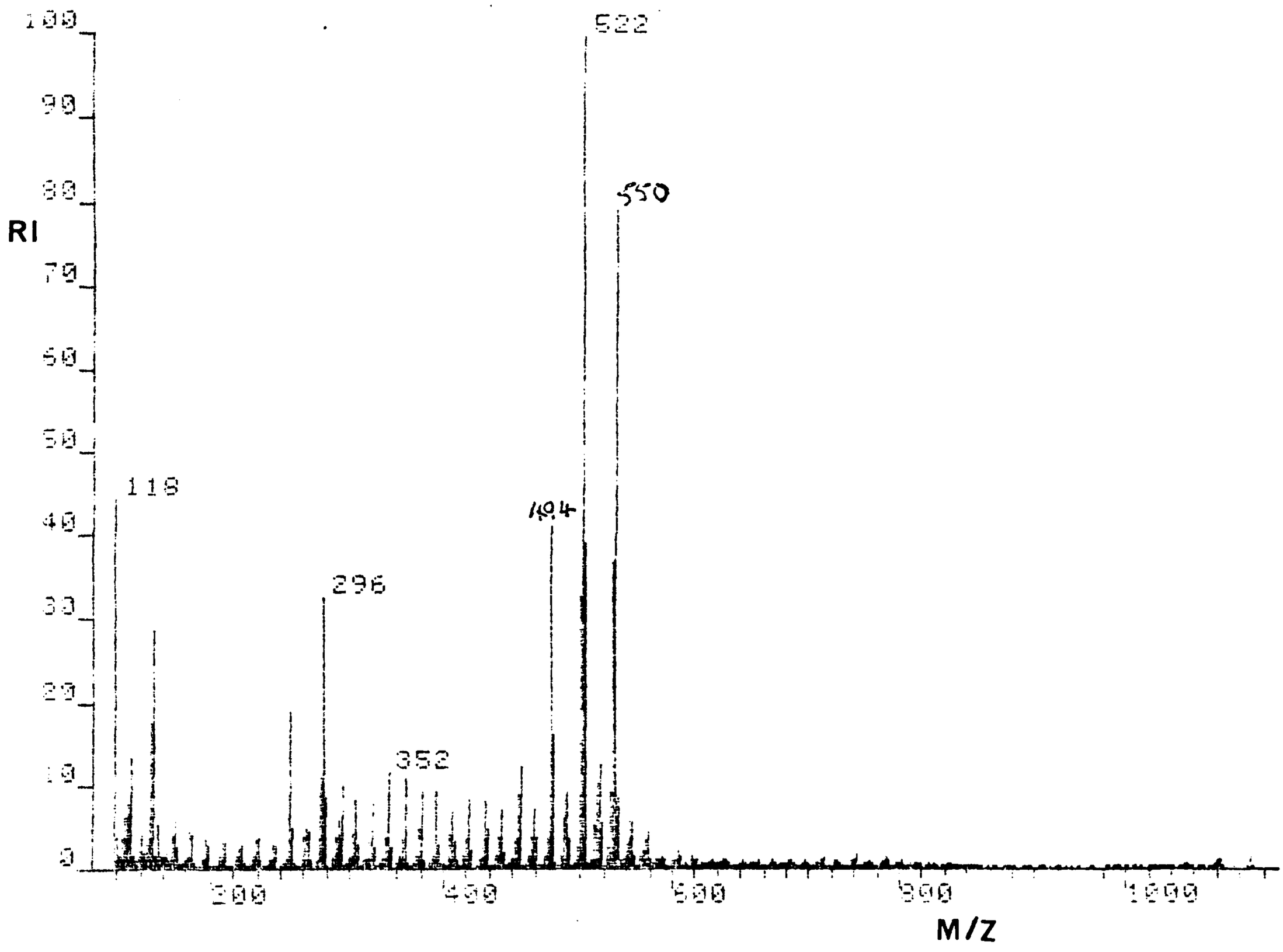

Fig. 3.1. FAB spectrum of Softlan JGE 930.

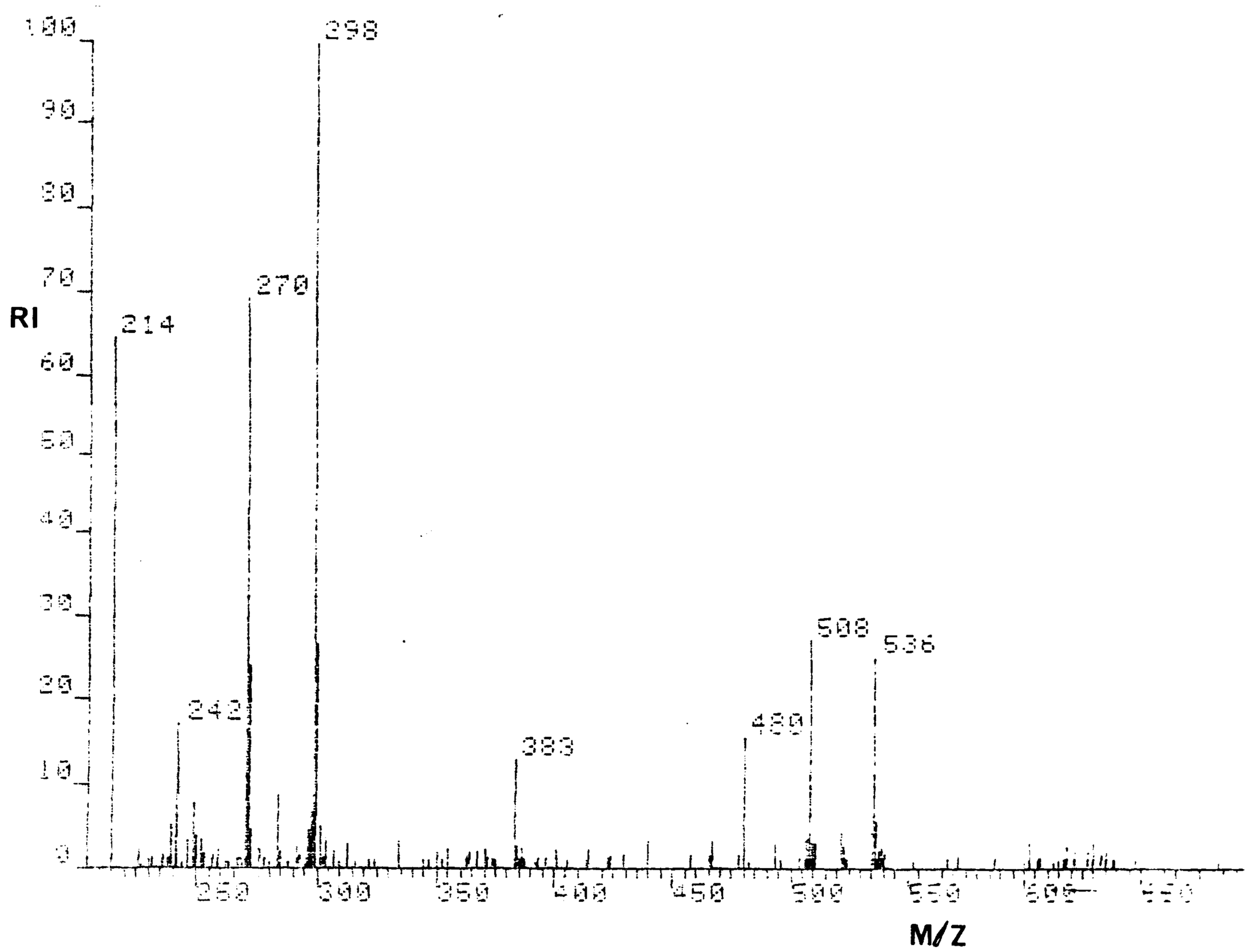

Fig. 3.2. Thermospray spectrum of Softlan JGE 930.

Fig 3.3 shows a FD spectrum obtained for Arquad NF. The only peaks observed were due to quaternary ammonium ions (m/z 270, $R_1 = R_2 = C_{10}H_{17}$) and m/z 326, $R_1 = R_2 = C_{10}H_{21}$), and cluster ions shown below;

$$[(C_8H_{17})_2N(CH_3)_2]_2Cl^+ \qquad (\underline{16})$$

m/z 575

$$[(C_8H_{17})_2N(CH_3)_2 - - (C_{10}H_{21})_2N(CH_3)_2]Cl^+ \qquad (\underline{17})$$

m/z 631

$$[(C_{10}H_{21})_2N(CH_3)_2]_2Cl^+ \qquad (\underline{18})$$

m/z 687

From these results it can be concluded that FAB produced good qualitative and surprisingly quantitative data. No severe discrimination effects were observed for these relatively simple mixtures. Occasionally different components gave the same mass ion, quantitative results could still be obtained by use of statistics[94]. Thermospray, however, was found not to be applicable to the analysis of these mixtures, because of the lack of intact quaternary ammonium ions, and extensive fragmentation observed. This was a surprising result, and so merited further work to deduce the fragmentation pathway occurring when thermospray ionisation was used with these mixtures.

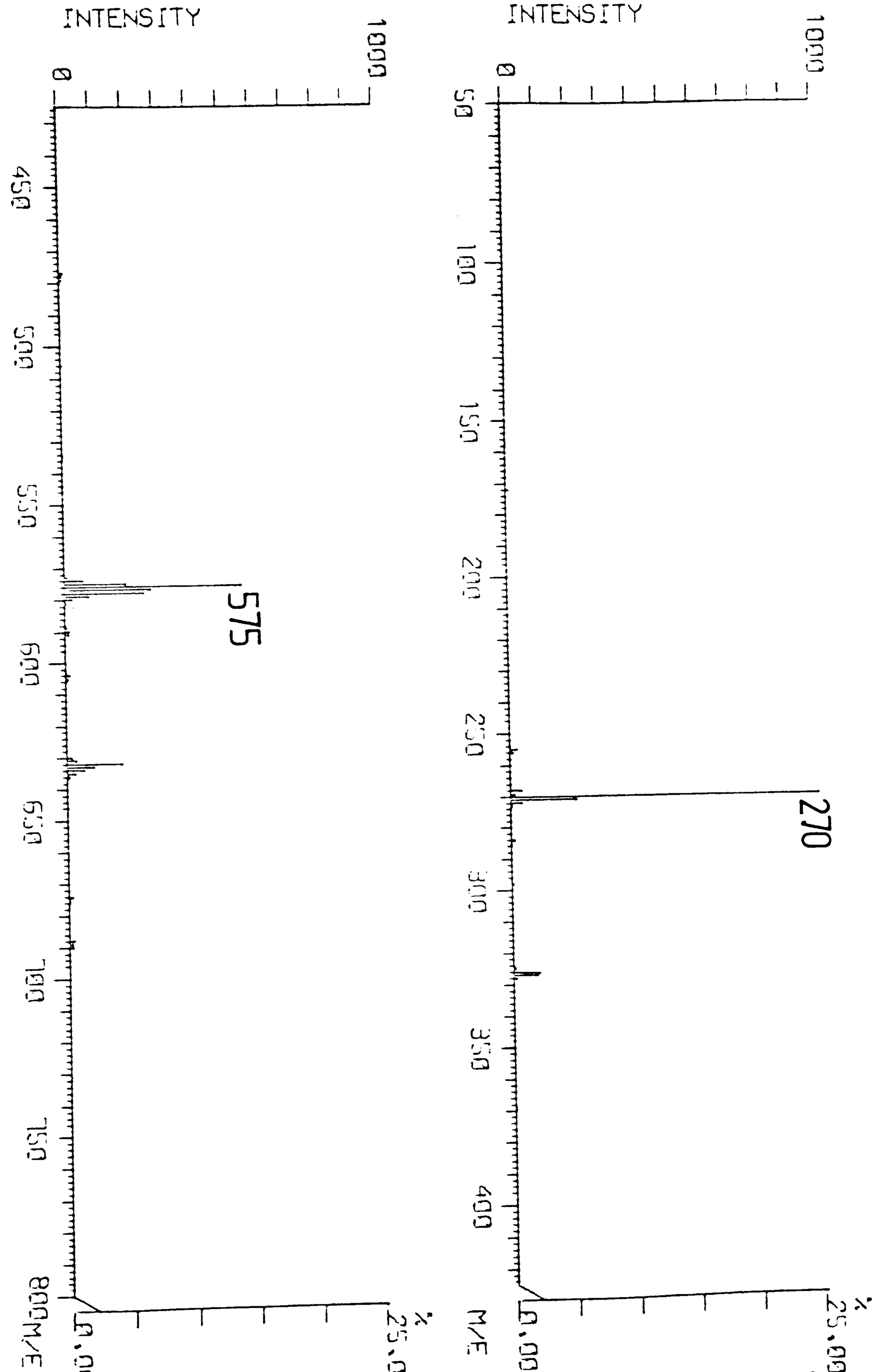

Fig. 3.3. FD spectrum of Arquad NF.

3.4 Thermospray Ionisation of Quaternary Ammonium Salts

There are three possible mechanisms:

(a) The first involves the thermal decomposition of a "molecule" or "ion pair" species ($R_4N^+X^-$). When quaternary ammonium salts of this type are heated they undergo one of two possible reactions[98]:

(i) Hoffman Elimination

$$R_4NX \longrightarrow R_3N + \text{alkene} + RX \qquad (26)$$

(ii) Alkyl Halide Elimination

$$R_4NX \longrightarrow R_3N + RX \qquad (27)$$

These reactions are often in competition with one another. For the Hoffman elimination to occur it is necessary for one of the alkyl groups to be an ethyl or larger. In general the alkyl group with the most β hydrogen atoms is eliminated, unless there is an alkyl with a β substituent which can stabilise a negative charge in which case the alkyl with the stabilising group is eliminated.

Alkyl halide loss is generally preferred when the negative counter ion is a weak base.

The tertiary amine formed, from either of these reactions can be subsequently protonated via the thermospray ionisation process to form the observed ions.

(b) The second fragmentation mechanism involves an intramolecular rearrangement, with migration of a β hydrogen atom to the nitrogen with the expulsion of an alkene neutral

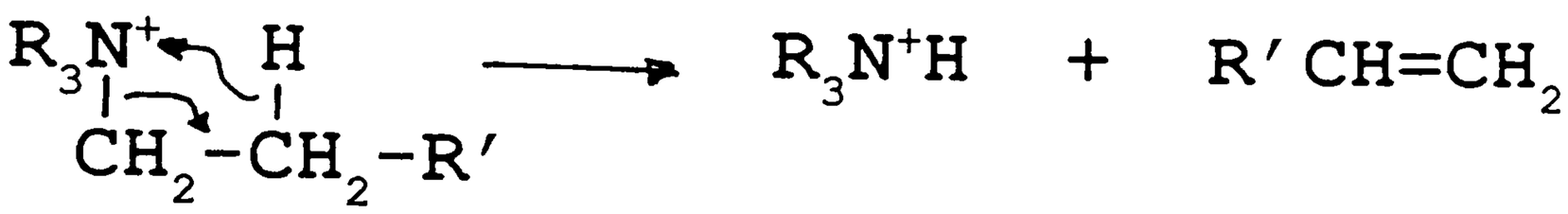

(28)

(c) Thirdly, it may be possible for an ion-molecule reaction involving a solvent molecule ($R'OH$) and a quaternary ammomnium ion (R_4N^+).

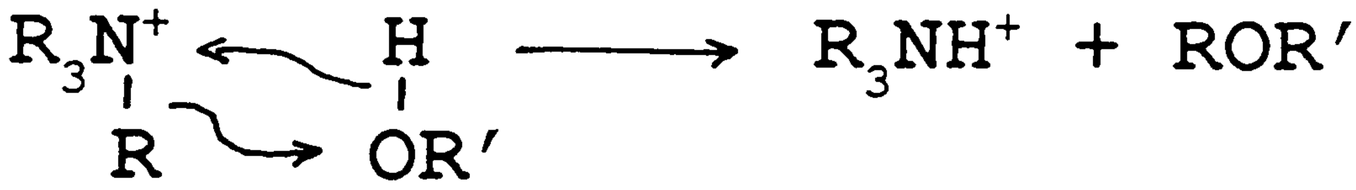

(29)

3.4.1 Experimental Investigation of Fragmentation Mechanism

A series of one component tetra-alkyl (tetramethyl - octyl) ammonium salts were studied. These compounds generated "clean" spectra comprising of only two, non background peaks; (i) intact quaternary ammonium ion, (ii) corresponding protonated tertiary amine.

Variation of the ratio of the quaternary ammonium ion peak to fragment ion peak intensities ($I(R_4N^+)/I(R_3NH^+)$) with a number of experimental parameters was investigated:

(a) Vaporiser Temperature

A plot of $I(R_4N^+)/I(R_3NH^+)$ against vaporiser temperature (Fig 3.4), for a 0.1 $moldm^{-3}$ tetrapentyl ammonium bromide solution, shows a linear reduction in the ratio (representing an increase in fragment ion intensity) with increasing vaporiser temperature.

The temperature range over which experiments could be performed was limited. Variation of $\pm 50^{o}$ from the optimum resulted in an unacceptable fall in intensity, and loss of stability of the ion beam.

This result indicates that the formation of the fragment ions occur via a thermal decomposition pathway.

(b) Source Temperature

Fig 3.5 shows the variation of the ratio $I(R_4N^+)/I(R_3NH^+)$ for a 0.1 $moldm^{-3}$ tetrapentyl ammonium bromide solution

Again a fall in the percentage of fragmentation was observed with increasing temperature. This provides further evidence for a thermal decomposition pathway.

Comparison of Fig 3.4 and 3.5 shows the greater influence of vaporiser than source temperature for thermospray. The slope of Fig 3.4 is steeper (0.11 K^{-1}) than that for Fig 3.5. (0.00926 K^{-1}) indicating that decomposition occurs mainly in the vaporiser.

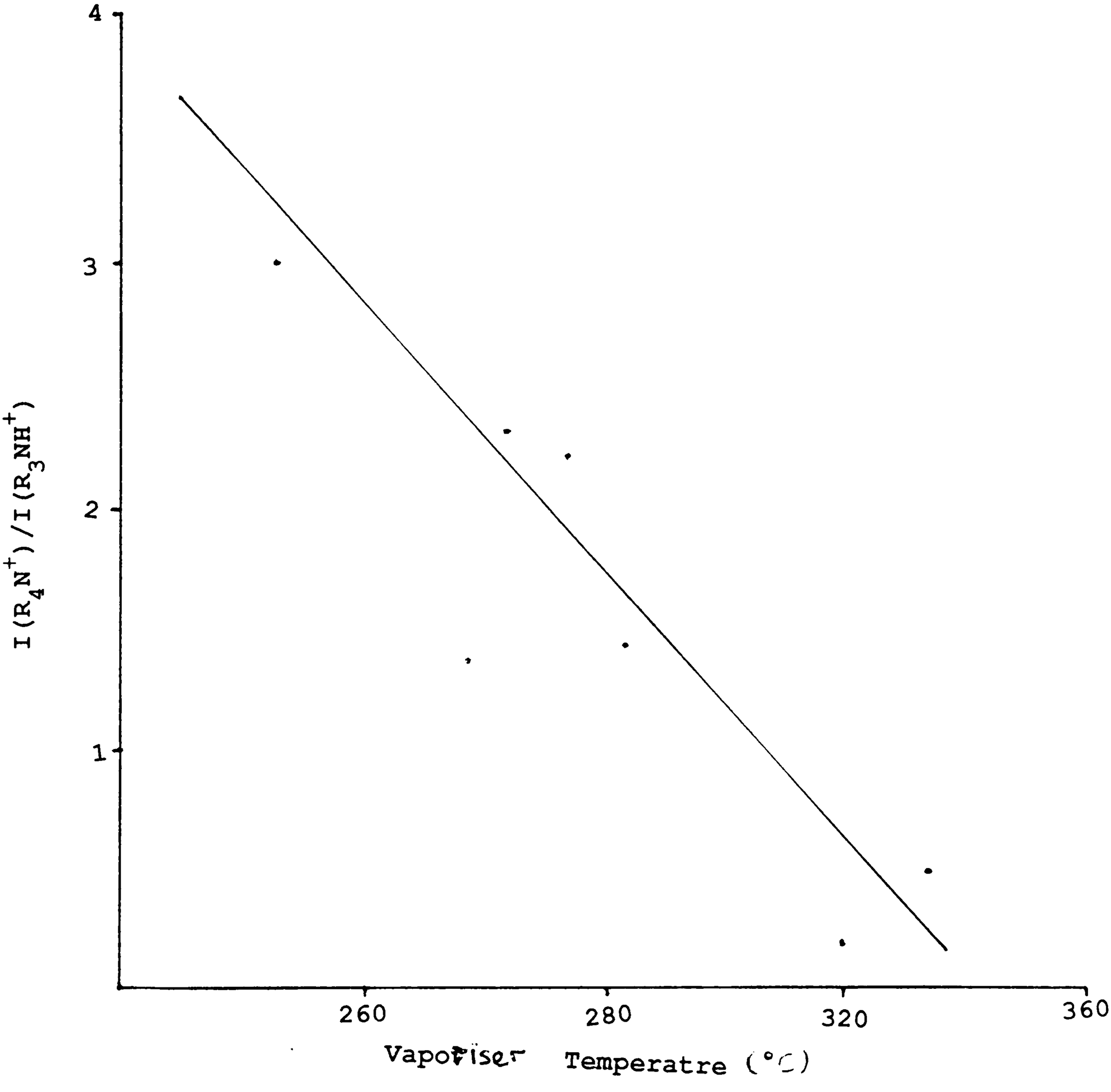

Fig. 3.4. Plot of $I(R_4N^+)/I(R_3N^+H)$ against vaporiser temperature.

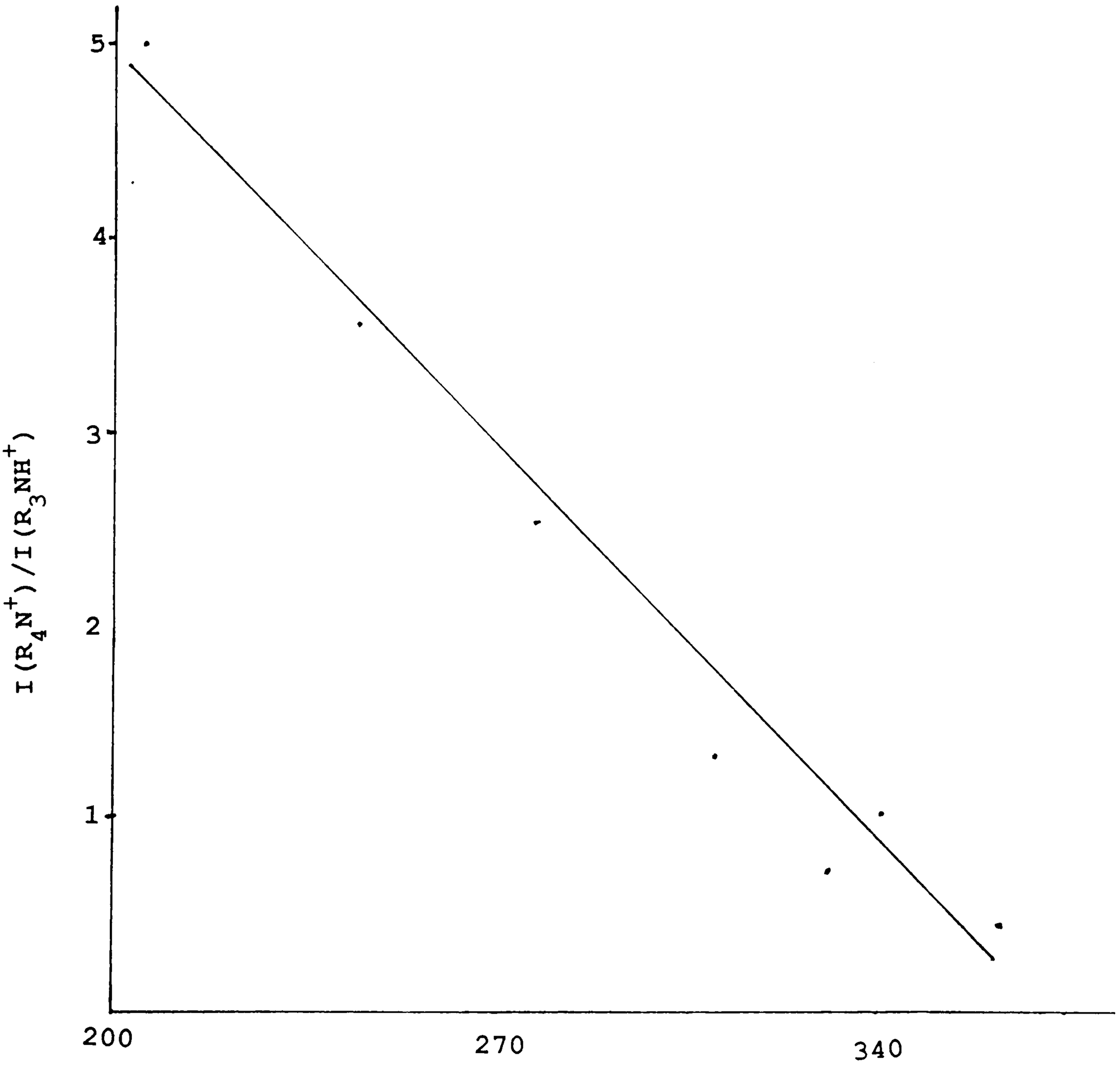

Fig. 3.5. Plot of $I(R_4N^+)/I(R_3N^+H)$ against source temperature.

(c) Quaternary Ammonium Salt Concentration

Fig 3.5 shows the variation of $I(R_4N^+)/I(R_3NH^+)$ with the concentration of tetrapentyl ammonium bromide. The range of concentrations used was limited by; (i) at low concentrations there were sensitivity problems, (ii) at high concentrations there was a danger of precipitation of the salt in the vapouriser which would block the microbore column.

Fig 3.6 indicates that the ratio increased as the concentration was reduced. This shows that the fragmentation requires the formation of a "molecule" or "ion pair". For an electrolyte AB

$$AB \longrightarrow A^+ + B^- \qquad (30)$$

The equilibrium constant (K) expression

$$K = \frac{[A^+][B^-]}{[AB]} \qquad (31)$$

If D is the degree of dissociation of the salt and c the concentration of AB

$$K = \frac{cD^2}{1-D} \qquad (32)$$

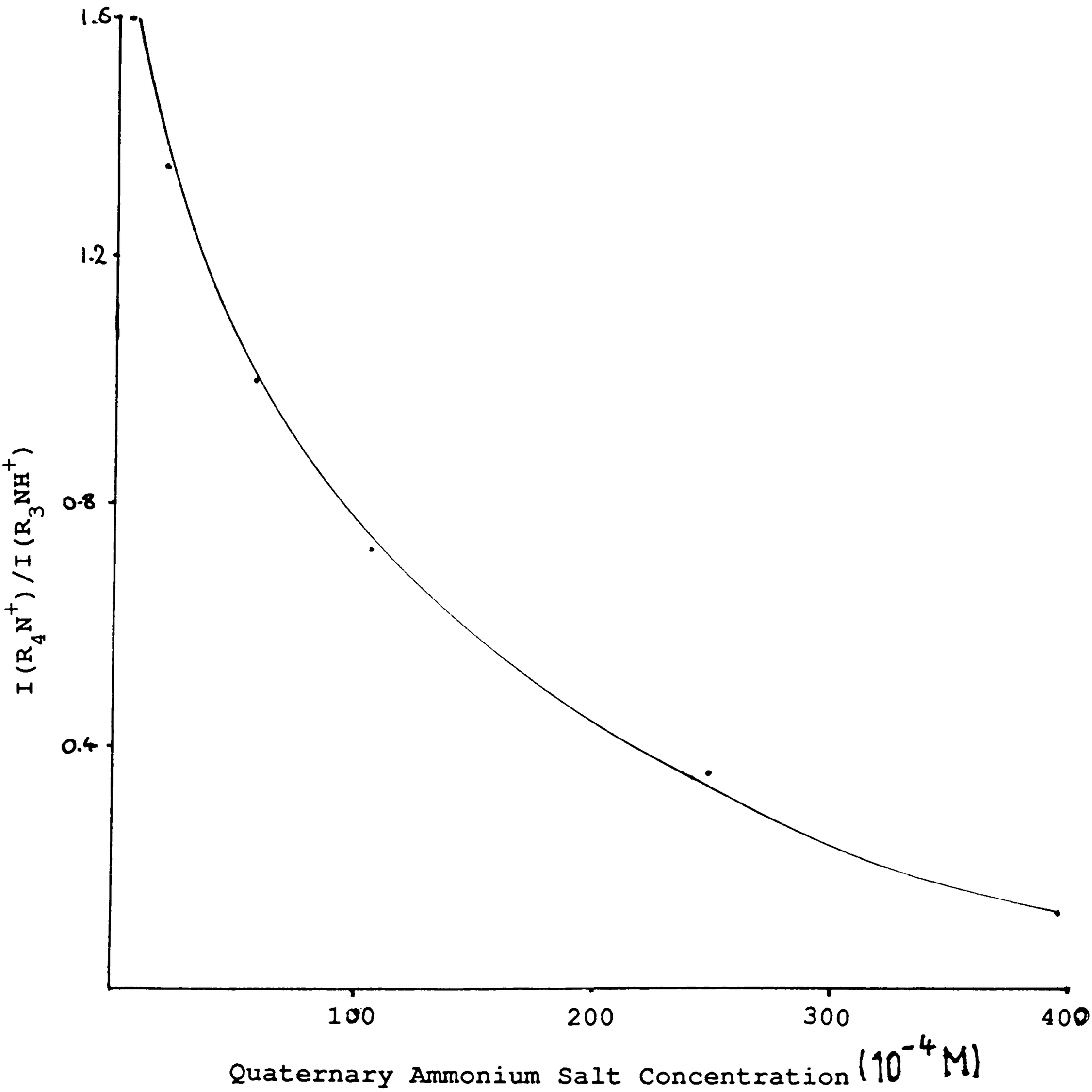

Fig. 3.6. Plot of $I(R_4N^+)/I(R_3N^+H)$ against quaternary ammonium salt concentration.

Therefore

$$D \propto \frac{1}{c} \qquad (33)$$

Hence as the concentration of the electrolyte decreases, the degree of dissociation increases with a corresponding increase in the relative concentration of free ions to ion pairs, and a rise in the $I(R_4N^+)/I(R_3NH^+)$ ratio.

This result provides supportive evidence for the first mechanism. If decomposition occurred via an intramolecular rearrangement no concentration dependence of the $I(R_4N^+)/I(R_3NH^+)$ ratio would be expected.

A fall in the ratio would be expected if the third mechanism occurred, since decreasing concentration increases the proportion of free ions to ion pairs, and hence the amount of reactive to unreactive species.

(d) Size of alkyl group

A plot of $I(R_4N^+)/I(R_3NH^+)$ against alkyl group size (Fig 3.7) indicates an inversely proportional relationship.

The same trend has been observed with the thermal vaporisation of quaternary ammonium salts[99].

Enthalpies of formation are available for only a few quaternary ammonium salts (tetramethyl[100], tetraethyl[101], and tetrapropyl[101] ammonium halides). The enthalpies of formation are available for all the respective alkyl halides, tertiary amines, and alkanes, as well as the

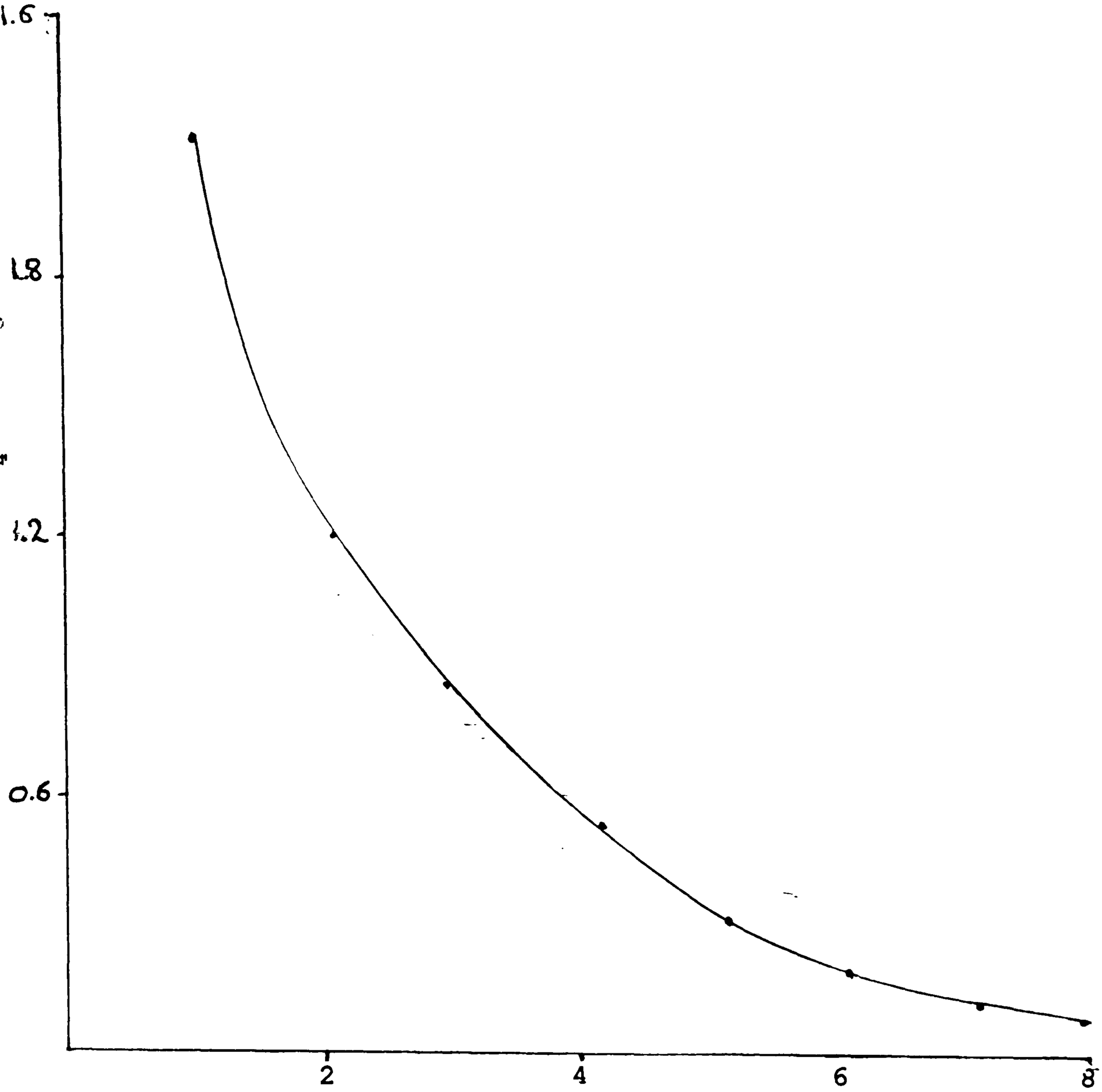

Fig. 3.7. Plot of $I(R_4N^+)/I(R_3N^+H)$ against alkyl group size.

enthalpies of vaporisation. From these data the enthalpies of reaction for alkyl halide elimination ($\Delta R'$) Hoffman elimination ($\Delta R''$), and enthalpies of formation for tertiary and protonated amines can be calculated (table 3.2)

R_4NX	$\Delta H_{R'}$ $KJmol^{-1}$	$\Delta H_{R''}$ $KJmol^{-1}$	$\Delta H_f(R_3NH^+)$ $KJmol^{-1}$	$\Delta H_f(R_3N)$ $KJmol^{-1}$
R = Me, X = Cl	157.56	-	564	-23.72
R = Me, X = Br	156.00	-	564	-23.72
R = Et, X = Cl	226.44	360.00	465	-98.70
R = Et, X = Br	220.64	375.02	465	-98.70
R = Pr, X = Cl	305.00	310.44	390	-161.10

Table 3.2 - Enthalpic values for reaction and formation of tetramethyl and ethyl chloride and bromide, and tetrapropyl chloride.

Consider the alkyl halide elimination reaction. The $H_{R'}$ values imply that the larger the alkyl group then the less favourable the reaction. $\Delta H_{R'}$ is increased by about 70 $KJmol^{-1}$ per methylene group, which is offset slightly by the more favourable protonation of the larger tertiary amines (10 - 20 $KJmol^{-1}$). Hence, increasing the alkyl group size reduces the likehood, in so far as enthalpies of reaction dictate the possibility of reaction. An analogous situation arises with the EI spectra of amines[104]. Increasing the alkyl group size enhances the probability of alkyl loss, whilst the

enthalpies of formation of the species indicate that alkyl loss should be less likely. This trend in EI spectra can be explained in terms of changes in entropy. Amines with larger alkyl groups have more degrees of freedom, and so it is more entropically favourable for the reaction to proceed.

The values for ΔH_R, indicate a more promising reaction with increasing alkyl size. This provides some evidence for a preference of an Hoffman elimination reaction, over alkyl halide elimination.

(e) Parameters not affecting the $I(R_4N^+)/I(R_3NH^+)$ ratio

The ratio was found to be independent of the solvent used. If mechanism (iii) was true some dependence would be expected.

The degree of fragmentation of the tetrabutyl ammonium salt was found to be independent of the counter ion (chloride, bromide, iodide and hydroxide). These results are not totally unexpected because there is no change in the enthalpies of reaction with counter ion (table 3.2), and no entropy differences would be predicted. Also the two alternative mechanisms would be independent of counter ion.

The degree of fragmentation was also found to be unaffected by changes in the concentration of ammonium acetate. This result is contrary to those obtained with doubly changed quaternary ammonium salts, where the fragment ion abundances decreased with ammonium acetate concentration. This provides evidence against the thermal decomposition pathways, because the neutral tertiary

amines are protonated by the ammonium ions in a manner resembling ammonia chemical ionisation. Removal of the ammonium ions should therefore reduce the relative abundance of these fragment ions. When tetramethyl ammonium bromide was injected into the thermospray inlet system in the absence of ammonium acetate, a prominent peak 14 amu below the intact quaternary ammonium ion peak was still observed. This can not possibly occur via a rearrangement process. Although this result seems to suggest the third mechanism it could be argued that protonation of the amine could occur via a different route, possibly from acidic proton transfer from the solvent.

3.4.2. Hoffman Elimination or Alkyl Halide Loss

Hoffman elimination is preferred to the alkyl halide elimination when a strong base is the counter ion. Furthermore, the enthalpies of reaction (table 3.2) for the Hoffman elimination predict the correct trend for ease of alkyl loss, whereas those for alkyl halide elimination forecast the opposite trend. Conversely, the thermospray spectrum (Fig 3.8) of benzyl triethyl ammonium chloride shows two major ions;

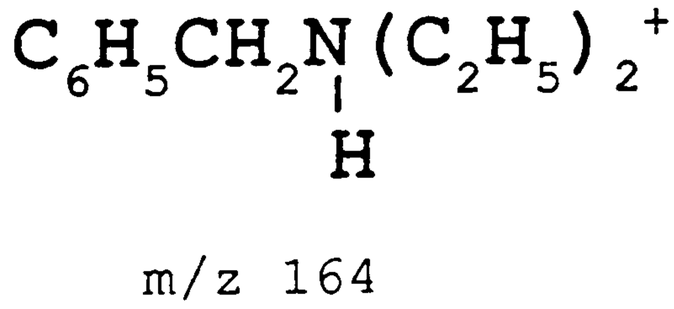

(19)

m/z 164

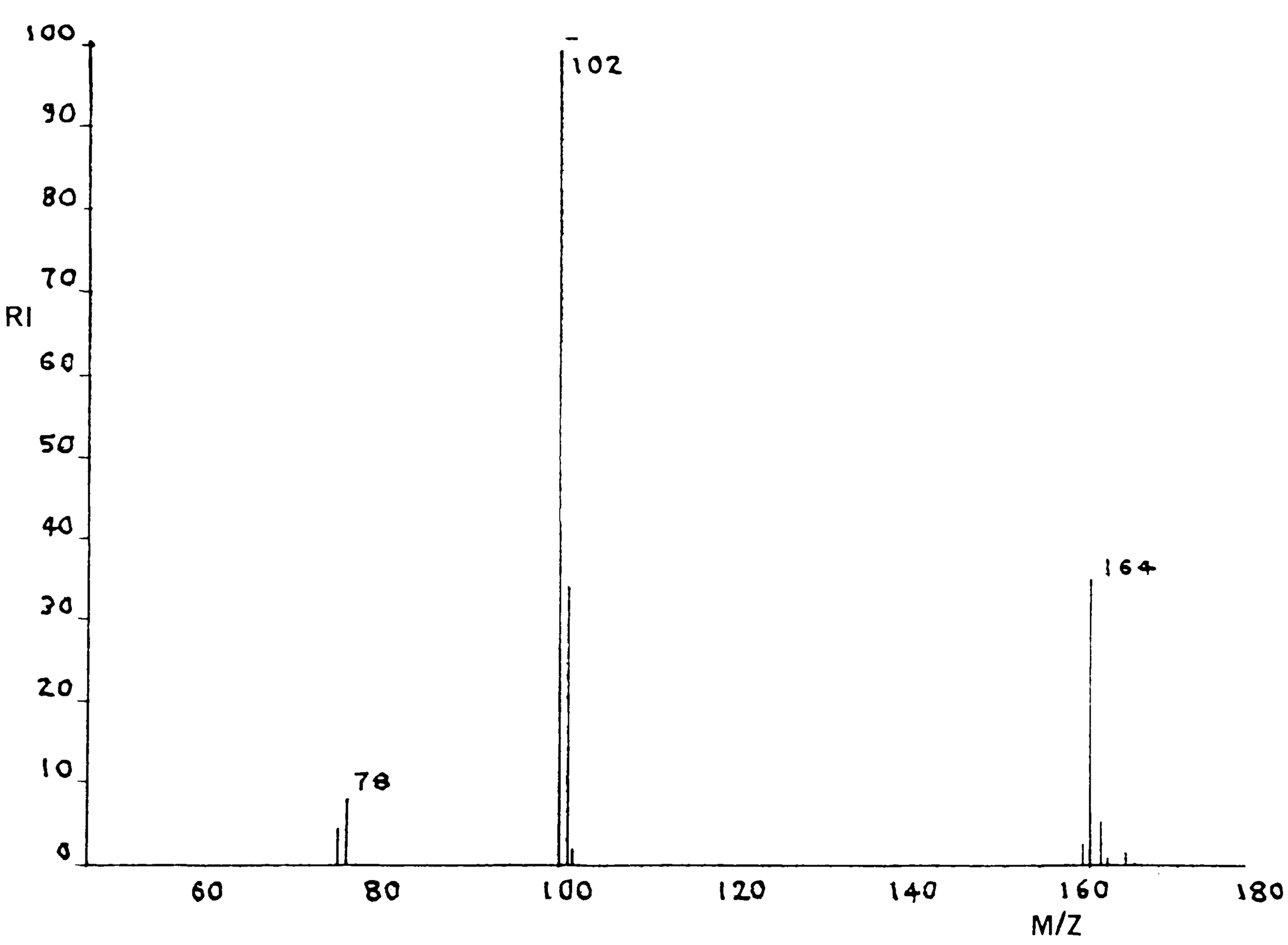

Fig. 3.8. Thermospray spectrum of benzyl triethyl ammonium chloride.

$$(C_2H_5)_3NH^+ \qquad (\underline{20})$$

m/z 102

This provides strong evidence for the loss of alkyl halide from the ion pair. Hoffman degradation dictates that the loss of ethene would be preferred to form (19) over the loss of the unlikely neutral C_7H_{16} to form (20). Fig 3.8 clearly indicates that benzyl loss was more prominent than ethyl loss.

3.5 Thermospray of Amines

Thermospray was found to be an excellent ionisation technique for analysing long chain primary, secondary and tertiary amines used as precursors for quaternary ammonium salts.

Fig 3.9 shows the thermospray spectra of such amines Syn 35 is a primary amine mixture; RNH_2R is a mixture of $C_{13}H_{27}$ and $C_{15}H_{31}$ alkyl groups. Protonated pseudo-molecular ions were observed at m/z 200 and 228. Also cluster ions were detected at m/z 399 - $(C_{13}H_{27}NH_2)_2H^+$, m/z 427 - $(C_{13}H_{27}NH_2...C_{15}H_{31}NH_2)H^+$ and m/z 455 - $(C_{15}H_{31}NH_2)H^+$. Syn 35M is a secondary amine; $RN(CH_3)H$, again protonated pseudo-molecular ions were observed, with a small degree of clustering. Some primary amine was also present (m/z 200 and m/z 228). Syn 35DM is a tertiary amine; $RN(CH_3)_2$, this spectrum shows a small amount of impurity at m/z 284, which probably corresponds to the protonated ion of $C_{17}H_{35}N(CH_3)_2$.

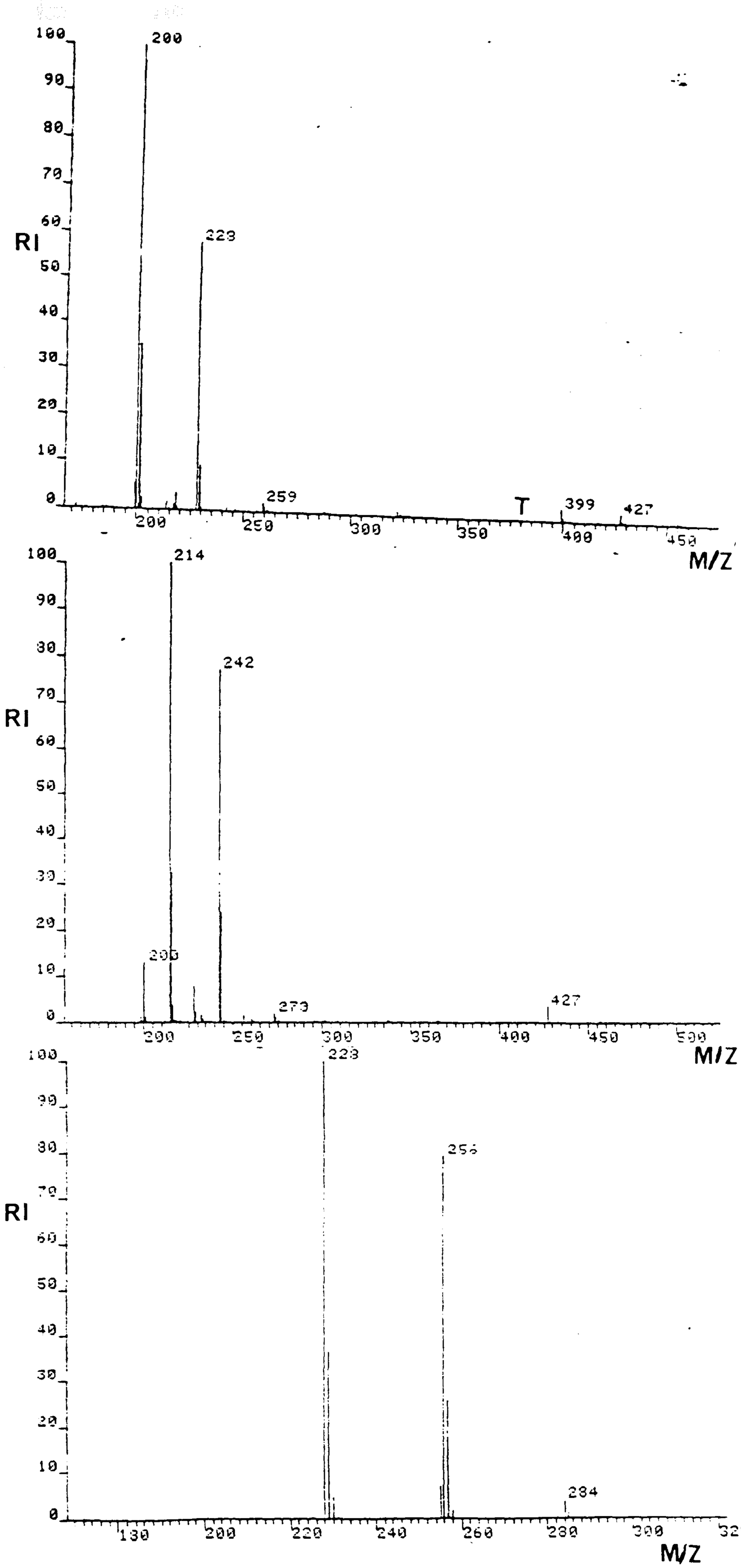

Fig. 3.9. Thermospray spectra of (a) Syn 35 (b) Syn 35M (c) Syn 35 DM.

3.6 Conclusion

Both FD and FAB provided good qualitative and quantitative data for quaternary ammonium salts. FAB is the preferred technique due to its simplicity in comparison to FD. Conversely thermospray spectra showed only decomposition products produced by thermal reaction of an "ion pair" to form the amine and alkyl halide. This complicated the spectra, consequently thermospray was found to be of no practical use for quaternary ammonium salt analysis.

Conversely thermospray was found to be ideal for analysis of long chain amines.

Chapter IV

MASS SPECTROMETRIC ANALYSIS OF ORGANO-TIN STABILISERS

4.1. Introduction

Polyvinyl-chloride (PVC) is a thermoplastic material of major importance[105]. It has many uses in such diverse areas as packing, clothing, electrical goods and construction.

Extensive applications of PVC have evolved despite one potentially major drawback; PVC is readily degraded by heat and short wavelength light. It is necessary, therefore, to incorporate stabilising compounds into the PVC formulation. These stabilising compounds are usually metal salts or esters. The largest group of stabilisers used consists of a range of organotin compounds.

Organotin stabilisers can be represented by the general formula

$$R_aSnX_b \qquad (21)$$

where $a + b = 4$

and $b = 1 - 3$

R is an alkyl group, and X is maleic acid or an ester of thioglycollic acid. The thioglycollates contain tin-sulphur linkages, and have been found to be the most effective stabilisers against thermal degradation[106].

Most organo-tin stabilisers are di-n-octyl compounds (ie a = 2), although some mono octyl compounds have been used. The mono alkyl stabilisers have been found to be particularly effective when used in conjunction with a diakyl compound in a PVC formulation.

Thermolysis of PVC is a complex process, and the mechanism is not fully understood. The generally accepted explanation requires the existence of active sites within the polymer, in particular allylic chlorine (-CH=CH-CHCl-). Loss of hydrogen chloride from these sites is thought to activate an adjacent chlorine atom in the polymer chain. The effectiveness of the stabiliser is then explained in terms of replacement of active chlorines with a thio ligand, which is more resistant to heat. The stabiliser will also react with the hydrogen chloride, and remove hydroperoxide sites in the polymer, which prevents catalysis of polymer degradation by these species.

Chemical analysis of organo-tin stabilisers is a lengthy process involving a number of "wet chemistry" separation, and instrumental analysis stages[107,108]. Analysis of pure stabilisers, and those extracted from PVC formulation is essential for quality control purposes. The work presented in this chapter involves the application of mass spectrometry and NMR spectroscopy to the analysis of organo-tin stabilisers.

4.2. Experimental

The experimental conditions used to obtain the FAB results have already been described in Chapter 2 and for FD in Chapter 3.

High collision energy daughter-ion linked-scan spectra were obtained on a Kratos MS50 operated with an accelerating voltage of 6 KV. The collision gas used was helium. A collision cell in the first field free region was filled with helium until the intensity of the parent ion of interest fell to approximately 30% of its original value. Low collision energy daughter ion spectra were performed on a ZABQQ (VG Analytical Instruments). This instrument is a reverse geometry magnetic sector instrument, with a first Rf only quadrupole acting as a collision cell (collision gas was helium), and a second "normal" quadrupole as a mass analyzer. The ion of interest was selected using the sector analyser and the resulting fragments, after collision, were analysed using the second quadrupole. Differing collision energies (0-500 eV) could be used by changing the potential on the ion retarding plates just prior to the collision quadrupole.

The CI spectra were obtained using an MS80 mass spectrometer operated with an accelerating voltage of 4 KV, electron energy of 100 eV and source pressure of about 1 Torr.

Tin-119 NMR spectra were obtained using a Bruker 400 FT NMR spectrometer operating at 149.21 MHz, with inverse gated (due to a negative magnetogyric ratio: -9.9707 $radr^{-1}s^{-1}$)^{109} broad band proton decoupling at 293 K. Typically spectra were acquired over 100 KHz sweep width, with 32,000 data points, and 500 - 2000 transients (recorded approximately every 2 seconds). Tetramethyl tin was used as a reference material.

4.3. Results and Discussion

Table 4.1. lists the standard tin stabilisers studied.

Reference	R	X	a	b	RMM
Dimethyl	CH_3	$SCH_2CO_2isoC_8H_{17}$	2	2	556
Di-n-butyl	C_4H_9	$SCH_2CO_2isoC_8H_{17}$	2	2	640
Di-n-octyl	C_8H_{17}	$SCH_2CO_2isoC_8H_{17}$	2	2	752
Mono-n-octyl	C_8H_{17}	$SCH_2CO_2isoC_8H_{17}$	1	3	842

Table 4.1. - Standard organo-tin stabilisers.

Where reference refers to the terminology used throughout this work for that compound and RRM is the relative molecular mass of that compound.

4.3.1. Probe CI

Fig 4.1. shows an ammonium CI spectrum of the di-n-butyl stabiliser. The spectrum is typical for probe temperatures up to 670 K. A peak at m/z 222 dominates the

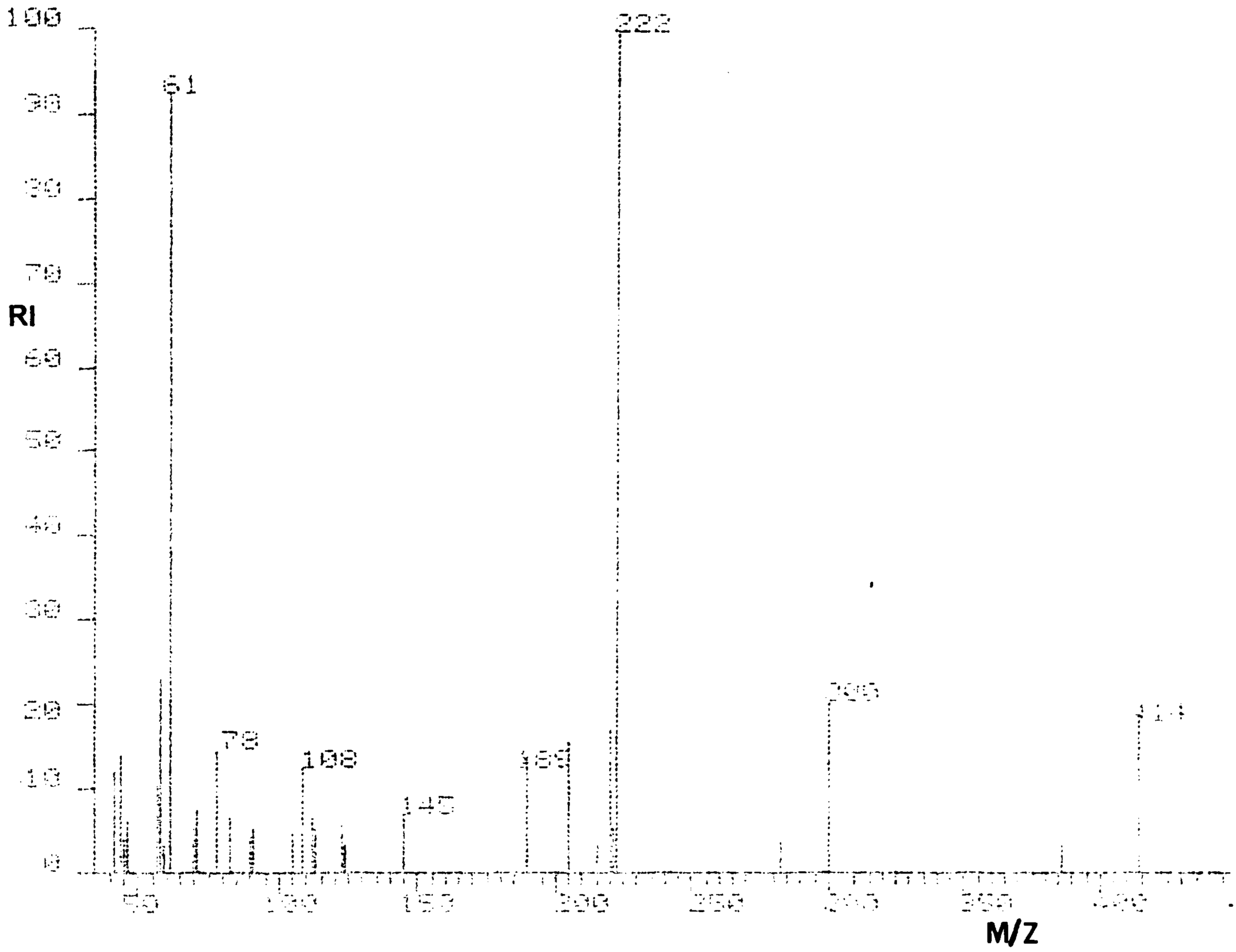

Fig. 4.1. Ammonium CI spectrum of dibutyl tin stabiliser up to probe temperatures of 670 K.

spectrum, which corresponds to the ammonium adduct of the thioglycollate ester ligand.

$$NH_4HSCH_2CO_2C_8H_{17} \qquad (\underline{22})$$

This ion probably arises from unco-ordinated ligand present in the sample, rather than from thermal degradation of the stabiliser because of the presence of the m/z 222 peak prior to heating the probe.

At higher probe temperature, peaks corresponding to tin-containing species were observed (Fig 4.2.)

Possible structures for the ions observed are shown below:

$$(C_4H_9)_2SnSCH_2CO_2C_8H_{17}$$
$$\llcorner SCH_2CO_2H$$

m/z 529 (<u>23</u>)

$$C_4H_9SnSCH_2CO_2C_8H_{17}$$
$$\llcorner SCH_2CO_2H$$

m/z 471 (<u>24</u>)

$$(C_4H_9)_2SnSCH_2CO_2C_8H_{17}$$

m/z 435 (<u>25</u>)

$$SnSCH_2CO_2C_8H_{17}$$

m/z 323 (<u>26</u>)

Probe mass spectrometry was found not to be applicable to the analysis of these compounds. The spectra obtained were transient, lasting for only one or two scans, and reproducibility was poor. Also, the sample peaks were of low intensity and no molecular ions were present.

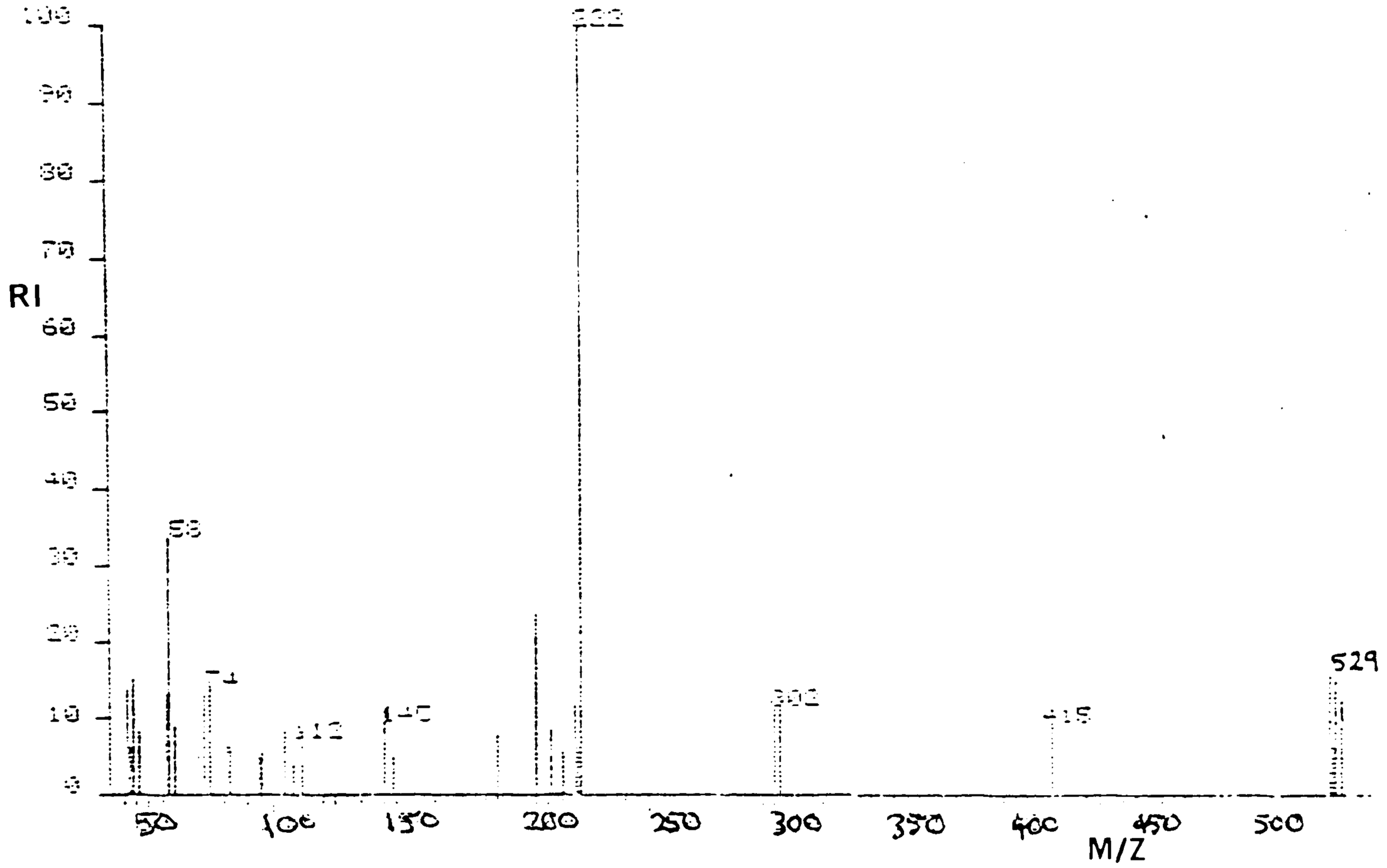

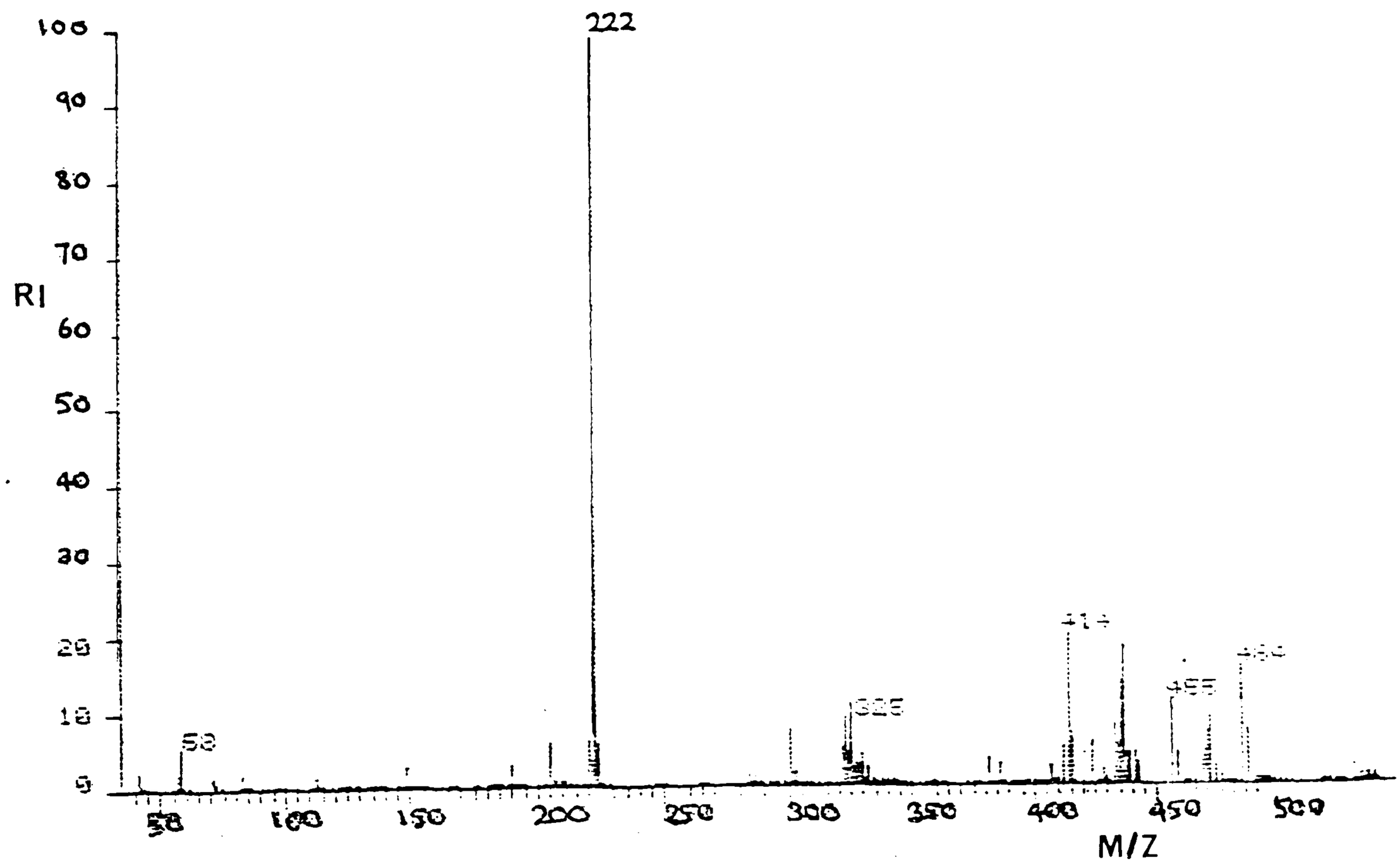

Fig. 4.2. Ammonium CI spectrum of dibutyl tin stabiliser at probe temperatures above 670 K.

4.3.2. Field Desorption

Fig 4.3. shows a FD spectrum of the dimethyl stabiliser. Peaks at m/z 203, 406, and 609 arose due to clustering of iso-octyl thioglycollate ligands - $(SCH_2CO_2C_8H_{17})_n$ - with n = 1, 2 and 3 respectively. A relatively strong molecular radical cation was observed at m/z 556. Fragment peaks occurred at m/z 541, and 353, the former was due to the loss of a methyl radical from the molecular ion, and the latter from the loss of a thioglycollate ester radical. The peak at m/z 759 is probably an adduct ion of a stabiliser and a thioglycollate ligand molecule.

4.3.3. Fast Atom Bombardment

Although FD provides good qualitative data, as stated earlier, its use has drawbacks. FAB is quicker, simpler, and a more reliable ionisation technique. The physical nature of these compounds (viscous liquids) makes them suitable to FAB analysis without a matrix.

Bentz et al[110] published a short paper on the FAB analysis of organo-tin stabilisers at the same time as we published our preliminary results[111]. Similar trends were observed with positive ion FAB, although a number of differences were noted with negative ion FAB.

4.3.3.1. Positive Ion FAB

Fig 4.4. shows a positive ion FAB spectrum of the dimethyl stabiliser. The general features of this spectrum are typical of those obtained for all the tin

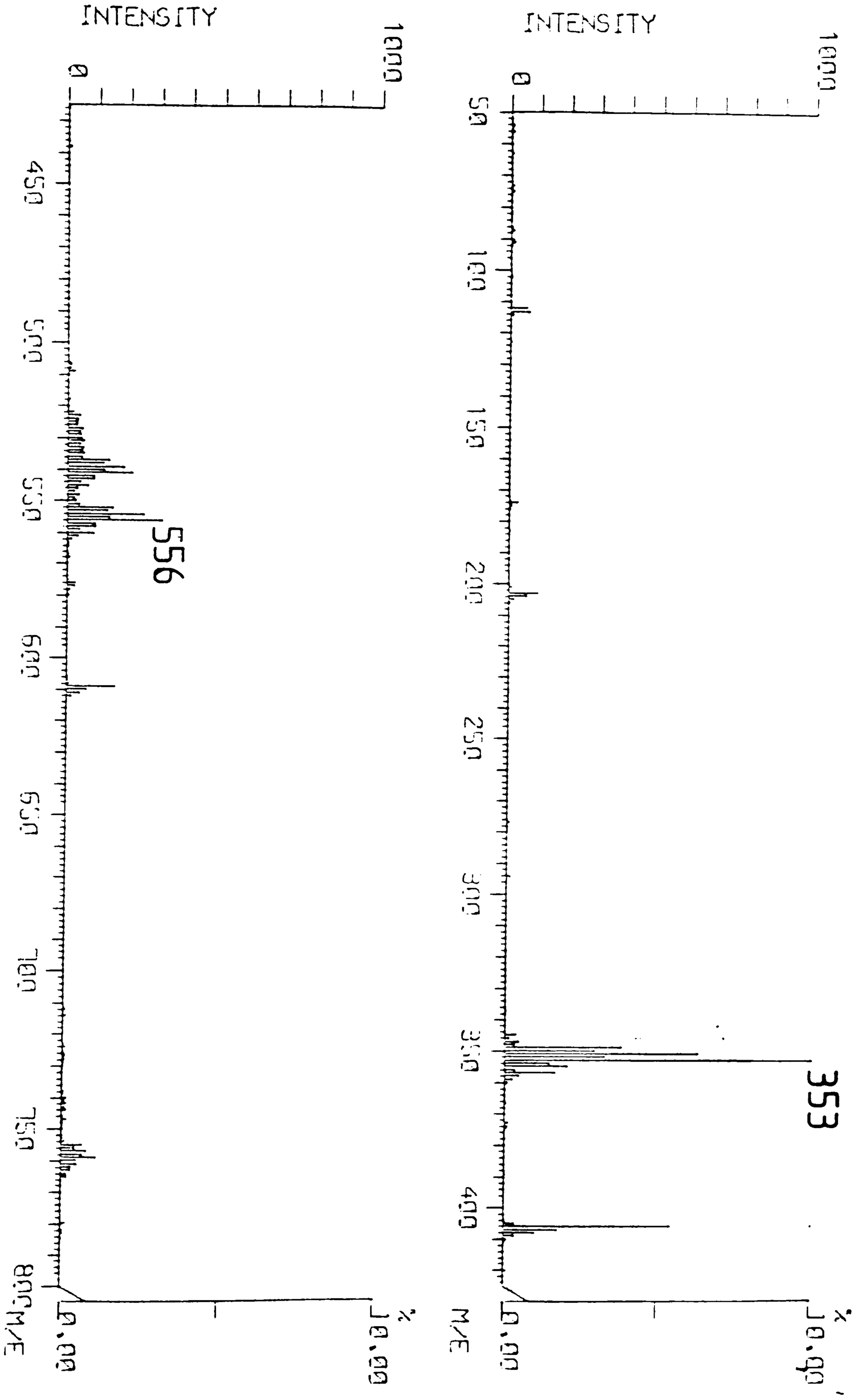

Fig. 4.3. FD spectrum of dimethyl tin stabiliser.

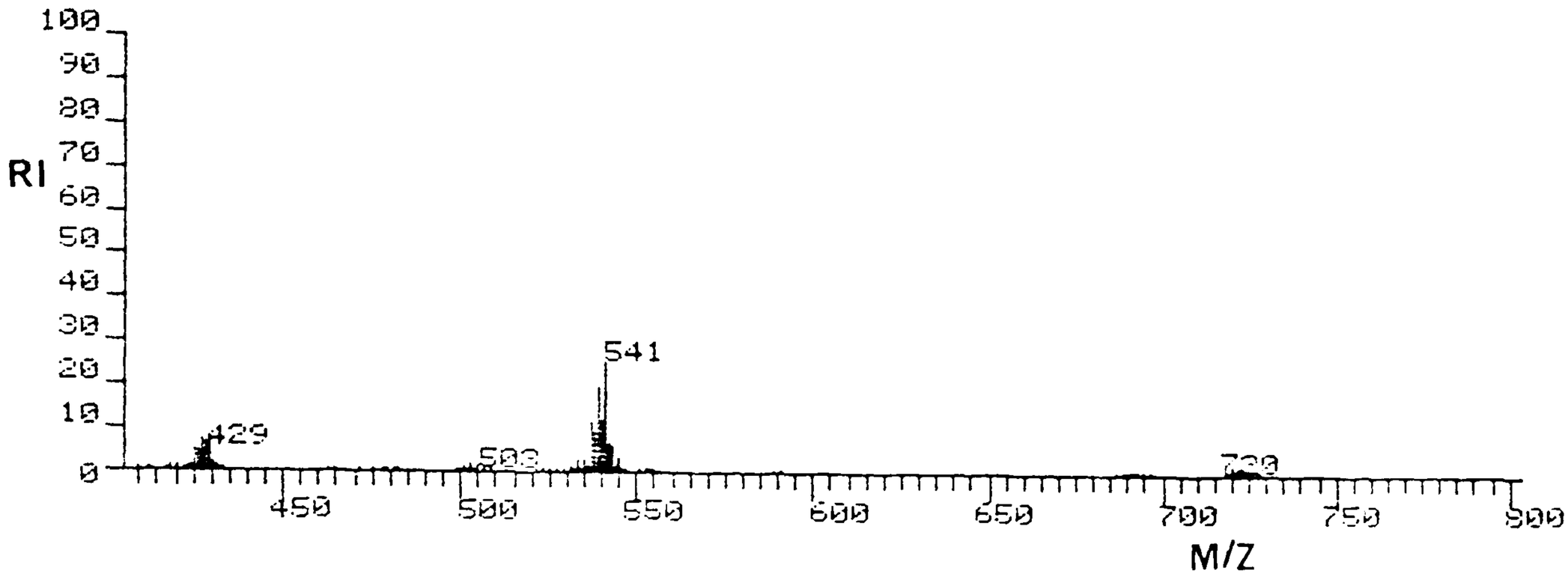

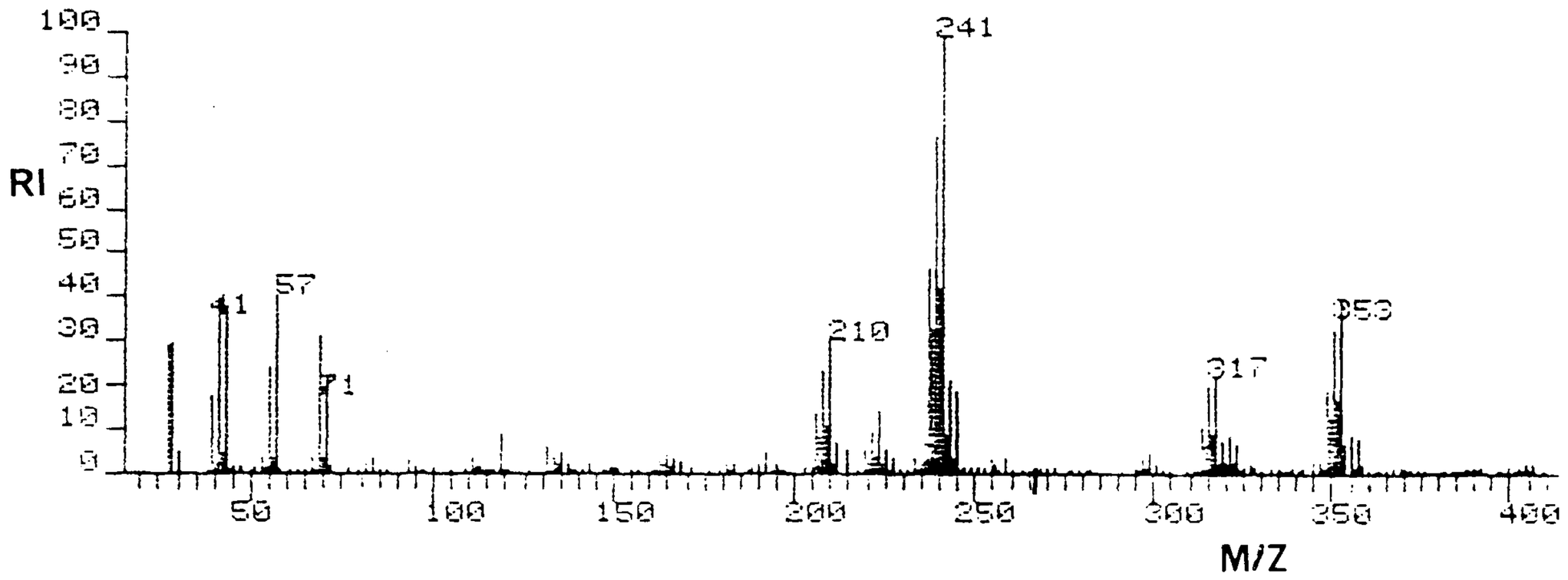

Fig. 4.4. Positive ion FAB spectrum of dimethyl tin stabiliser.

stabilisers studied. The spectrum shows a radical molecular cation of low abundance, with major peaks arising from fragmentation processes. These results are somewhat unusual in that FAB spectra of neutral analytes consist of a reasonably intense protonated pseudo-molecular ion peak, with little fragmentation. Acidic matrices (eg thioglycerol) and acidified matrix (eg glycerol, triethanolamine) solutions were used in an effort to produce protonated pseudo-molecular ions, without any success.

Lack of a molecular ion of reasonable abundance makes it difficult to assign the correct nature of an unknown. In these situations the normal course of action is to add a salt solution. This normally facilitates the formation of pseudo-molecular ions.

Addition of a saturated salt solution produced a cation adduct pseudo-molecular ion peak of three to four times the intensity of the molecular ion peak. The abundance was only marginally dependent upon the cation used, lithium being better than sodium, and potassium showing the least intense pseudo-molecular ion peak of the three. This trend can be explained in terms of the smaller ions having higher charge densities, and hence stronger binding with the analyte molecules. Although lithium is more efficient than sodium, it produces pseudo-molecular ion peaks 7 amu higher than the radical molecular ion peaks, the large number of tin isotope peaks causes confusion. Whereas sodium addition provides pseudo-molecular ion peaks 23 amu higher, preventing

ambiguity in identification. Although these pseudo-molecular ion peaks are only marginally more intense than the molecular ion peaks, their appearance on addition of a sodium salt confirms the molecular weight of the sample.

The appearance of radical molecular ions as opposed to protonated pseudo molecular ions is probably due to the low ionisation potential of tin (elemental tin has an ionisation potential of 7.3 eV)[65]. This theory has been used to rationalise the appearance of radical molecular ions in FAB.

Ion structures and fragmentation pathways can be deduced by use of CAD daughter ion spectra over a range of collision energies.

Fig 4.5 - 7 shows a series of low energy CAD daughter ion spectra for the sodium adduct pseudo molecular ion of the mono-n-octyl stabiliser.

As may be expected, increasing the collision energy enhances the degree of fragmentation. With a collision energy of 38 eV, the level of fragmentation observed was comparable to that seen with high energy CAD (8 KeV) obtained on a magnetic sector instrument. At a collision energy of 10 eV, two major daughter peaks were seen at m/z 639 and m/z 527. The peaks at m/z 639 arose from loss of a sodium and a thioglycollate ligand. The peak of m/z 527 occurs due to the loss of a sodium, a thioglycollate ligand, and an octene from a second thioglycollate ligand.

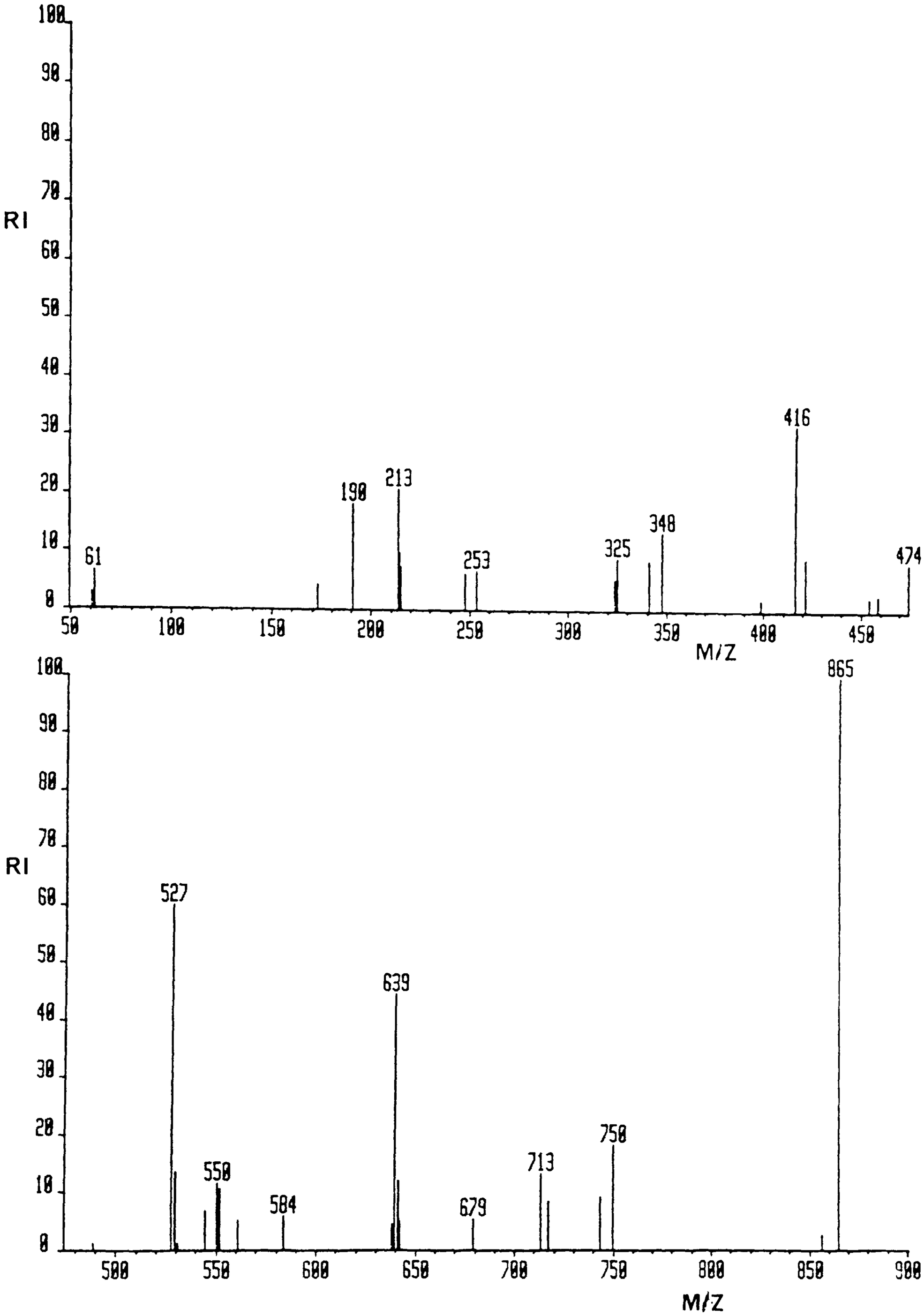

Fig. 4.5. CAD daughter ion spectrum of the m/z 865 ion from mono-n-octyl at a collision energy of 38 eV.

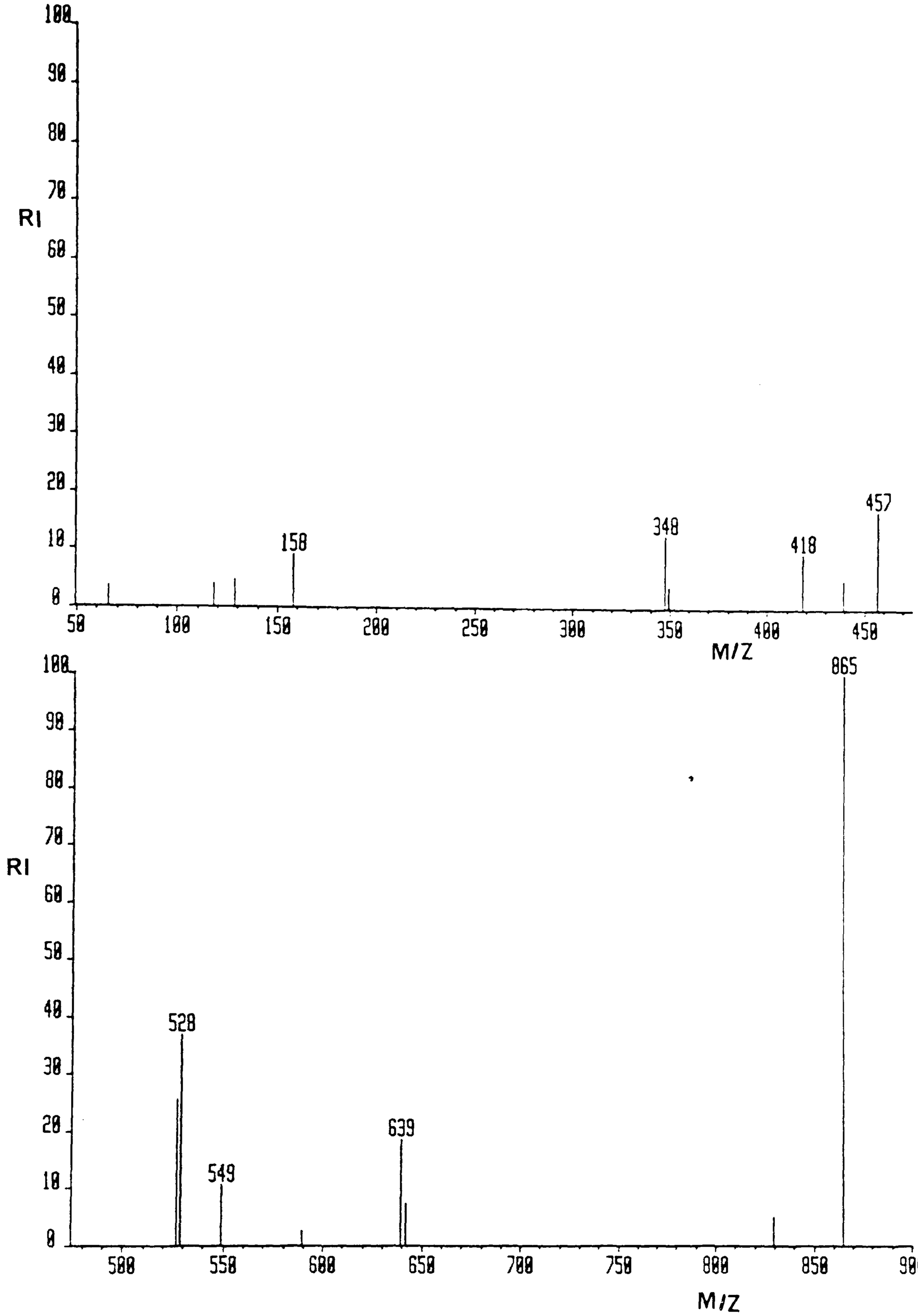

Fig. 4.6. CAD daughter ion spectrum of the m/z 865 ion from mono-n-octyl at a collision energy of 24 eV.

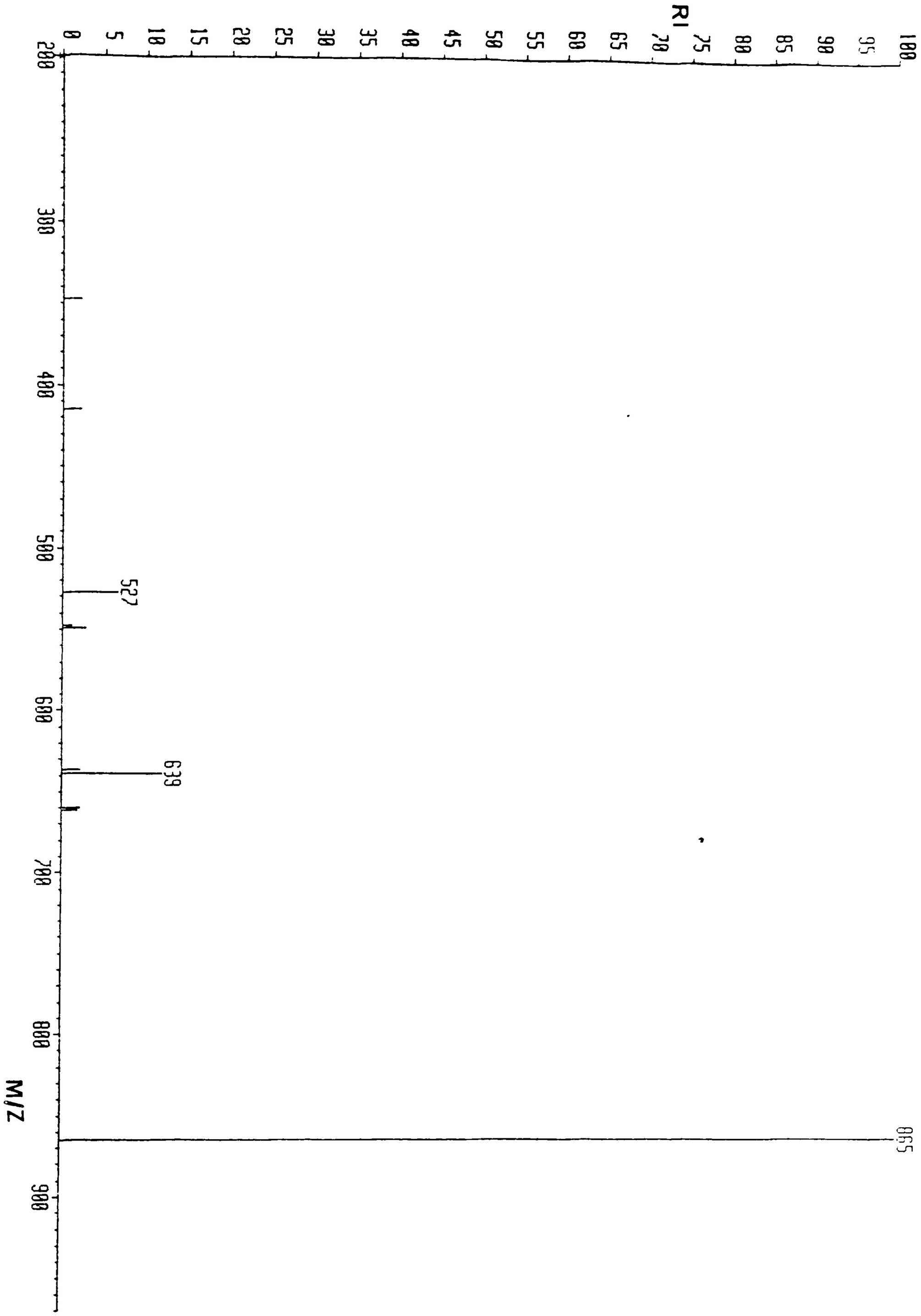

Fig. 4.7. CAD daughter ion spectrum of the m/z 865 ion from mono-n-octyl at a collision energy of 10 eV.

Fig 4.8 shows a 10 eV CAD daughter ion spectrum for the sodium adduct pseudo-molecular ion of the dimethyl stabiliser (m/z 579).

There were two major fragment ions: (a) m/z 457, arising from loss of a thioglycollate ligand. (b) m/z 263, corresponding to the loss of an octene, and a thioglycollate ligand. Therefore the sodium was retained in the fragment ions. This was also observed in the high energy CAD spectra obtained at 8 keV. In the case of the di-n-butyl stabiliser, both types of fragment ions were observed, with and without sodium retention. Therefore the presence of sodium in the fragment ion is dependent upon the size of the alkyl group bounded to tin. Decreasing alkyl group size favours sodium retention in the fragment ion.

A generalised series of fragmentation pathways may be drawn up for these compounds (Fig 4.9)

Three major unimolecular decomposition reactions are evident:

(a) Radical loss. A radical molecular cation can lose either an alkyl radical, which is bonded directly to tin or a thioglycollate ester radical.

(b) Alkyl migration. The following reaction scheme shows the migration of an alkyl group from tin to the

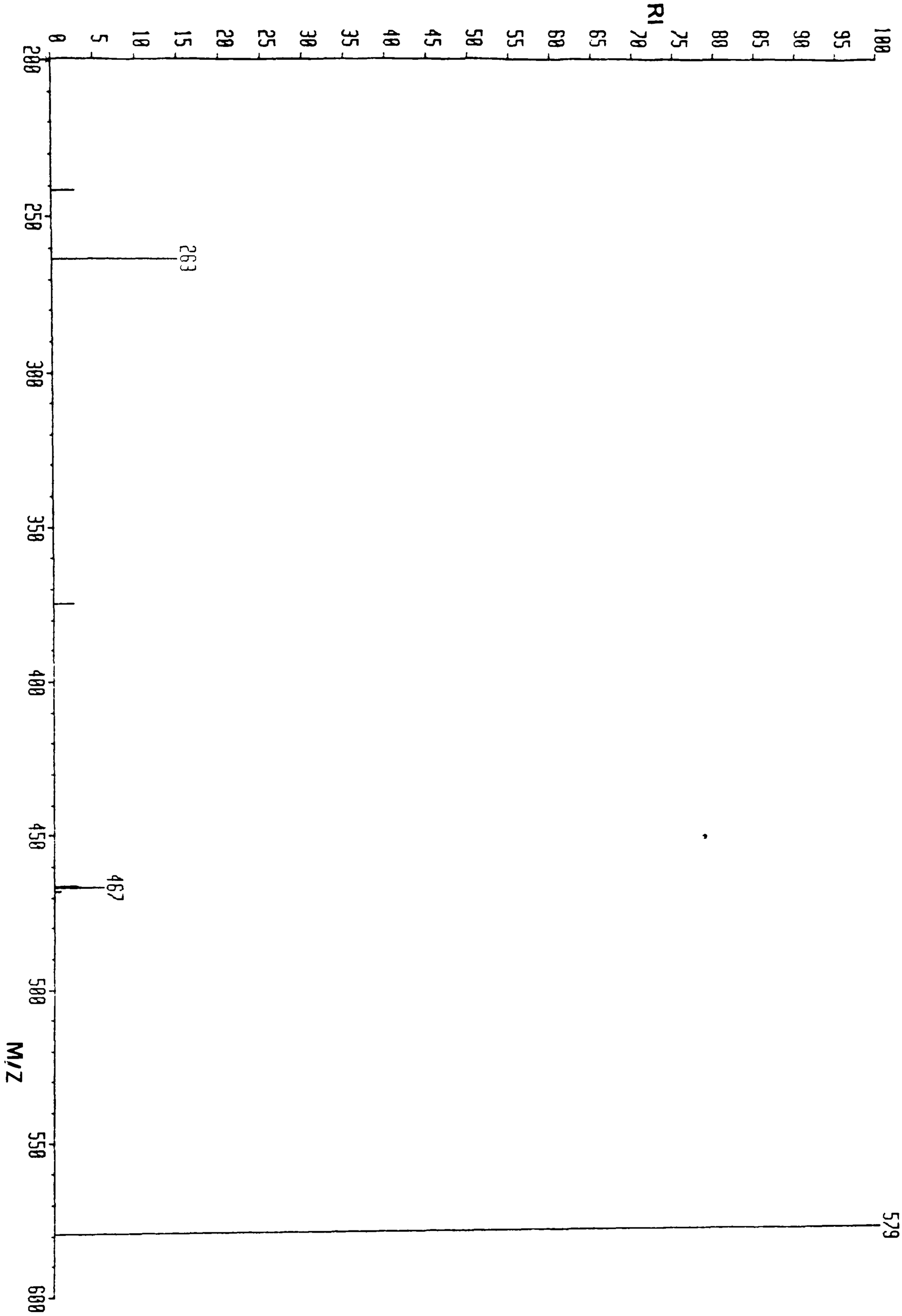

Fig. 4.8. CAD daugther ion spectrum of m/z 579 from dimethyl tin stabiliser at a collision energy of 10 eV.

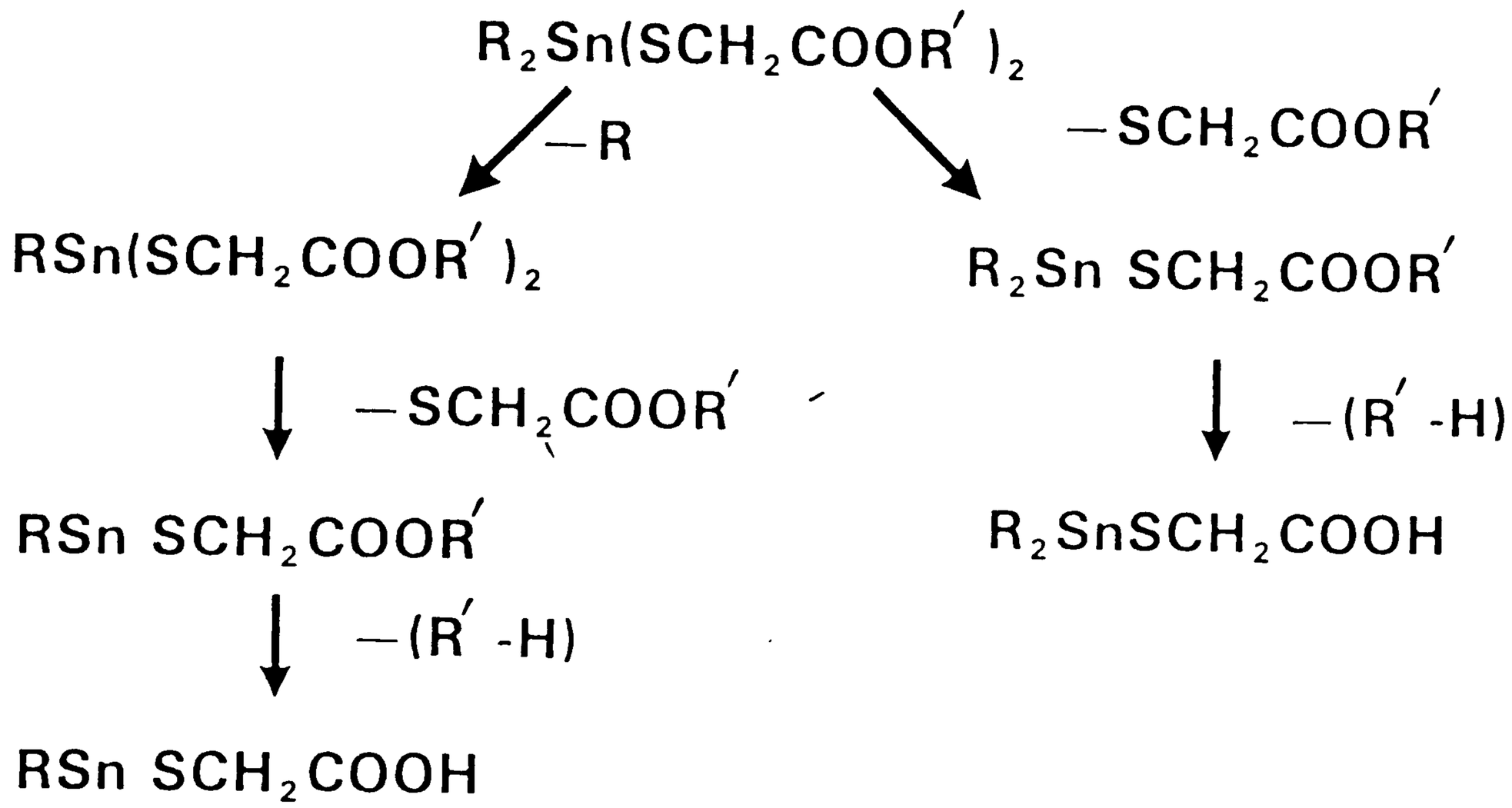

Fig. 4.9. Fragmentation pathways for organo-tin stabilisers.

sulphur of a thioglycollate ester, with subsequent expulsion of a neutral molecule.

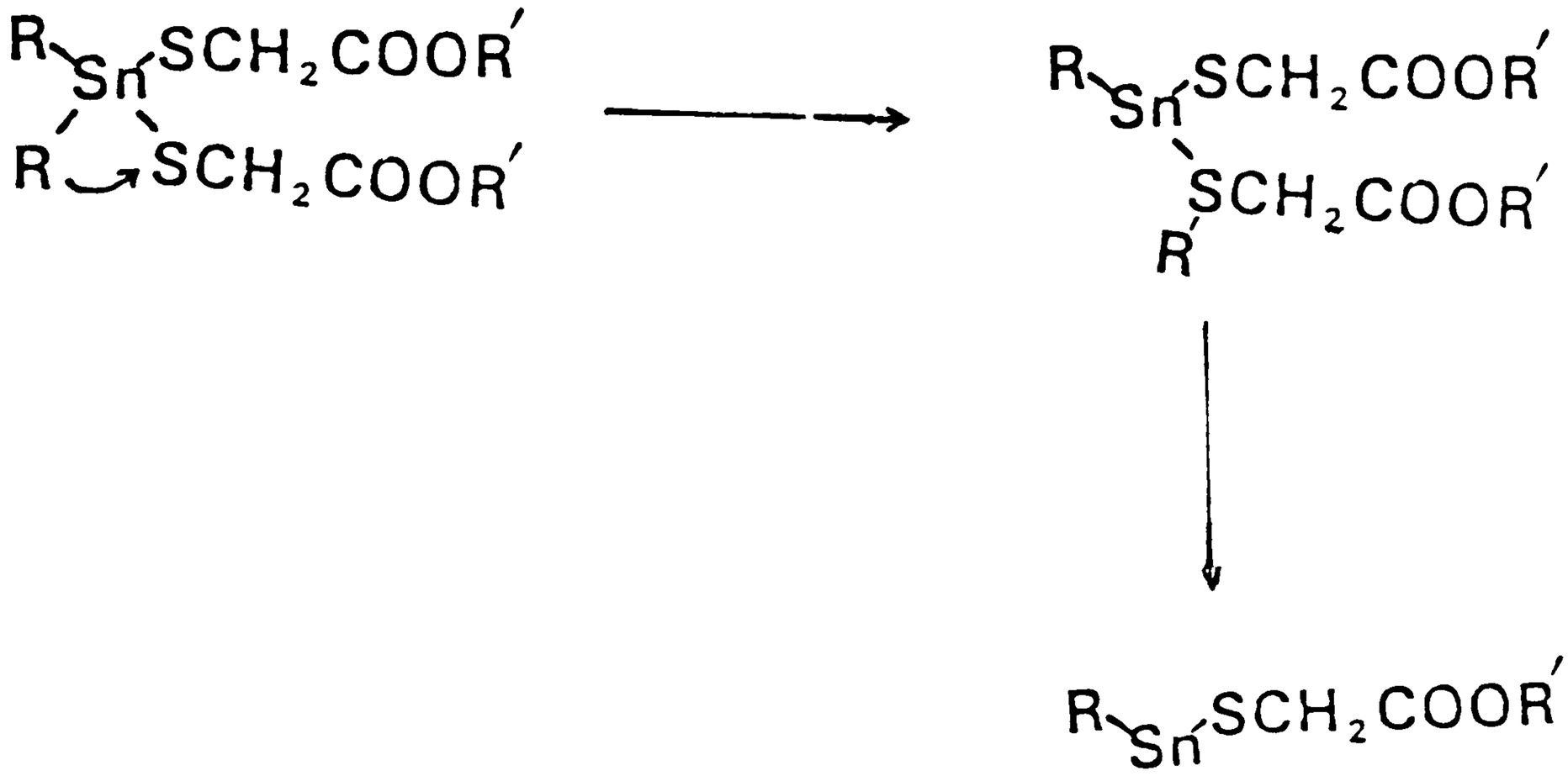

(34)

(c) Proton migration. Proton transfer from a thioglycollate alkyl, to the carbonyl of the thioglycollate can readily occur. With the compounds studied this resulted in the loss of an octene neutral.

The dominant peak in the dimethyl stabiliser spectrum occurs at m/z 241, which is due to the ion - $(CH_3)_2SnSCH_2CO_2H$. A dealkylated peak arose at m/z 211 corresponding to the ion - $SnSCH_2CO_2H$ which has a relative (to m/z 241) intensity of approximately 30%. Conversely the di-n-octyl compound provides spectra with the dominating peak m/z 211. The peak at m/z 437 - $(C_8H_{17})_2SnSCH_2CO_2H$ has a relative intensity (with respect to m/z 211) of about 60%. Therefore the ease of loss of a tin bonded alkyl group was dependent upon the size of that group, with an increasing propensity for alkyl loss with size.

In all cases thioglycollate ester radical loss was preferred to the loss of an alkyl radical. This is not surprising because of the greater stability of the thioglycollate to alkyl radical.

Unlike FAB, FD spectra showed only ions resulting from loss of radicals, with no rearrangement reactions being observed. This was due to the short residence times of ions within the source with FD (10^{-9} - 10^{-12} s) compared to FAB (10^{-4} - 10^{-6} s). As already stated radical loss decompositions have larger A factors than rearrangement reactions (hence faster rate constant), and are therefore predomently observed in an FD source. Since tin stabilisers undergo facile rearrangement reactions, lower relative molecular ion abundances occurred when FAB ionisation was employed compared with FD.

Close investigation of the FAB spectra of these compounds revealed the presence of tin containing species at higher masses than the molecular ion. The structures of these ions were deduced by the use of high energy CAD in conjunction with daughter ion linked scans.

The highest mass ion detected for the di-n-octyl occurred at m/z 1016.

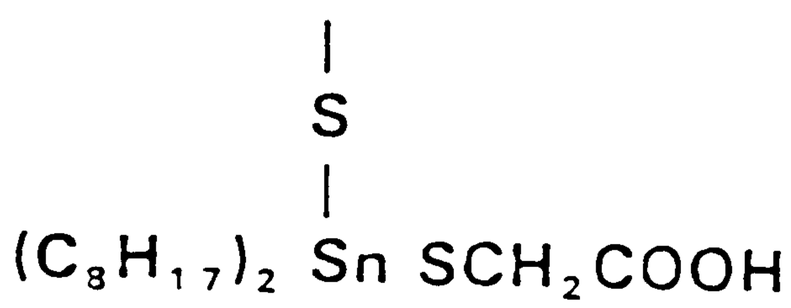

(27)

Addition of a saturated salt solution did not produce any higher mass peaks.

The calculated mass of the ion is 1018 amu using the relative atomic masses of the most abundant isotopes. The difference of two amu is due to the superimposition of all the isotope patterns of the elements in the ion. This ion can fragment in a number of ways, these are indicated in Fig 4.10.

From this, all the other high mass peaks could be identified.

Confirmation of the ions' composition was obtained by comparison of the calculated theoretical (computer generated) and experimental isotope patterns. The latter were an average of over fifty scans at a scan speed of 30 secdec^{-1} in order to reduce statistical fluctuations in the isotope pattern which occur when studying FAB generated ions of such low abundance. It is, of course,

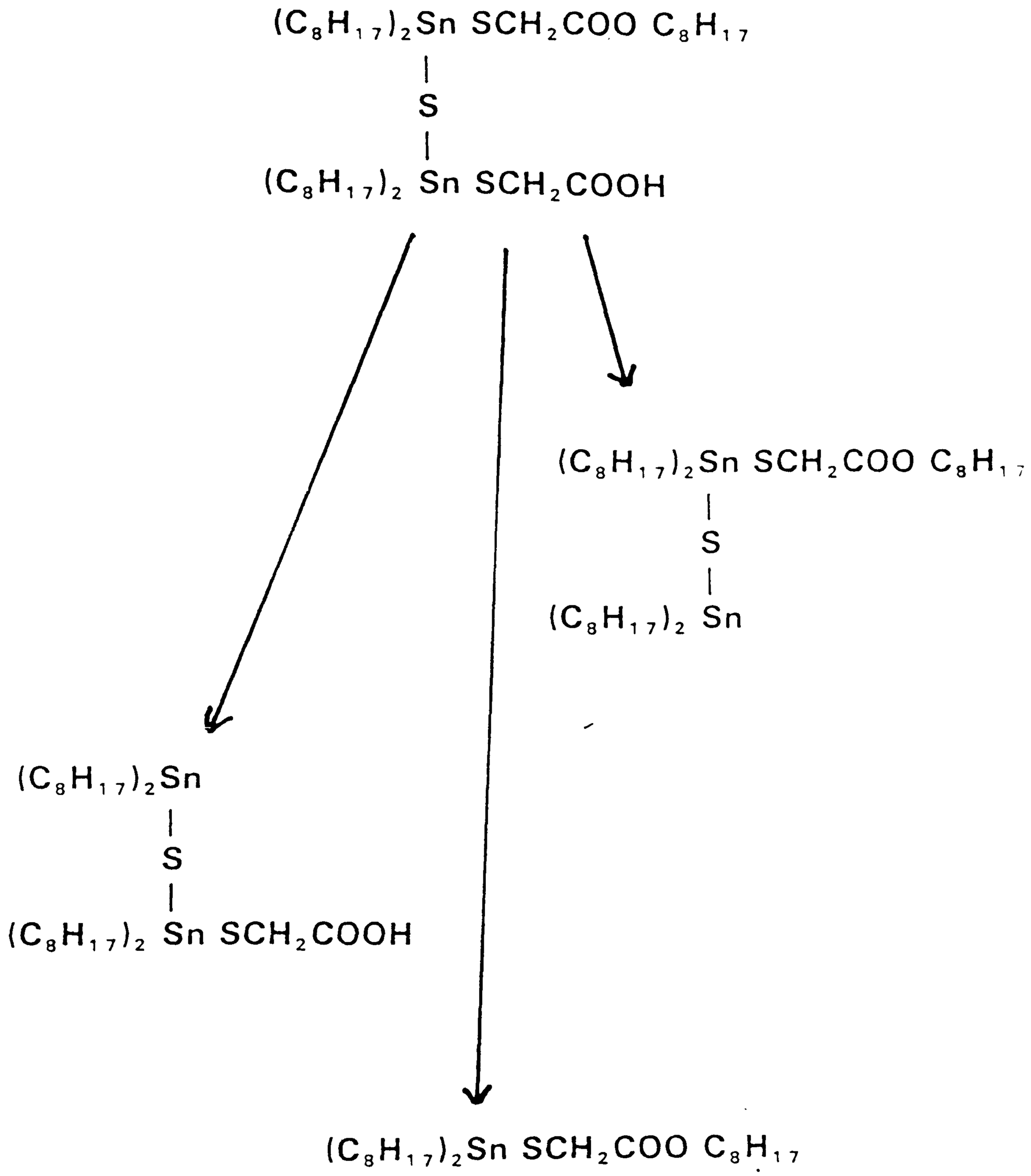

Fig. 4.10. Fragmentation pathways for ion m/z 1016.

possible that the origin of the ions depicted in Fig 4.10 was a molecule of the structure depicted below.

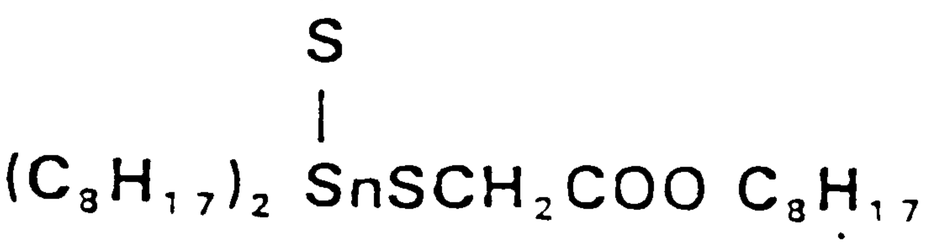

(22)

The isotope cluster centered at 1016 amu arose from a rearrangement loss of an octene neutral. No ion could be detected which corresponds to the above formula. This would not be surprising because of the low abundance of molecular ions obtained with these compounds.

4.3.3.2 Negative Ion FAB

Fig 4.11 shows a negative ion FAB spectrum of the mono-n-octyl stabiliser. Our results differ somewhat from Bentz et al. In contrast to the positive ion FAB spectra, they did not detect any tin containing ions in their spectra.

The major peaks in Fig 4.11 arise at m/z 203. This may be due to either (a) loss of a thioglycollate ligand with charge retention on the ligand or (b) proton abstraction from unbound ligand in the sample, which has been shown to be present in these samples.

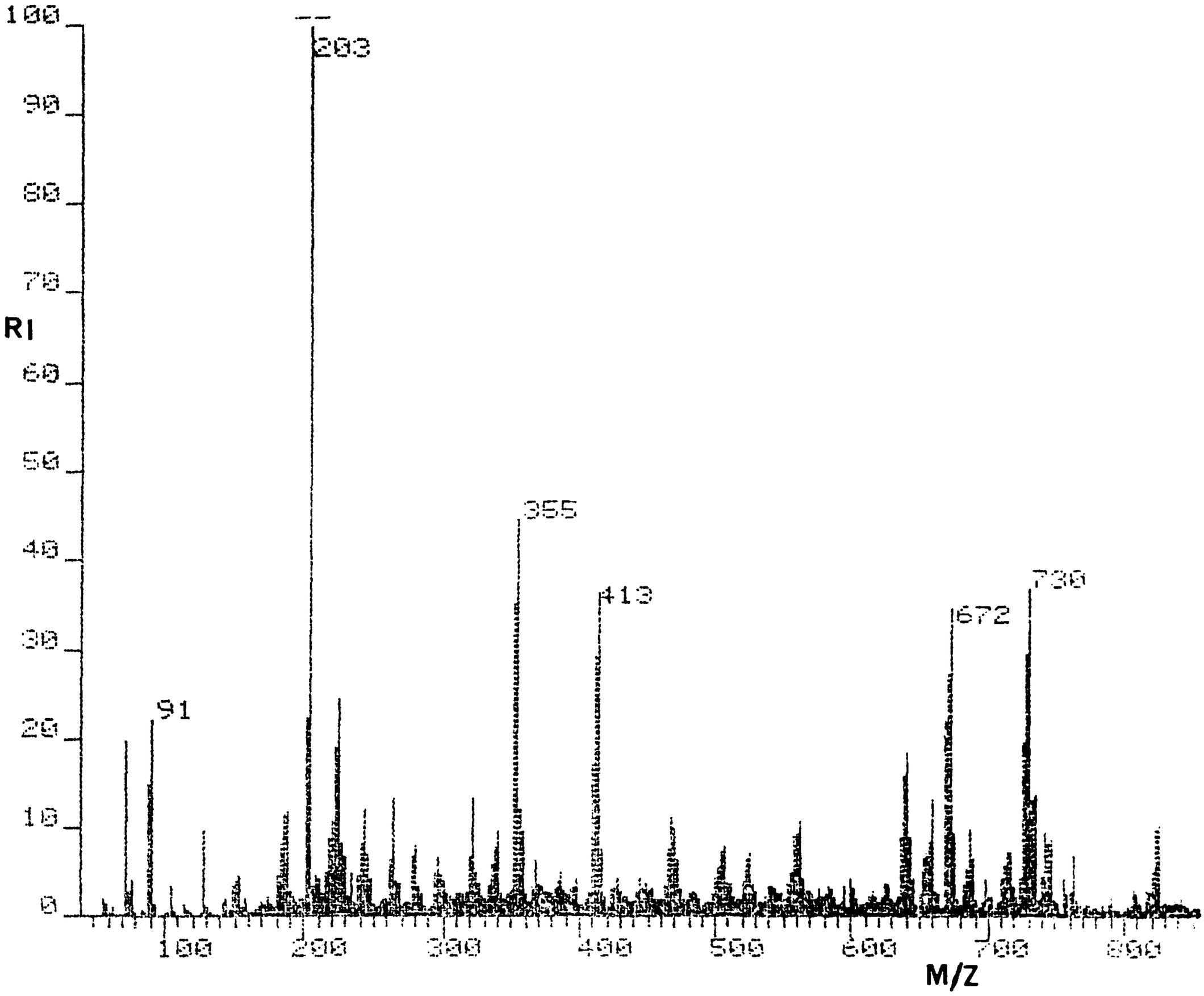

Fig. 4.11. Negative ion FAB spectrum of mono-n-octyl tin stabiliser.

The negative ion spectra obtained were similar to the positive ion in that no discernable molecular ion peaks were observed. Major tin-containing peaks in the negative ion spectra could arise from: (a) Alkyl loss from the thioglycollate ester (b) loss of $CH_2CO_2C_8H_{17}$. These losses lead to ions of two types

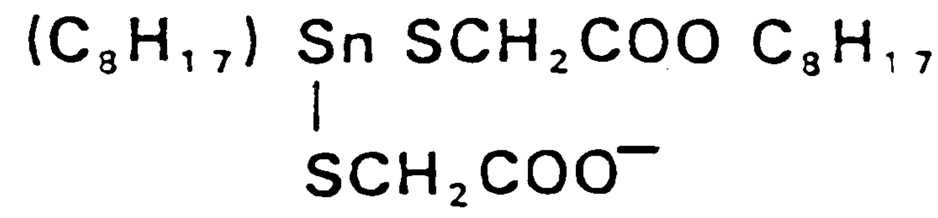

(29)

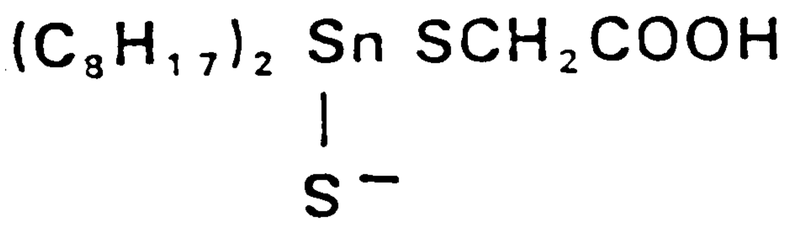

(30)

In an attempt to create negative molecular anions by proton abstraction from the molecular neutral, strong base was added. Also anionic attachment was tried in a bid to provide pseudo-molecular ions. Neither of these methods provided molecular weight information.

4.3.4. ^{119}Sn NMR

There are two NMR active tin nuclei; ^{117}Sn and ^{119}Sn. They both have spin of a half, and are of roughly the same natural abundance, although ^{119}Sn NMR is more sensitive than ^{117}Sn NMR. Therefore the ^{119}Sn isotope was studied. Since the spectra were acquired under proton decoupled conditions they were simple, comprising of only one or two peaks. In contrast the carbon and proton spectra were highly complex.

All the ^{119}Sn NMR spectra consisted of singlets, except for the di-n-octyl stabiliser. The chemical shifts obtained were; dimethyl 74 ppm, di-n-butyl 60 ppm, mono-n-octyl 61 ppm (relative to the external standard).

Fig 4.12 shows the ^{119}Sn NMR spectrum of the di-n-octyl stabiliser. The presence of the two peaks indicates the possibility of two tin containing species. Doping of a di-n-octyl sample with mono-n-octyl stabiliser increased the relative intensity of the peak at 61 ppm suggesting some mono-n-octyl stabiliser was present in the di-n-octyl sample. No mono-n-octyl species was observed in the FAB spectrum of the di-n-octyl sample. This was probably due to the greater concentration of di-n-octyl in the sample, in comparison to the mono-n-octyl. In addition, the di-n-octyl species is probably more surface active than the mono-n-octyl, so suppressing the latter. The greater surface activity of the di-n-octyl stabiliser is due to the replacement of a more hydrophillic thioglycollate ester by the hydrophobic octyl group.

Presence of the di-tin species is not obvious from the NMR spectrum, because the chemical environment of the tin atoms is similar in both cases. Careful study of the peak at 66.5 ppm indicates the presence of a shoulder. This could be due to the di-tin species.

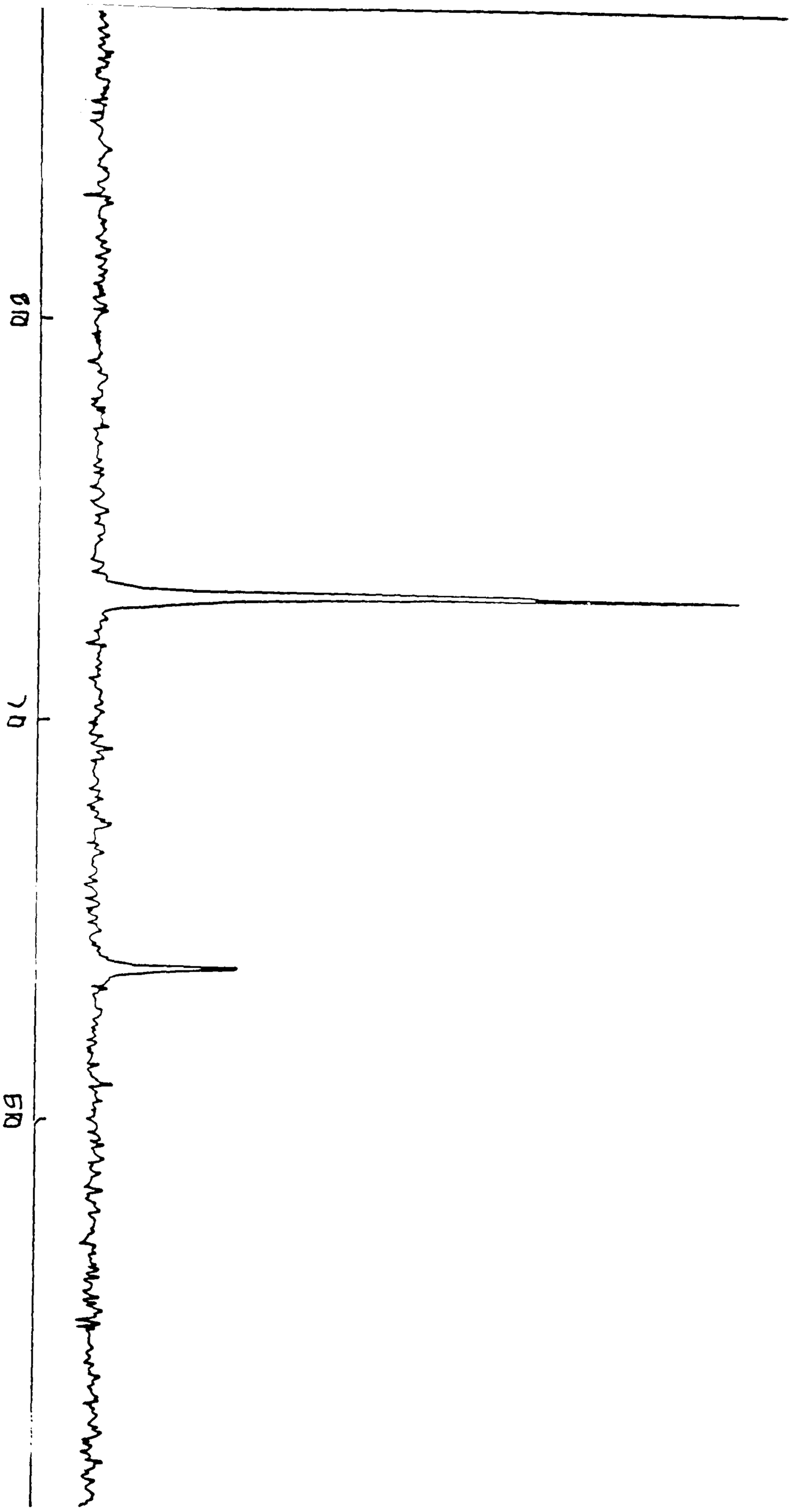

Fig. 4.12. ^{119}Sn NMR spectrum of the di-n-octyl tin stabiliser.

4.3.5. Analysis of an Extracted Tin Stabiliser

The extraction of tin stabilisers from plastic bottles is well documented[107,108]. A sixteen hour soxhlet extraction using diethyl ether as solvent, removed the tin stabiliser present from a weighed amount of homogenized PVC bottle. A sample of ether extract (10 µl) was placed on the FAB probe tip. This was then placed in the solids inlet line, enabling the solvent to be pumped away. The process was repeated a total of five times. Nitrobenzyl alcohol (5 µl) was added to the tip as a matrix. Positive ion FAB spectra were then acquired, a representative of which is shown in Fig 4.13. Comparison of this spectrum with those spectra obtained for the standards, showed that the extracted stabiliser was di-n-octyl tin di-iso-octyl thioglycollate. Confirmation of this result came from the ^{119}Sn NMR spectrum.

Also present in the ether extract are: (a) plasticisers eg esters of aliphatic and aromatic di and tri carboxylic acids and of phosphoric acids. (b) Lubricants eg long chain aliphatic acids, esters and alcohols. Even in the presence of these other additives FAB produces analytically useful spectra for determining the organo-tin stabiliser present.

4.4 Conclusion

Positive ion FABMS was found to provide reasonable qualitative data for organo-tin stabilisers, although the relative abundance of the molecular ion region was low. Confirmation could be obtained by use of FD, and ^{119}Sn NMR.

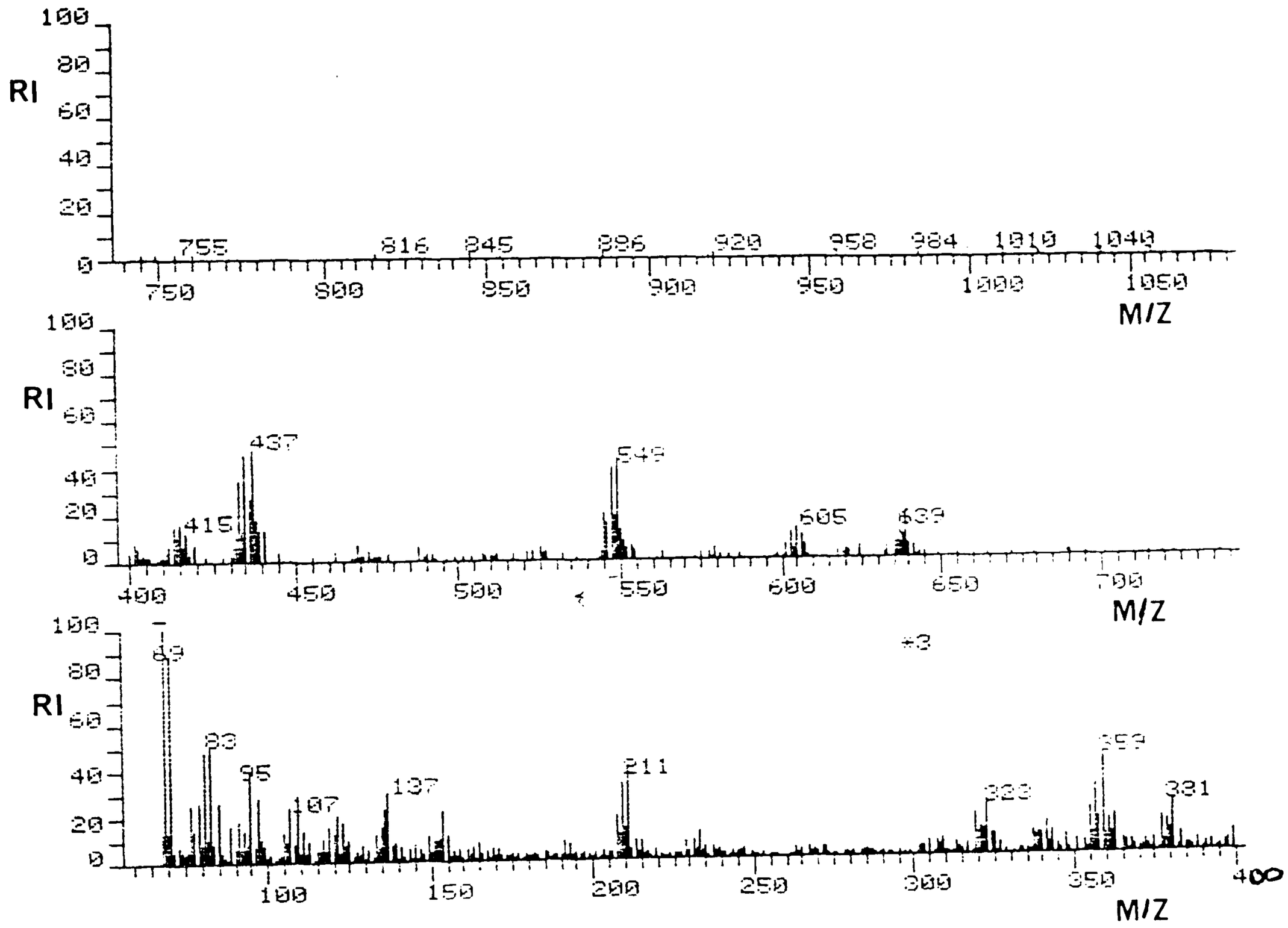

Fig. 4.13. Positive ion FAB spectrum of extracted tin stabiliser from PVC bottle.

Chapter V

MASS SPECTRA OF 3-NITRO-CHROMENES, 3-NITRO-CHROMANS AND CORRESPONDING CHROMAN-3-ONE-OXIMES

1. Introduction

3-Nitrochromenes (31), constitute a class of biologically active oxygen heterocycles[112,113,114]. These compounds can be synthesized by condensation of o-hydroxybenzaldehydes with b-nitrostyrenes, in the presence of basic alumina, using sonic acceleration[115]. Interest in nitrochromenes reflects the reported[116] radioprotective properties of chromenes containing electron attracting substituents at the 3-position. The corresponding saturated analogues, 3-nitrochromans (32), have only recently been synthesized by reduction of the corresponding 3-nitrochromenes with sodium borohydride in methanol/tetrahydrofuran[117]. Chroman-3-one oximes (33), are a new class of oxygen heterocycles, which have only recently been synthesized by the tin dichloride reduction of the corresponding 3-nitrochromenes[118]. These oximes are important stable derivatives of the reactive and almost unstudied chroman-3-ones[119]. In view of the biological activity of the chromenes, and novelty of the chromans and oximes, it was thought a study of their mass spectra would be of interest.

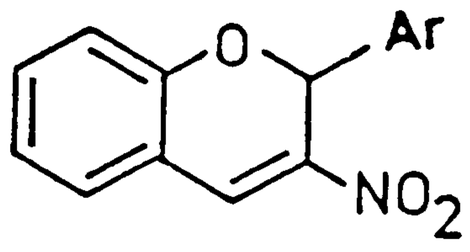

(31)

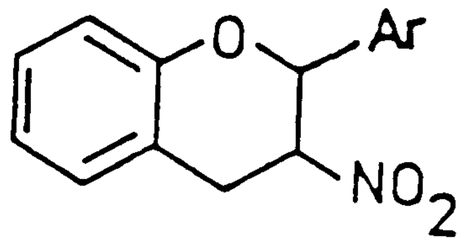

(32)

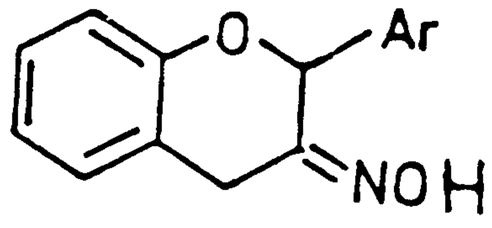

(33)

5.2. Experimental

The synthesis of the compounds studied have been published[115,117,118].

2-Phenyl-3,4-dideuterio-3-nitrochroman was prepared by reduction of 2-phenyl-3-nitrochromene with sodium borohydride in CH_3OD/tetrahydrofuran. All of the chromans and chromenes studied were obtained from R. S. Varma, University of Tennessee.

Mass spectra were recorded using a MS80 (Kratos Analytical) double focusing mass spectrometer operating at an accelerating voltage of 4 KV. EI spectra were obtained by ionisation with 70 eV electrons at a source pressure of about $2x10^{-6}$ Torr, and temperature of 528 K. The instrument was operated with a mass resolution of 1000, and a scan speed of 3 $secdec^{-1}$. Structural identity of ions in the spectra was confirmed by high mass resolution measurements (7,800), using perfluorokerosine as an internal standard.

The resonance electron capture spectra were obtained using ammonia as a buffer gas at a source pressure of approximately 1 Torr.

5.3. Comparison of 3-Nitrochromenes and 3-Nitrochromans

The mass spectra obtained for a series of eight 2-aryl-3-nitrochromenes and ten corresponding chromans show a number of interesting features, which are discussed below.

5.3.1. Electron Impact Mass Spectra

Table 5.1. shows the major peaks observed in the EI mass spectra of eight 2-aryl-3-nitrochromenes expressed as a percentage of the base peaks. Peaks with relative intensities of less than 15% of the base peaks are omitted. The EI mass spectra of ten corresponding 2-aryl-3-nitrochromenes are given in table 5.2.

Upon careful inspection of the spectra, a number of differences become apparent between the two compound classes. These differences can be graphically shown by a comparison of the spectra from the parent 2-phenyl compounds (Fig 5.1.)

(a) Although all the compounds showed significant molecular ion peaks, the intensities observed for the chromenes tended to be higher than for the analogous chromans. Thus the relative intensities of the molecular ion peaks in the spectra of the corresponding pairs (i) and (ix), (ii) and (x), (iii) and (xii), (iv) and (xiii) are 41% and 18%, 45% and 28%, 30% and 9%, 21% and 9% respectively. This trend probably reflects a real difference in the stability of the ionised molecules, with respect to fragmentation, because the percentage of the total ion current carried by the molecular ion was systematically higher for chromenes (typically 3 - 8%) than for the analogous chromans (typically 1 - 5%). The relative abundance of the molecular ion in both classes of heterocycle was increased by the presence of electron rich alkoxy substituents in the 2-aryl group or at the 8-

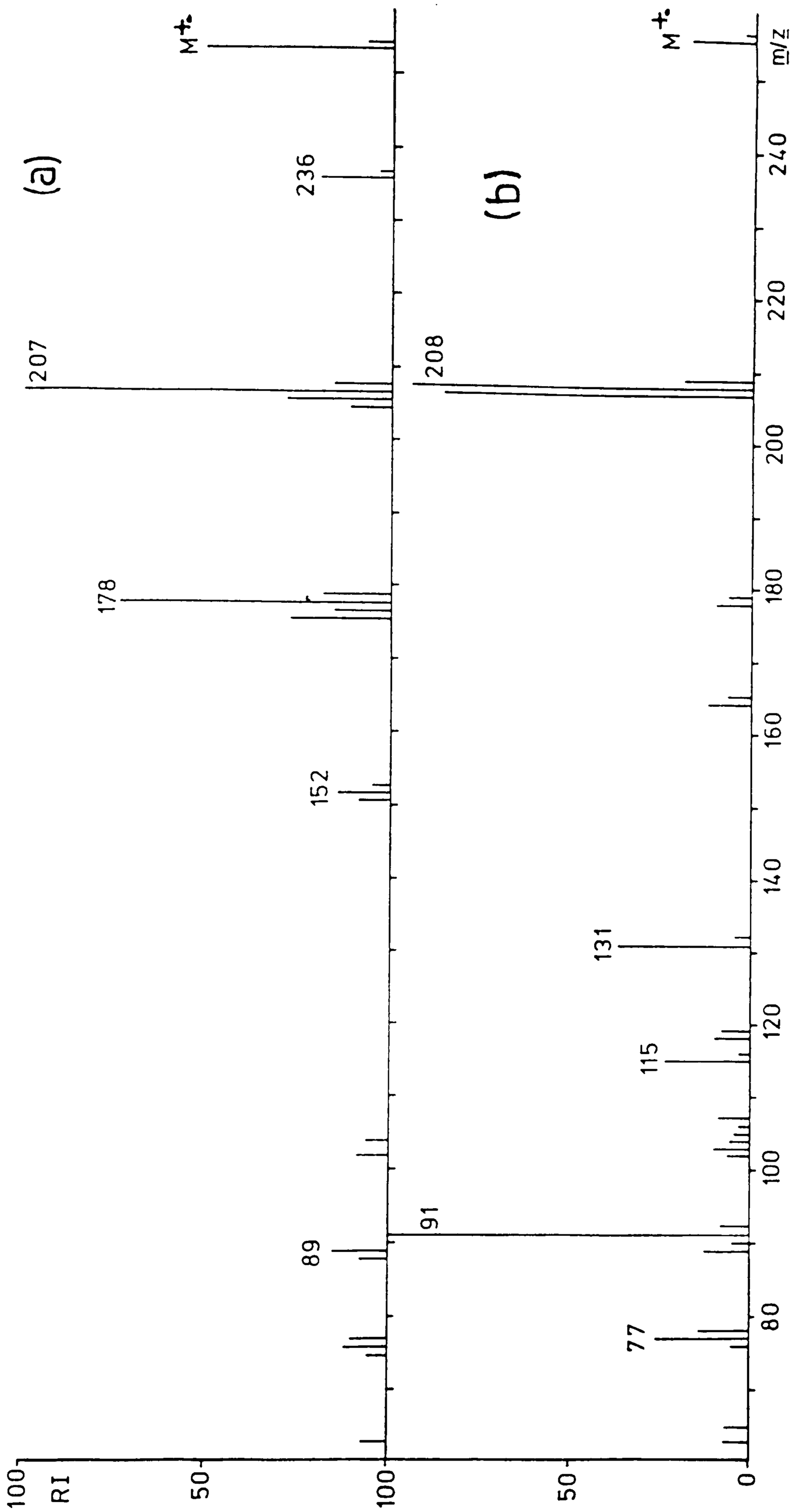

Fig. 5.1. EI spectra for (a) 2-phenyl-3-nitrochromene (b) 2-phenyl-3-nitrochroman.

Compound	m/z and relative abundance
2-phenyl-3-nitrochromene (I)	254 (7); 253 [M$^{+\cdot}$] (41); 236 (19); 208 (16); 207 (100); 206 (30); 205 (12); 179 (19); 178 (74); 177 (16); 176 (28); 152 (15); 89 (16)
2-(4-isopropyl-phenyl)-3-nitro-chromene (II)	296 (10); 295 [M$^{+\cdot}$] (45); 278 (22); 250 (49); 249 (100); 248 (18); 235 (18); 234 (71); 233 (68); 220 (15); 207 (28); 205 (24); 179 (21); 178 (29); 176 (29)
2-(1-naphthyl)-3-nitro-chromene (III)	304 (4); 303 [M$^{+\cdot}$] (30); 258 (30); 257 (100); 256 (24); 255 (58); 229 (40); 228 (28); 227 (18); 226 (22)
2-(2-naphthyl)-3-nitrochromene(IV)	304 (4); 303 [M$^{+\cdot}$] (21); 258 (23); 257 (100); 256 (19); 255 (30); 249 (15); 229 (26); 228 (33); 227 (16); 226 (24)
2-(3,4-diethoxy-phenyl)3-methoxy-3-nitrochromene (V)	372 (24); 371 [M$^{+\cdot}$] (84); 326 (35); 325 (100); 298 (15); 297 (72); 281 (19); 269 (39); 268 (20); 253 (16); 252 (18); 206 (28); 152 (20); 115 (16)
2-(1-naphthyl)-3-methoxy-3-nitro-chromene (VI)	334 (11); 333 [M$^{+\cdot}$] (50); 316 (17); 288 (24); 287 (100); 286 (30); 285 (41); 272 (27); 271 (70); 257 (25); 255 (23); 244 (26); 243 (22); 228 (17); 227 (15); 226 (17); 216 (22); 215 (67); 213 (18); 189 (41); 165 (16); 152 (23); 107 (37)
2-(1-naphthyl)-6-chloro-3-nitro-chromene (VII)	340 (2); 339 (10); 338 (7); 337 [M$^{+\cdot}$] (30); 293 (27); 292 (26); 291 (97); 290 (28); 289 (56); 256 (68); 253 (100); 228 (40); 227 (28); 226 (62); 223 (15); 128 (19); 113 (50); 101 (18)
2-phenyl-3,6-dinitro-chromene (VIII)	299 (5); 298 [M$^{+\cdot}$] (23); 281 (37); 253 (18); 252 (100); 251 (30); 207 (14); 206 (85); 205 (34); 178 (20); 177 (25); 176 (31); 165 (18); 152 (23); 151 (16); 102 (15); 76 (16)

Table 5.1 - Relative peak intensities for EI mass-spectra of eight 2-aryl-3-nitrochromenes

Compound	m/z and relative abundance
2-phenyl-3-nitrochroman (IX)	256 (3); 255 [M'·] (18); 209 (20); 208 (95); 207 (86); 131 (38); 115 (25); 91 (100); 78 (15); 77 (27)
2-[4-isopropyl-phenyl)-3-nitro-chroman (X)	298 (6); 297 [M'·] (28); 251 (29); 250 (97); 249 (64); 235 (26); 208 (17); 207 (70); 134 (15); 133 (100); 131 (37); 118 (40); 117 (30); 115 (33); 107 (19); 105 (36); 103 (15); 91 (39); 77 (29)
2-phenyl-8-methoxy-3-nitrochroman (XI)	286 (8); 285 [M'·] (48); 239 (11); 238 (43); 237 (23); 149 (21); 136 (15); 115 (19); 91 (100); 77 (14)
2-(1-naphthyl)-3-nitro-chroman (XII)	306 (2); 305 [M'·] (9); 258 (14); 257 (13); 165 (30); 152 (21); 141 (100); 131 (16); 128 (19); 127 (19); 107 (33); 77 (
2-(2-naphthyl)-3-nitrochroman (XIII)	306 (2); 305 [M'·] (9); 257 (14); 258 (57); 257 (27); 165 (15); 156 (18); 155(20); 141 (100); 131 (19); 127 (27)
2-(3,4-diethoxy-phenyl)-3-nitro-chroman (XIV)	344 (13); 345 [M'·] (55); 297 (10); 296 (34); 239 15); 180 (14); 179 (100); 165 (19); 152 (18); 151 (94); 131 (73); 123 (90); 118 (21); 107 (16); 77 (28)
2-phenyl-6-chloro-3-nitro-chroman (XV)	291 (2); 290 (1); 289 [M'·] (6); 244 (7); 243 (9); 242 (20); 241 (16); 91 (100); 89 (17); 77 (20)

Compound	m/z and relative abundance
2-(1-naphthyl)-8-methoxy-3-nitro-chroman (XVI)	336 (3); 335 [$M^{+\cdot}$] (14); 289 (4); 288 (9); 165 (22); 152 (18); 141 (100); 137 (19); 91 (32)
2-phenyl-3-nitro-5,6-benzchroman (XVII)	306 (3); 305 [$M^{+\cdot}$] (18); 257 (14); 258 (62); 257 (35); 181 (38); 152 (15); 128 (29); 115 (37); 91 (100); 77 (21)
2-(1-naphthyl)-3-nitro-5,6,-benzchroman (XVIII)	350 (6); 355 [$M^{+\cdot}$] (24); 309 (11); 308 (44); 307 (17); 181 (19); 165 (48); 153 (24); 152 (42); 141 (100); 128 (23); 127 (17)

Table 5.2 - Relative peak intensities for EI mass spectra of ten-2-aryl-nitrochromans

position, but it was reduced by the substitution of a 2-naphthyl group for the 2-phenyl group.

(b) Loss of an hydroxyl radical from the molecular ion produced only a small peak in the spectra of nitrochromenes and nitrochromans. This reaction, which is often of importance for ionised nitrocompounds[104], was of marginally greater significance in the nitrochromenes series. However, at the low internal energies appropriate to the decomposition of metastable ions, hydroxyl elimination become the dominant reaction of the ionised nitrochromenes. Conversely the corresponding nitrochroman radical cation did not expel hydroxyl radicals to any appreciable extent in metastable transitions.

(c) The third difference between the spectra of nitrochromenes and nitrochromans concerns the intensity of the peaks produced by loss of NO_2 and HNO_2 from the molecular ion. The base peak in the spectra of each of the eight nitrochromenes studied in this work corresponds to the loss of a nitro group: $[M-NO_2]^+$. Only a much smaller peak was present at $[M-HNO_2]^{+\cdot}$, although there was often a peak at $[M-NO_2-H_2]^+$ of sizable intensity. In contrast, $[M-HNO_2]^{+\cdot}$ was the most abundant of the group of three ions at $[M-NO_2]^+$, $[M-HNO_2]^{+\cdot}$ and $[M-NO_2-H_2]^+$ in the spectra of nitrochromans. However even in the cases of (ix) and (x), $[M-HNO_2]^{+\cdot}$ was not the most abundant ion in the spectrum, though it did rival the base peak in intensity. The intensity of the peak at $[M-HNO_2]^+$ declined sharply on progressing to the

2-naphthyl-3-nitrochromans, or on adding substituents at the 6- or 8- positions. Nevertheless, loss of HNO_2 remains of importance at low internal energies, as evidenced by the appearance of a metastable peak for the process.

This reaction is rare for ionised nitrocompounds. It seems likely that HONO, rather than HNO_2, was lost.

Hydrogen transfer from the 2-position of the ionised chroman to oxygen, leads to the stabilised cation radical subsequent expulsion of HONO then produces an extremely stable daughter ion. This mechanism is supported by the behaviour of the deuterium labelled analogue shown in reaction (36). This compound expeled specifically [HNO_2] in metastable transitions. The only plausible alternative mechanism would involve hydrogen abstraction from the 4 position, but this would not yield a daughter ion having the stabilising structural features of (39).

Elimination of an hydrogen radical from [M-HNO_2]$^{+\cdot}$ would lead to the formation of the benzopyrilium cation (40), which would be expected to be extremely stable.

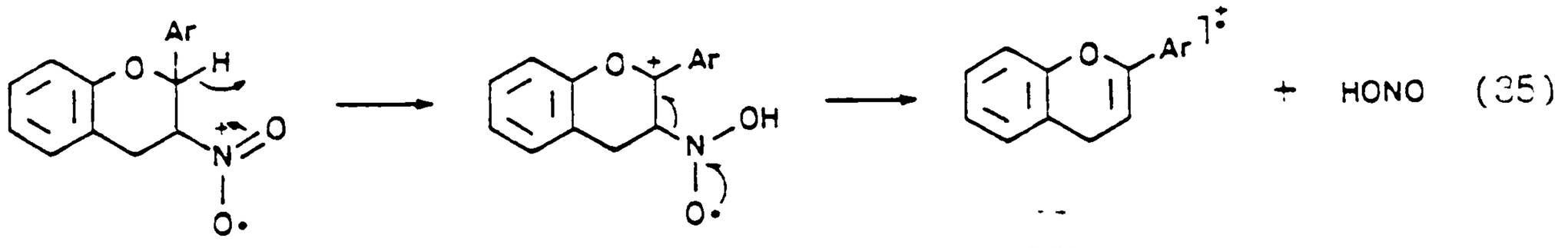

(34) (35) (36)

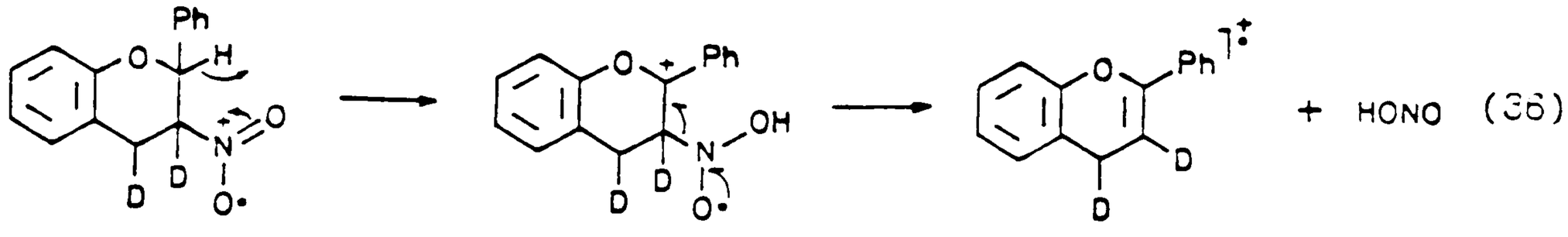

(37) (38) (39)

However, other routes to the ion at $[M-(H_2NO_2)]^-$ are possible, including hydrogen loss from $[M-NO_2]^+$. Despite this uncertainty, the greater abundance of the ions at $[M-(HNO_2)]^{+\cdot}$ and $[M-(H_2NO_2)]^+$ in the spectra of the chromans can be interpreted in terms of the enhanced stability of these ions compared to the corresponding species in the chromene spectra.

(d) The fourth contrast between the spectra of the chromenes and those of the chromans was the appearance of a structurally informative ion of nominal structure ($ArCH_2$) as the base peak in the spectra of the chromans. Consequently the formula of the 2-aryl substituent in these nitrochromans was defined by this peak. A possible route for the production of the ion at $[ArCH_2]$ is given in Fig 5.2. (37).

Following $NO_2\cdot$ loss from the molecular ion, the derived ion, (42), undergoes a hydride shift to form the stabilised ion (43), which may be represented as (44). Ring opening of (44) to (45), and a subsequent hydride shift, leads to (46), which cyclises to (47). Cleavage of the exocyclic carbon carbon bond the results in expulsion of benzofuran and formation of $[ArCH_2]^+$. Other mechanisms are feasible, including a modification of the proposed scheme to allow for production of the isomeric tropylium cation as the daughter ion. When 2-phenyl-3,4-dideuterio-3-nitrochroman was investigated, the relative abundance of the ion at m/z 91,92, and 93 were 15:100:18. The preponderance of $C_7H_6O^+$ (m/z 92) can be

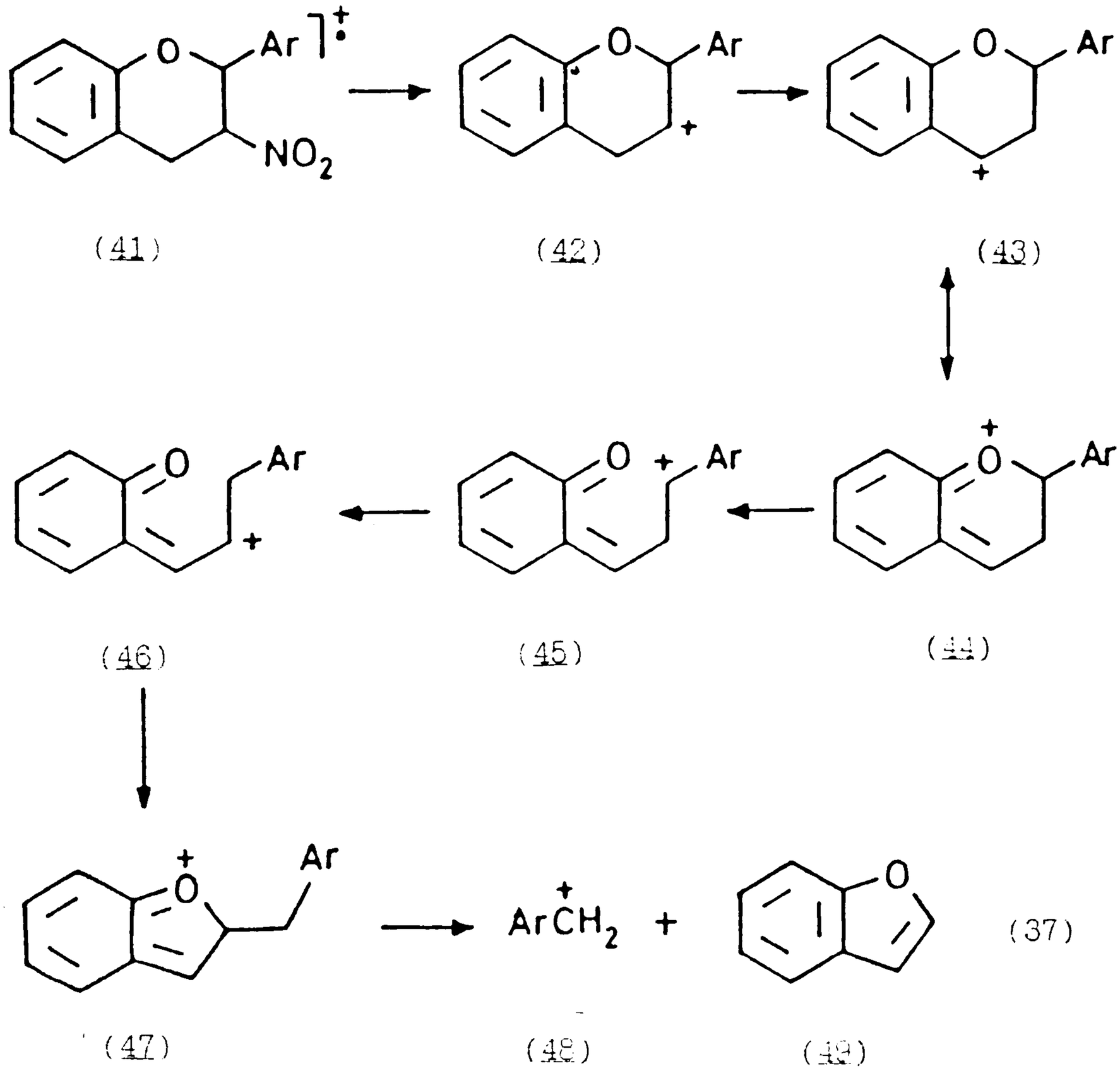

Fig. 5.2. Formation of $ArCH_2^+$.

explained using the shown reaction, on the assumption that the hydride (or deuteride) shifts one largely irreversible. In the absence of an isotope effect, the expected relative abundance of m/z/ 91, 92 and 93 are 33:100:8. Therefore, it would seem that some exchange of hydrogen and deuterium atoms occurs prior to formation of these ions.

Unfortunately it was not possible to probe this process more deeply by investigating metastable ions because the reaction did not give rise to a significant metastable peak. Notwithstanding this limitation, it is logical to associate the $[ArCH_2]^+$ peak with benzofuran loss from $[M-NO_2]^+$. The absence of comparable peaks in the nitrochromene spectra would be expected since there is no parallel mechanism for its formation by expulsion of a stable neutral species from $[M-NO_2]^+$.

(e) The fifth distinction between the spectra of the chromans and the chromenes was the presence of an ion at $[M-(NO_2 + ArH)]^+$ for some nitrochromans. This ion, which is of only occasional importance (for example m/z 131 in the spectrum of xiv at a relative abundance of 73%), is probably produced by consecutive loss NO_2 and ArH. The likely structure of the daughter ion is the benzopyrylium cation.

In the 5,6-benzochroman series, the peak corresponding to this dissociation appeared at m/z 181, as would be predicted on the basis of the shift rule[121]. However, the abundance of these $[M-NO_2-ArHO]^+$ ions was always sufficiently high to permit their use as a reliable source of structural information.

Similar remarks may be applied to the ion which was present at $[M-HNO_2-CO]^+$ in the spectra at a number of chromenes. This peak was very intense (74% relative intensity] in the spectrum of the 2 phenyl compounds, it persisted at reduced importance in the spectra of the 2-(4-isopropylphenyl) and 2-(naphthyl) compounds (15 - 33%), but was only of minor significance in the spectra of the remaining chromenes. Loss of CO from $[M-HNO_2]^{+\cdot}$ clearly requires extensive rearrangements, this reaction presumably competes effectively with more direct dissociations because it produces very stable daughter ions. In the case of the 2-phenyl parent chromene, likely structures for the resultant $[C_{14}H_{10}]^+$ ions are ionised anthracene, phenanthrene or 1,2-diphenyl-ethyne. However, the data does not allow the mechanism of this unusual process to be defined. The corresponding chromans did not show related ions in their spectra, due to there being no daughter ions of comparable stability to those possible with the chromenes. This contrast between the spectra of the chromenes and chromans was particularly striking for

the 2-phenyl derivatives, but it was less obvious for the higher homologues.

Other interesting features observed in the mass spectra include the successive loss of two nitro groups from the ionised dinitrochromene, and the elimination of HCl from the $[M-NO_2]^+$ ion in the spectrum of the chloronitrochromene. The former process constitutes a violation of the even-electron rule, however, consecutive loss of nitro radicals from dinitro-compounds is not particularly unusual[104]. In addition, diethoxyphenyl derivatives showed successive losses of neutral species having a mass of 28 amus (C_2H_4). With the diethoxyphenyl chroman these peaks (m/z 252 - 94%, m/z 123 - 90%) provided further information on the nature of the 2-aryl group, whose gross structure was defined by the $[ArCH_2]^+$ peak at m/z 179. Apart from these instances, there were relatively few fragmentations of high abundance which could be associated with the presence of specific functional group in the nitrochromenes or nitrochromans.

5.3.1. Electron Capture CI

The electron attracting nature of the nitro group would be expected to make the nitrochromenes and nitrochromans yield abundant radical molecular anions by electron capture, at a high level of sensitivity, when subjected to negative ion chemical ionisation. Resultant electron attachment spectra did in fact contain radical molecular anions of moderate abundance (typically 10 -

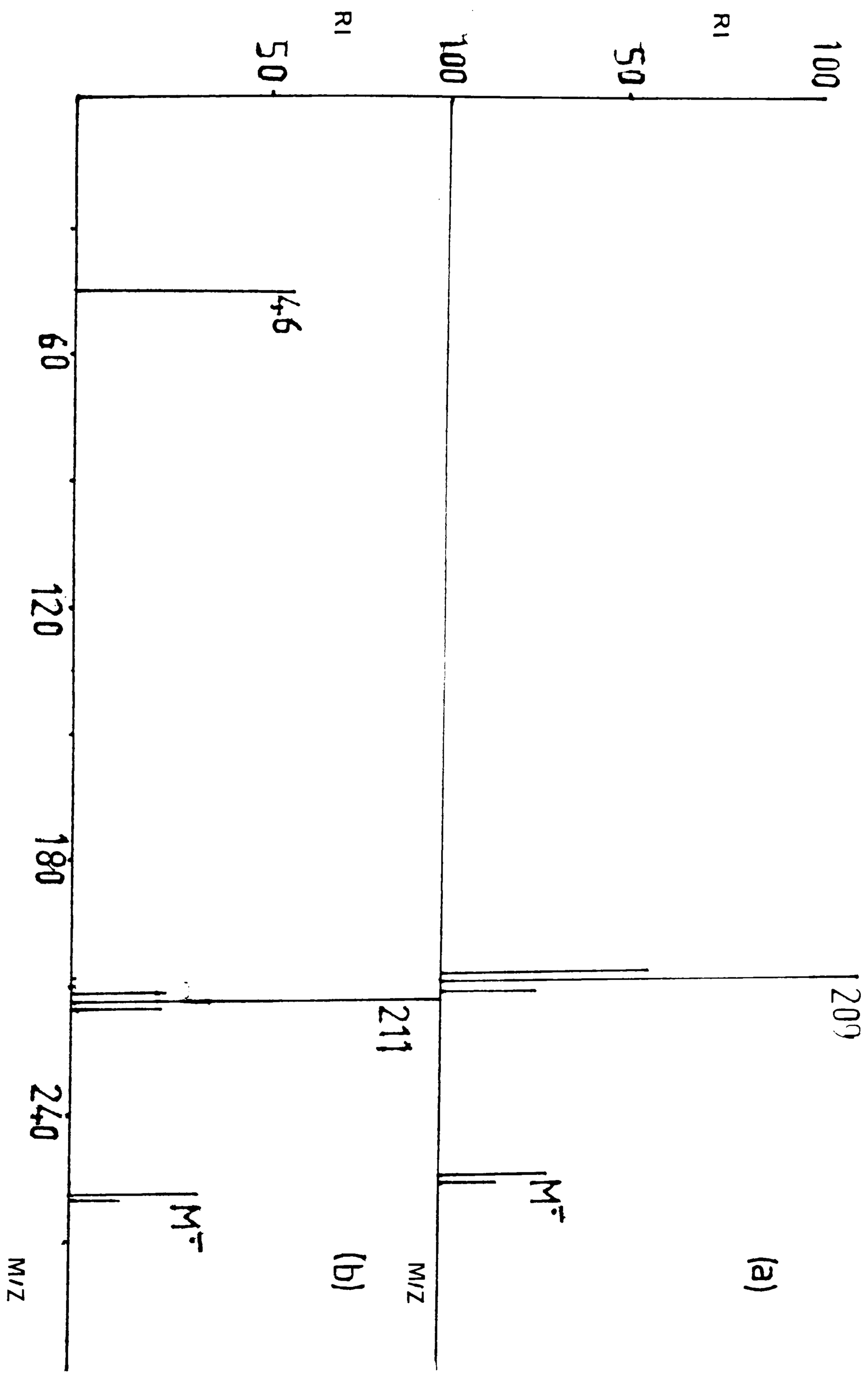

Fig. 5.3. Electron capture spectra for (a) 2-phenyl-3-nitrochromene (b) 2-phenyl-3-nitrochroman.

20%) and intense signals corresponding to loss of a nitro radical, as the base peak. Fig 5.2. shows both a spectrum for the parent 2-phenyl nitrochroman and corresponding chromene.

Ions other than $[M]^{+\cdot}$ and $[M-NO_2]^-$ or related ions, such as $[M-HNO_2]^{-\cdot}$, at very similar m/z were rare. However, some loss of CH_2O occurred from the molecular ion and $[M-NO_2]^-$ in the spectrum of the methoxynitrochromene.

The only major difference between the spectra of the chromenes and chromans was the appearance of a significant peak at m/z 46 ($[NO_2]^{-\cdot}$). in the chroman spectra. This divergence of behaviour could reflect the greater ability of $[M-NO_2]$ to retain the electron in the unsaturated series, perhaps because the charge is formally located in an sp^2 orbital, rather than in an sp^3 orbital as is necessary in the chroman series. Abundance of the $[NO_2]^{-\cdot}$ in the nitrochroman spectra was occasionally very high, and some peaks arising from attachment of the nitro anion to the parent nitrochroman did appear in these circumstances.

5.4. EI of 2-Aryl-chroman-3-one Oximes

The EI mass spectra of five 2-aryl-chroman-3-one oximes are represented in table 5.3.

A pictorial version of the parent 2-phenyl oxime is shown in Fig 5.3.

Substituents	m/z (relative abundance, %)
2-phenyl	240 (12); 239[M]$^{+\cdot}$(63); 223 (21); 222 (96)[$C_{15}H_{12}NO$]$^{+}$; 220 (18);207 (18); 165 (16); 145 (22); 133 (19); 131 (30); 116 (43); 115 (44); 107 (100) [C_7H_7O]$^{+}$; 106 (18); 105 (26); 91 (37) [C_7H_7]$^{+}$; 90 (19) [C_7H_6]$^{+\cdot}$; 89 (57) [C_7H_5]$^{+}$; 78 (32); 77 (60); 63 (30); 52 (18); 51 (43); 50 (19)
2-phenyl-8-methoxy	270 (17); 269 [M]$^{+\cdot}$ (92); 253 (23); 252 (100); 250 (15); 237 (18); 236 (27); 220 (20); 207 (23); 179 (27); 137 (60); 116 (19); 115 (27); 91 (27); 89 (20); 77 (22); 65 (23)
2-(1-naphthyl)	290 (20); 289 [M]$^{+\cdot}$ (96); 273 (27); 272 (100); 270 (25); 183 (41); 166 (27); 136 (21); 128 (16); 127 (17); 107 (52)
2-(1-naphthyl)-8-methoxy	320 (23); 319 [M]$^{+\cdot}$ (100); 303 (26); 302 (88); 287 (18); 286 (34); 195 (19); 183 (76); 167 (19); 166 (47); 165 (25); 152 (17); 141 (23); 140 (22); 139 (35); 137 (91); 128 (21); 127 (23); 115 (18); 77 (16); 65 (28); 63 (15)
2-phenyl-6-nitro	285 (19); 284 [M]$^{+\cdot}$ (88); 268 (23); 267 (98); 251 (18); 221 (29); 220 (28); 208 (44); 207 (27); 191 (19); 178 (20); 165 (25); 153 (15); 152 (80); 133 (39); 132 (18); 130 (15); 117 (17); 116 (78); 115 (37); 106 (44); 105 (46); 104 (19); 103 (21); 102 (21); 91 (59); 90 (32); 89 (83); 88 (22); 79 (28); 78 (33); 77 (84); 76 (34); 75 (23); 65 (26); 64 (20); 63 (20); 62 (24); 52 (22); 51 (100); 50 (41)

Table 5.3. Relative peak intensities for EI mass spectra of five 2-aryl chroman-3one-oximes.

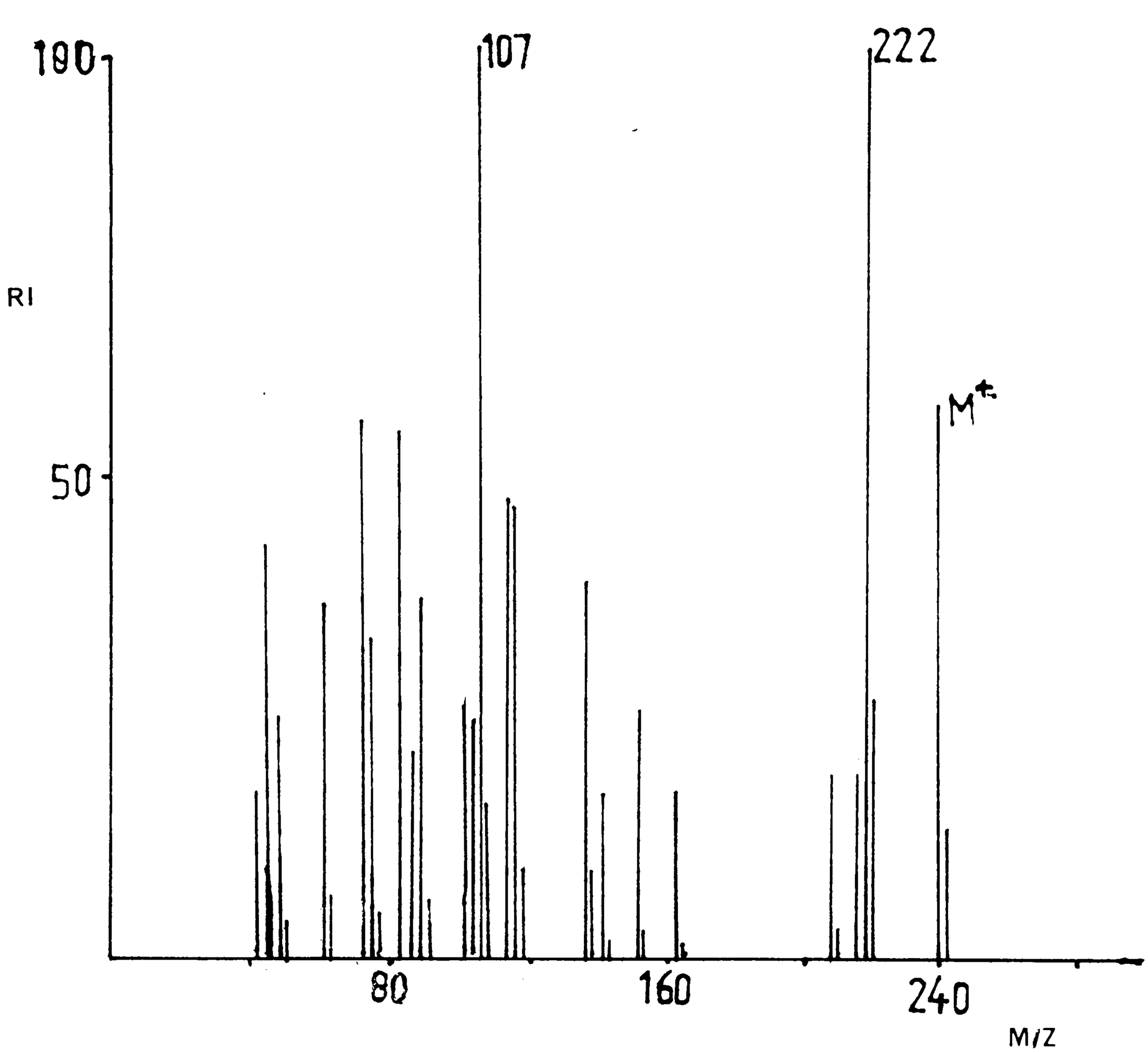

Fig. 5.4. Electron impact spectrum of 2-phenyl-chroman-3-one oxime.

These spectra are analytically useful and provide interesting comparisons to the corresponding 3 nitrochromans just described. The main spectral differences are probably due to the strength of the carbon-nitrogen double bond in the oximes which results in their retention of the nitrogen on the B ring, whereas the nitro group is easily lost in the nitrochromans.

The oximes shows facile loss of an hydroxyl radical (relative intensity 88 - 100%).

In addition, there was a sizable peak at $[M-O]^+$ (relative intensity 21 - 27%). This behaviour is characteristic of oximes, though there is evidence that $[M-O]^-$ in the spectra of oximes actually arises by thermal elimination of an oxygen radical prior to ionisation[122].

A third major peak in the spectra (relative intensity 52 - 100%) corresponds to a structurally informative cleavage of the B ring, with subsequent hydrogen transfer.

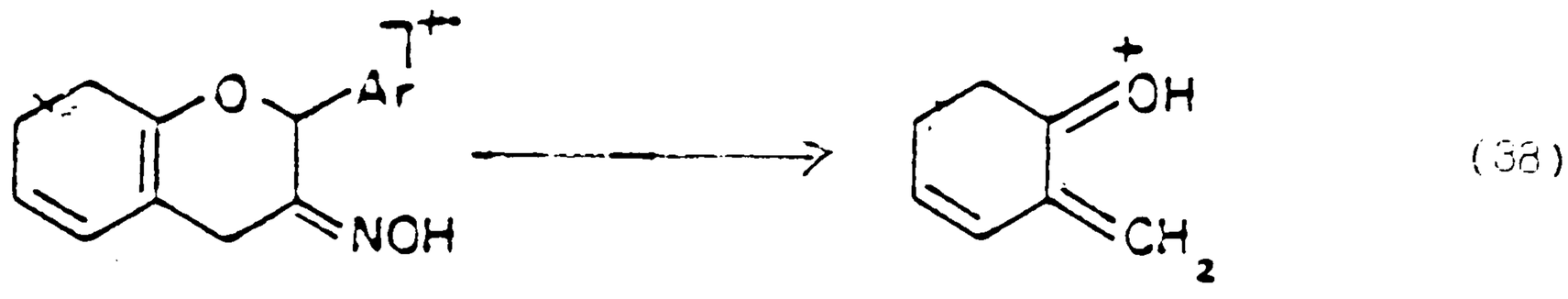

(38)

Thus, the formula of a substituent in ring A may be deduced from the mass of this fragment ion (e.g., m/z 107, X = H; m/z 137, X = OCH_3; m/z 152, X = NO_2). Similar results have been reported in the mass spectra of chroman-3-ol, and chroman-3-ol acetate[123]. A complementary peak (relative intensity 41 - 75%), corresponding to elimination from the molecular ion of a quinomethane, was of importance in the mass spectra of 2-(1-naphthyl)-chromanone oximes.

The lower abundance (10 - 40%) of this $[ArC_2H_2NO]^+$ ion when Ar was phenyl probably reflects the higher ionisation energy of the $[ArC_2H_2NO]$ species and the consequent poor stability of the resultant ion. No such series of peaks were observed for the 3 nitrochromans.

Finally, there is a collection of three peaks corresponding to $[ArCH_2]^+$, $[ArCH]^+$, $[ArC]^+$ (typical relative intensities 15 - 40%, 15 - 20%, and 20 - 55% respectively). As with the 3 nitrochromans these results confirm the nature of the 2 aryl group. $[ArCH_2]^+$ can originate from a similar mechanism to that explained earlier for the chroman $[ArCH]^+$ comes from the following scheme.

The $[ArC]^+$ ion originates from loss of an hydroxyl radical followed by hydrogen transfer to the nitrogen with the subsequent expulsion of $[ArC]^+$. The formation of these ions is shown in Fig 5.5.

5.5 Conclusions

3-nitrochromenes, 3-nitrochromans and chroman-3-one oximes are amenable to analysis by mass spectrometry. Several characteristic fragmentations exist in the electron impact mass spectra, and there are clear differences between the behaviour between these compound types. Unambiguous determination of the molecular masses of these heterocycles could be achieved.

References

1. "Mass Spectrometry, Principles and Application". I. Howe, D.H. Williams, R.D. Bowen. 1981 McGray-Hill

2. "Interpretaion of Mass Spectra" F.W. McCrafferty. 1980, University Science Books

3. "Practical Organic Mass Spectrometry". J. R. Chapman 1985. John Wiley and Sons.

4. "Rays of Positive Eletricity and Their Application to Chemical Analysis:. J. J. Thompson. Longman, Green and Co. 1913.

5. F.W. Aston. Phil. Mag. 38, 707, 1919.

6. A.J. Dempster. Phys. Rev. 11, 316, 1918.

7. "Modern Practice of Gas Chromatography". R.L. Grob, Marcell Dekker, 1977.

8. E.G. Johnson, A.O. Nier. Phys. Rev., 91, 10, 1953.

9. R.P. Morgan, J.H. Beynon, R.H. Bateman, B.W. Green, Int. J. Mass. Spectrom. Ion Phys., 28, 171, 1978.

10. P.E. Miller, M.B. Denton, J. Chem. Educ., 63, 617, 1986.

11. G.C. Goode, R.M. O'Malley, A.J. Ferrier-Correia, K.R. Jennings, Chem. in Britain, 7, 12, 1971.

12. "Time of Flight Mass Spectrometry". D. Price, J.E. Williams, Pergamon Press, Oxford, 1969.

13. G. C. Stafford, P.E. Kelly, S.E. Syka, W.E. Reynolds, J.F.J. Todd, Int. J. Mass. Spectrom. Ion Pro., 60, 85, 1985.

14. A.E. Schoen, J.W. Amy, J.D. Ciapeli, R.G. Cooks, P. Dobberstein, G. Juny. Int. J. Mass Spectrom. Ion Pro., 65, 125, 1985.

15. M.L. Gross, E.K. Chess, P.A. Lyon, F.W. Crow, S. Evans, H. Tudge. Int. J. Mass Spectrom. Ion Pro., 42, 243, 1982.

16. J. Mattauch, R.F.K. Herzog, Z. Physik, 89, 786, 1934.

17. G. J. Outer, A.W. Buijserd, A.J.H. Boerboom. Int. J. Mass Spectrom. Ion Phys., 46, 131, 1983.

18. K. Watanabe, J. Chem. Phys., 26, 542, 1957.

19. I. Dzidic, D.J. Carroll, R.N. Stillwell, E.C. Horning, Anal. Chem., 48, 1763, 1976.

20. H.D. Beckey, Angew. Chem. Int. Edn. Eng., 9, 633, 1969.

21. H.M. Rosenstock, M.B. Wallenstein, A.G. Watirhaftig, H. Eyring. Proc. Natl. Acad. Sci. USA, 38, 667, 1952.

22. U. Lohle, Ch. Ottinger, J. Chem. Phys., 51, 3097, 1969.

23. A. Mandelbaum, Org. Mass Spectrom., 15, 53, 1980.

24. R.D. Bowen, A. Maccoll. Org. Mass Spectrom. 19, 379, 1984.

25. "Chemical Ionisation Mass Spectrometry". A.G. Harrison, C.R.C. Press Inc Florida, 1984.

26. A.G. Harrison, K.R. Jennings, J. Chem. Soc. Faraday Trans. II, 72, 1601, 1976.

27. D.F. Hunt, G.C. Stafford, F.W. Crow, J.W. Russell. Anal. Chem., 48, 2098, 1976.

28. "Analytical Pyrolysis". W.J. Irwin, Marcell Dekker, 1982.

29. R.D. Macfarlane, Anal. Chem., 55, 1247 A, 1983.

30. M.A. Baldwin, F.W. McLafferty, Org. Mass Spectrom., 7, 1353, 1973.

31. R.J. Cotter, Anal. Chem., 52, 1589, 1980.

32. D.M. Hercules, R.J. Day, K. Balasanmugam, T.H. Dang, C.P. Li. Anal. Chem., 54, 280A, 1982.

33. H.D. Beckey, Angew. Chem. Int. Edn. Eng., 24, 403, 1975.

34. R.S. Leherle, I.C. Robb, D.W.J. Thomas, Sci. Instrum., 39, 458, 1962.

35. M. Barber, R.S. Bardoli, R.D. Sedgwick, A.N. Tyler. J. Chem. Soc. Chem. Commun., 325, 1981.

36. W.A. Donaldson, R.P. Huges, J. Am. Chem. Soc., 104, 4846, 1982.

37. J.L. Gower, Biomed. Mass Spectrom., 12, 191, 1985.

38. G. Bojesen, J. Moller, Int. J. Mass Spectrom. Ion Pro., 68, 239, 1986.

39. E. Clanton, A. Wakefield, J. Chem. Soc. Chem. Commun., 969, 1984.

40. C.W. Magee, Int. J. Mass Spectrom. Ion Pro., 49, 211, 1983.

41. G.R. Schronk, R.J. Cotter, Biomed. Environ. Mass Spectrom., 11, 522, 1986.

42. R.M. Caprioli, Anal. Chem., 55, 2387, 1983.

43. B.D. Musselman, J.T. Watson, C.K. Chang, Org. Mass. Spectrom., 21, 215, 1986.

44. T. Keough, Anal. Chem., 57, 2027, 1985.

45. J.A. Sunner, A. Morales, P. Kabarle, Anal. Chem., 59, 1378, 1987.

46. J.A. Sunner, A. Morales, P. Kabarle, Anal. Chem., 60, 98, 1988.

47. J.A. Sunner, R. Kalatunga, P. Karble, Anal. Chem., 58, 2009, 1986.

48. O.W. Huang, G.C. Wa, H.T. Tang. Int. J. Mass Spectrom. Ion Pro., 70, 145, 1986.

49. J. Bartmess, L.B. Phillips. Adv. Mass Spectrom., 10, 1581, 1985.

50. C.R. Blakey, M.L. Vestal, Anal. Chem., 55, 750, 1983.

51. A.J. Alexander, P. Kabarle, Anal. Chem., 58, 471, 1986.

52. "Tandem Mass Spectrometry" Ed. F.W. McLafferty, John Wiley and Sons, 1983.

53. "Collision Spectroscopy". R.G. Cooks, Plenum, 1978.

54. P.N.T. van Velzen, W.J. van der Hart, Org. Mass Spectrom., 19, 190, 1984.

55. M.E. Bier, R.G. Cooks, J. Amy, G. Stafford, P.C. Ceja, K.P. Syka, ASMS Denver, 279, 1987.

56. R.B. Cody, B.S. Freiser, Anal. Chem., 59, 1054, 1987.

57. M.J. Farncombe. PhD Thesis 1984 references therein, 1984.

58. G.C. Glish, S.A. Mclinckey, R.G. Cooks. Int. J. Mass Spectrom. Ion Proc., 39, 1981.

59. R.A. Yost, C.G. Enke, Anal. Chem., 51, 1251A, 1979.

60. K. Sato, T. Asada, M. Ishihara, F. Kunihiro, Y. Kammell, E. Kubota, C.E. Costello, S.A. Martin, H.A. Scodle, K. Bieman, Anal. Chem., 59, 1652, 1987.

61. E.B. Ledford, S. Gradevi, C.L. Wilkins, M.L. Gross, Adv. Mass Spectrom., 8A, 1707, 1980.

62. J.N. Louris, R.G. Cooks, J.E.P. Syka, P.E. Kelley, G.C. Stafford, J.F.J. Todd, Anal. Chem., 59, 1677, 1987.

63. "Quantitative Mass Spectrometry". H.J. Millard, Heydon and Son, 1978.

64. P.L. Layman, Chem. Eng. News, 17, 1984.

65. "Handbook of Chemistry and Physics" Ed. R. C. West, C.R.C. Press, 1984.

66. "Surfactants and Interfacial Phenomena". M.J. Rosen, John Wiley and Sons, 1978.

67. "Surfactant Science Series" Various authors, Edward Arnold publishers, 1967.

68. G. Libster, G. Eppent, Z. Chem., 19, 69, 1979.

69. A. W. O'Connell. Anal. Chem., 49, 855, 1977.

70. P. Taylor, G.C. Nickless, J. Chromatogr., 178, 259, 1979.

71. H. Heilman, Fressenius Z. Anal. Chem., 294, 397, 1979.

72. S.H. Hoke, A.G. Collins, C.A. Reynolds, Anal. Chem., 51, 859, 1979.

73. "Anionic Surfactant Analysis - Chemical Analysis" J. Cross Ed, Marcel Delker, New York, 1977.

74. E. Julia-Danes, A.M. Casanovas, Tenside Deterg., 16, 317, 1979.

75. R.A. Clanabo, R.A. Jamiason, Anal. Chem., 53, 174R, 1981.

76. P. Daehling, F.W. Roelgen, J.J. Zwinselman, R.H. Fokkens, N.M.M. Nibbering, Fresenius. Z. Anal. Chem., 312, 335, 1982.

77. R.A. Sanders, A.J. DeStefano, T. Keough. Org. Mass Spectrom. 15, 348, 1980.

78. T. Keough, A.J. DeStefano, R.A. Saunders. Org. Mass Spectrom., 15, 351, 1980.

79. R.O. Mumma, F.J. Vastola. Org. Mass Spectrom., 6, 1373, 1972.

80. H. Kosuge, K. Matzumoto, Fresenius Z. Anal. Chem., 312, 317, 1982.

81. E. Schneider, K. Levsen, P. Dahling, K Rollgen, Fresenius Z. Anal. Chem., 316, 488, 1983.

82. P.A. Lyon, W.G. Stebkings, F.W. Crow, K.B. Tonner, D.L. Lippstres, M.L. Gross, Anal. Chem., 56, 8, 1984.

83. M. Barber, R.S. Bardoli, G.J. Elliott, R.D. Sedgwick, A.W. Tyler, J. Chem. Soc. Faraday Trans. I, 79, 4249, 1983.

84. W.V. Ligon, S.B. Dorn, Int. J. Mass Spectrom. Ion Pro., 57, 75, 1984.

85. D.H. Williams, C. Bradley, G. Bojesen, S. Santikarn, L.C.E. Taylor, J. Am. Chem. Soc., 103, 5700, 1981.

86. S. Naylor, A.F. Findeis, B.W. Gibson, D.H. Williams, J. Am. Chem. Soc., 108, 6359, 1986.

87. W.V. Cigon, S.B. Dorn, Int. J. Mass Spectrom. Ion Pro., 61, 113, 1984.

88. E. De Pauw, G. Pelzer, D. Dao Viet, J. Marien, J. Biochem. Biophys. Res. Commun., 123, 27, 1984.

89. C.F. Beckner, R.M. Caprioli, Biomed. Mass Spectrom., 11, 60, 1984.

90. K. Linhart, K. Wrobelz, Tenside Deterg., 15, 19, 1978.

91. R.A. Lieonardo, T.A. Neubecker, Anal. Chem., 55, 93R, 1983.

92. J. Congell, W.D. Mariece, Analyst, 80, 167, 1985.

93. M. Malat, Z. Fresenius Anal. Chem., 297, 417, 1979.

94. M. Taylor, G. Manton, J.H. Scrivens, Private Communication, 1986.

95. E. Schneider, K. Levsen, P. Duhlung, F.W. Rollgen, Fresenius Z. Anal. Chem., 316, 277, 1985.

96. G. Schnelzeizen-Redeker, U. Geissman, F.W. Rollgen, Angew. Chem. Int. Ed. Engl., 23, 892, 1984.

97. G. Schnelzeizen-Redeker, M. A. McDowell, U. Geissman, K. Levesen, F.W. Rollgen, J. Chromatogr., 323, 127, 1985.

98. "Chemistry of the Amino Group". E.H. White, D.J. Woodcock, John Wiley and Son, 1968.

99. U. Schude, R. Stoll, F.W. Rollgen, Org. Mass Spectrom., 16, 441, 1981.

100. J. Wilson, J. Chem. Soc. Dalton Trans., 890, 1976.

101. A. Finch, F.M. Hall, J. Chem. Soc. Dalton Trans., 915, 1982.

102. "Thermochemistry of Organic and Organometallic Chemistry". J.D. Cox G. Pilcher.

103. S.G. Ciar, J.F. Kielsmann, R.D. Levin, J. Phys. Chem. Ref. Data, 13, 1984.

104. "The Mass Spectra of Organic Compounds". H. Budzikiewicz, C. Djerassi, D.H. Williams, 1967, Holden Day.

105. S.C. Stinson, Chem. Eng. News, 27, 1984.

106. R.R. Stromberg, S. Straus, B.G. Achammen, J. Polymer Sci., 35, 355, 1959.

107. J. Urdis, Analyst, 96, 130, 1971.

108. I.D. Newton, I.C.I. Chemicals and Polymers, Private Communication.

109. "NMR of the Periodic Table" Ed. R.K. Harris, B.E. Mann, Academic Press 1978.

110. B.L. Bentz, P.J. Gale, M.E. Labib, Proc. 10th IMSC Swansea, 1533, 1985.

111. D. Mitchell, K.R. Jennings, J.H. Scrivens, Proc. 10th IMSC Swansea, 1601, 1985.

112. L. Rene, L. Blanco, R. Royer, R. Cavier, J. Lemione, Eur. J. Med. Chem. - Chim. Ther., 12, 385, 1977.

113. L. Rene, R. Royer, Eur J. Med. Chem. - Chim. Ther., 10, 72, 1975.

114. T.S. Roo, R.K. Singh, G.K. Trivedi, Heterocycles, 22, 1377, 1984.

115. R.S. Varma, G.W. Kabalka, Heterocycles, 23, 139, 1985.

116. M. Fatome, L. Andrien, J.D. Laval, R. Royer, La Rene, Eur. J. Med. Chem. - Chim. Ther., 11, 81, 1976.

117. R.S. Varma, M. Kadkhodayan, G.W. Kabalka, Heterocycles, 24, 1647, 1986.

118. R.S. Varma, M. Varma, Y. Z. Gai, G.W. Kabalka, Heterocycles, 24, 2581, 1986.

119. "Chromenes, Chromamones and Chromones". Ed. G.P. Ellis, Wiley New York, 1977.

120. K. Biermann, G. Spiteller, Tet. Letts., 229, 1961.

121. P.C. Vijfhnizen, W. Heerma, G. Dijkstra, Org. Mass Spectrom., 10, 919, 1975.

122. H. Budzikiewicz, U. Lenz, Org. Mass Spectrom., 10, 992, 1975.